

VITA-SALUTE SAN RAFFAELE UNIVERSITY

International PhD Course in Molecular Medicine
Curriculum in Basic and Applied Immunology and Oncology

**EXPLORING THE ROLE OF TISSUE
RESIDENT MEMORY T CELLS IN
PROSTATE CANCER: IMPLICATIONS
FOR ONCOLOGICAL OUTCOMES**

DoS: Prof. Alberto Briganti 
Second Supervisor: Dr. Carmen Priolo

PhD Thesis of Vito Cucchiara

Registration number 017646

XXXVI PhD Cycle

SSD MED/24

Academic Year 2022/2023

CONSULTAZIONE TESI DI DOTTORATO DI RICERCA

I, the undersigned Vito Cucchiara

Registration number 017646

Born in Alcamo (TP)

On 24/08/1989

Author of the PhD Thesis titled:

“Exploring The Role Of Tissue Resident Memory T Cells In Prostate Cancer: Implications For Oncological Outcomes”

DO NOT AUTHORIZE the public release of the thesis for 12 months from the PhD thesis date, specifically from 22/02/2024 to 22/02/2025.

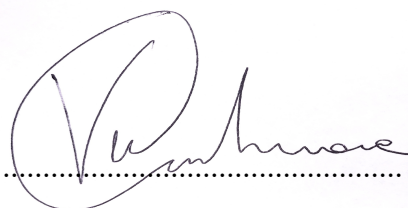
Because:

- The whole project or parts of it may be the subject of a patent application;
- Parts of the thesis have been or are being submitted to a publisher or are in the press;
- The thesis project is financed by external bodies that have rights over it and its publication.

Reproduction of the thesis in whole or in part is forbidden.

Date: February 22, 2024

Signature

A handwritten signature in black ink, appearing to read 'Vito Cucchiara', is written over a dotted line. The signature is enclosed within a light purple rectangular box.

DECLARATION

This thesis has been composed by myself and has not been used in any previous application for a degree. Throughout the text I used 'We' interchangeably. This thesis has been written according to the editing guidelines approved by the University.

All the results presented here were obtained by myself, except for:

- 1) *Identification of antibodies used in the Flow Cytometry Panel were performed in collaboration with Dr. Cristian Gabriel Beccaria and Dr. Valentina Venzin (San Raffaele Scientific Institute, Milan, Italy).*
- 2) *Extemporaneous pathological assessments were performed by Dr. Roberta Lucianò and Dr. Nazario Tenace (Department of Pathology, IRCCS San Raffaele Hospital, Milan, Italy).*
- 3) *Selection of optimal formalin-fixed paraffin-embedded samples for immunohistochemistry and immunofluorescence were performed in collaboration with Prof. Claudio Doglioni, Prof. Maurilio Ponzoni, Dr. Stefano Grassi, (Department of Pathology, IRCCS San Raffaele Hospital, Milan, Italy).*
- 4) *Library preparation for single-cell RNA sequencing was performed by Dr. Dejan Lazarevic and Dr. Lorenza Moronetti (Center for Omics Sciences, San Raffaele Scientific Institute, Milan, Italy).*
- 5) *Single-cell RNA sequencing bioinformatic analysis were performed in collaboration with Dr. Marco Morelli and Dr. Francesca Genova (Center for Omics Sciences, San Raffaele Scientific Institute, Milan, Italy).*

Figures in the introduction chapter are used for educational purpose. For those images subject to copyright, we have relied on the principle of fair use, which allows for the use of copyrighted materials for purposes such as information dissemination, criticism, or educational activities without requiring explicit authorization from the copyright owner. The Italian Legislative Decree no. 68 of 9 April 2003, aligning with Directive 2001/29/EC on copyright within the information society, has established a stance similar to the US fair use doctrine through Article 70 of Italian copyright law.

All sources of information are acknowledged by means of reference.

ABSTRACT

INTRODUCTION: CD103⁺ CD8⁺ tissue-resident memory T cells (TRMs) have emerged as a critical immune subset, potentially playing a pivotal role in orchestrating anticancer adaptive immune responses. This study aims to comprehensively characterize TRMs and their prognostic and predictive implications in prostate cancer (PCa), shedding light on their potential role in tumor progression and patient outcomes.

METHODS: TRMs were profiled in both tumor and healthy prostate tissues, employing a comprehensive molecular approach to characterize their function and abundance. Utilizing multiplex immunofluorescence analysis, we precisely quantified TRMs in primary PCa specimens and investigated their association with adverse pathological outcomes. Furthermore, to gain insights into the molecular mechanisms underlying TRMs function, we employed single-cell RNA sequencing and flow cytometry. We examined the transcriptional profile and functionality of tumor-infiltrating TRMs, providing valuable information on their role within the tumor microenvironment.

RESULTS: Reduced infiltration of TRMs was significantly associated with high-grade pathology in PCa. Cox regression analysis identified CD103⁺ CD8⁺ T cells as an independent prognostic marker for clinically significant disease (Gleason Score 7-10) in PCa patients (p-value: 0.05). Single-cell RNA sequencing analysis revealed downregulation of cytokine-related genes such as *IRF2BP2*, *IRF1*, *IL2RB*, *NFKB1*, and *NFKB2* in TRMs expressing *CD8B*, *ITGAE*, and *CXCR6* from high-grade tumors, indicative of an exhausted profile. Flow cytometry results demonstrated that TRMs from high-grade tumors exhibited lower levels of IFN- γ , IL-2, and TNF- α compared to those from healthy or low-grade disease. Furthermore, our investigation of CD39 expression, showed that CD39⁺CD103⁺CD8⁺ TRMs relative abundance was an independent prognostic factor for high-grade disease (p-value: 0.027) and lymph node invasion in PCa patients (p-value: 0.032).

CONCLUSION: Our research underscores the pivotal role of TRMs as a crucial functional subset within PCa. Through a comprehensive molecular characterization, we demonstrate that TRMs from aggressive prostatic disease display an exhausted profile, thus potentially contributing to the impaired antitumor immunity.

TABLE OF CONTENTS

1. ACRONYMS AND ABBREVIATIONS.....	3
2. LIST OF FIGURES AND TABLES.....	5
3. INTRODUCTION.....	7
3.1 Epidemiology.....	7
3.2 Risk Factors.....	9
3.3 Prostate Anatomy.....	10
3.4 Prostatic Carcinoma Histotypes.....	12
3.5 Grading of Prostatic Adenocarcinoma.....	13
3.5.1 Gleason System.....	14
3.5.2 International Society of Urological Pathology (ISUP) Grading System.....	15
3.5 Risk Group Classification.....	17
3.6 Diagnosis and Staging.....	19
3.6.1 Clinical Presentation.....	19
3.6.2 Methods of Diagnosis.....	20
3.7 Clinical and Pathological Staging.....	24
3.8 Management of prostate cancer patients.....	25
3.9 Tumor Microenvironment (TME) of Prostate cancer.....	28
3.9.1 Low Mutational Burden and Genomic alterations.....	29
3.9.2 Adaptive immune cells.....	31
3.9.3 Immune Checkpoint Expression.....	34
3.9.4 Immunosuppressive Cell Types.....	35
3.9.5 Stromal Influence.....	38
3.10 Immunotherapy in Prostate Cancer.....	39
3.10.1 Immune checkpoint inhibitors.....	41
3.10.2 Dendritic cell vaccines: Sipuleucel T.....	43
3.10.2 Prostate Specific Membran Antigen (PSMA) CAR T therapy.....	43
3.10.3 Bi-specific T cell engagement (BiTE).....	44
4 AIM OF THE WORK.....	45
5 RESULTS.....	46
5.1 Unveiling Prostate Immune Cell Composition.....	46
5.1.1 Patient Cohort and Tissue Retrieval.....	46
5.1.2 Flow cytometry – t-SNE analysis on fresh prostate samples.....	48
5.1.3 PD-1 and CTLA4 analysis on prostate tissues.....	50
5.1.4 Multiplex Immunohistochemical Phenotyping.....	52
5.1.6 Peripheral Blood Samples as a source of Immune biomarkers.....	59
5.2 Characterization of T Cells subsets in Healthy and Prostate Cancer tissue.....	62

5.2.1	<i>Unsupervised analysis on CD4⁺ cells</i>	64
5.2.2	<i>Unsupervised analysis on CD8⁺ cells</i>	67
5.2.3	<i>Spatial localization of T Cell Infiltration through Multiplex Analysis</i>	70
5.3	Transcriptional and Functional Profiling of CD8+CD103+ Cells	74
5.3.1	<i>Gene expression profiling of prostate samples</i>	74
5.3.2	<i>Intracluster Analysis of CD8B Gene-Expressing Cells in Prostate Tissue</i>	78
5.3.3	<i>Characterization of transcriptional profiles in CD8+CD103+ T cells</i>	81
5.3.4	<i>Flow Cytometry Analysis of Cytokine Production in CD8+ and CD8+CD103+ T Cells</i>	84
5.3.5	<i>Cytokine Production in CD4+ T Cells Using Flow Cytometry</i>	88
6	DISCUSSION	89
7	MATERIALS AND METHODS	95
8	REFERENCES	103

1. ACRONYMS AND ABBREVIATIONS

ADT:	Androgen Deprivation Therapy
AR:	Androgen Receptor
ARSI:	Androgen Receptor Signaling Inhibitors
ATM:	Ataxia Telangiectasia Mutated
BCR:	Biochemical Recurrence
BPH:	Benign Prostatic Hyperplasia
BRCA 1/2:	Breast Cancer Gene
CCR4:	C-C Motif Chemokine Receptor 4
CCL3:	C-C Motif Chemokine Ligand 3
CCL4:	C-C Motif Chemokine Ligand 3
CHEK2:	Checkpoint Kinase 2
CRPC:	Castration-Resistant Prostate Cancer
CS PCa:	Clinically Significant Prostate Cancer
CXCR6	C-X-C Motif Chemokine Receptor 6
DCs:	Dendritic Cells
DDR:	Dna Damage Repair.
DRE:	Digital Rectal Examination
EAU:	European Association Of Urology
ECM:	Extracellular Matrix
ENC1:	Ectodermal-Neural Cortex 1
EPCAM:	Epithelial Cell Adhesion Molecule
ERK1/2:	Extracellular Signal-Regulated Kinase 1 And 2
GLNY:	Granulysin
GMZK:	Granzymes
GS:	Gleason Score
HLA-DR:	Human Leukocyte Antigen – DR Isotype
HOXB13:	Homeobox Protein Hox-B13
IFN 1:	Interferon 1
IFNg:	Interferon Gamma
IL-2:	Interleukin-2
IL-6:	Interleukin-6
IL-8:	Interleukin-8
INKT:	Invariant Natural Killer
ISUP:	International Society Uro-Pathology

ITAGE:	Integrin Subunit Alpha E
JAK:	Janus Kinase
LHRH:	Luteinizing Hormone-Releasing Hormone
M1:	Type-1 Macrophage
M2:	Type-2 Macrophage
mAb:	Monoclonal Antibody
mCSPC:	Metastatic Castration-Sensitive Prostate Cancer
MDSCs:	Myeloid-Derived Suppressor Cells
MHCS:	Major Histocompatibility Complexes
MLH 1/2:	Mutl Protein Homolog
MMPS:	Matrix Metalloproteases
MSH6:	Muts Homolog 6
N0:	Negative Lymph Nodal Status
N1:	Positive Lymph Nodal Status
NCCN:	National Cancer Center Network
NK:	Natural Killer
NKG2D:	Natural Killer Group 2 Member D
NKT:	Natural Killer T
PAP:	Prostatic Acid Phosphatase
PARP:	Poly(Adp Ribose) Polymerase
PCa:	Prostate Cancer
PD-1:	Programmed Cell Death Protein
PD-L1:	Programmed Cell Death Ligand 1
PSA:	Prostate-Specific Antigen
RP:	Radical Prostatectomy
TAMs:	Tumor-Associated Macrophages
TBX:	MRI-Target Biopsy
TCR:	T Cell Receptor
TRM:	Tissue Resident Memory T Cells
TGFb:	Transforming Growth Factor-Beta
Th17:	Helper T Cells 17
Th2:	T Helper 2
TME:	Tumor Microenvironment
TREG:	T Regulatory
XCL1:	Chemokine (C Motif) Ligand

2. LIST OF FIGURES AND TABLES

Figure 1: Prostate cancer incidence and mortality rate	8
Figure 2: Prostate Anatomy and relations of different glandular zones	12
Figure 3: The Tumor Immune Microenvironment (TME) in Prostate Cancer	28
Figure 4: Comprehensive examination of immune system pathways and targets in prostate cancer	41
Figure 5: Composition and tissues retrieval pipeline of samples from study cohort of patients	47
Figure 6: t-Distributed Stochastic Neighbor Embedding (tSNE) analysis of CD45 ⁺ T cells in healthy and tumoral prostate tissue	49
Figure 7: PD-1 and CTLA-4 surface expression on CD4 ⁺ and CD8 ⁺ T cells do not correlate with high-risk prostate cancer disease	51
Figure 8: Composition and characteristics of study cohort of patients for multiplex immunohistochemical phenotyping	52
Figure 9: CD4 ⁺ and CD8 ⁺ T cell infiltration evaluation on patients affected by localized prostate cancer	53
Figure 10: M1 and M2 infiltration evaluation on patients affected by localized prostate cancer	55
Figure 11: tSNE analysis of CD45 ⁺ T cells in tissue prostate samples from stratified low, intermediate and high-risk disease patients	58
Figure 12: CD103 ⁺ CD8 ⁺ T cell population as an independent predictor of clinically significant PCa	59
Figure 13: tSNE analysis of CD45 ⁺ T cells in the blood of stratified low, intermediate and high-risk disease patients	61
Figure 14: tSNE analysis of CD45 ⁺ T cells in tissue samples of patients stratified as control, Insignificant and Clinically Significant patients	63
Figure 15: tSNE analysis of CD4 ⁺ T cells in prostate tissue samples of patients affected by localized prostate cancer	65
Figure 16: tSNE analysis of CD4 ⁺ T cells in prostate tissue samples of insignificant and clinically significant PCa patients	66
Figure 17: tSNE analysis of CD8 ⁺ T cells in prostate tissue samples of patients affected by localized prostate cancer	67
Figure 18: tSNE analysis of CD8 ⁺ T cells and a supervised analysis on CD103 ⁺ CD8 ⁺ T cells	69
Figure 19: CD103 ⁺ CD8 ⁺ T cells in prostate tissue samples of insignificant and clinically significant PCa patients	70
Figure 20: CD103 ⁺ CD8 ⁺ T cells infiltration and quantification in prostate tissue samples	71

Figure 21: <i>CD39⁺CD103⁺CD8⁺ T cell population as an independent predictor of high grade disease and lymph node invasion</i>	73
Figure 22: <i>Single-Cell RNA sequencing analysis on CD45⁺ cells</i>	75
Figure 23: <i>Characterization of immune populations in prostate samples by single-cell RNA sequencing</i>	77
Figure 24: <i>CD8B Gene Expression on CD45⁺ prostate populations</i>	78
Figure 25: <i>Single-cell analysis of CD8⁺ populations in prostate samples</i>	80
Figure 26: <i>ITGAE Gene Expression in CD8⁺ T cells of prostate samples</i>	81
Figure 27: <i>Differential Expression of Cytokine-Associated Genes in CD103⁺ CD8⁺ T Cells from Tumors and Healthy prostate tissue</i>	83
Figure 28: <i>Cytokine production capacity of CD8⁺T cells in prostate cancer tissue samples</i>	85
Figure 29: <i>Reduced cytokine production capacity of CD8⁺T cells from high grade prostate cancer tissues</i>	86
Figure 30: <i>Reduced cytokine production capacity of tissue-resident memory CD8⁺T cells from clinically relevant tumors</i>	87
Figure 31: <i>Reduced cytokine production capacity of CD4⁺T cells from clinically significant disease</i>	88
Table 1: <i>Histological definition of ISUP Grading System</i>	16
Table 2: <i>European Association of Urology (EAU) risk groups for localized and advanced disease</i>	17
Table 3: <i>Rate of Prostate Cancer diagnosed in relation to serum PSA</i>	21
Table 4: <i>The 2009 TNM (Tumor Node Metastasis) classification for PCa</i>	24
Table 5: <i>Study cohort of patients for identification of immune cells in tissue and blood samples</i>	57
Table 6: <i>Study cohort of patients for the characterization of T cells in tissue samples</i>	62
Table 7: <i>Patient Composition and Characteristics for Flow Cytometry Analysis of Cytokine Production</i>	84
Table 8: <i>List of reagents and antibodies for Multiparameter flow cytometry</i>	97
Table 9: <i>Reagents and Antibodies used for Multiplex Ventana phenotyping</i>	100

3. INTRODUCTION

3.1 Epidemiology

In 2020, prostate cancer (PCa) garnered approximately 1.4 million diagnoses globally, making it the second most frequently diagnosed cancer in men (Culp et al., 2020). PCa typically affects men aged 50 and older, with its occurrence rising in correlation with age. The majority (about 85%) of PCa cases are diagnosed in individuals over the age of 65, peaking between 70 and 74 years old. Rarely does this cancer occur in men under 50, representing less than 0.1% of all PCa patients within this age group. Conversely, when a man reaches 85, the cumulative risk of PCa diagnosis jumps to 20% (Sung et al., 2021). It's important to note that these values are based on clinically detected tumors, potentially underestimating the actual incidence as clinically silent cases are not considered.

African American men have the highest reported incidence of PCa globally at 272/100,000, followed by Caucasians at 169/100,000 and Asians at 101/100,000. Native Americans exhibit a significantly lower incidence at 50/100,000. The mortality rate for African American men is around 68/100,000, more than double that of Caucasians (about 27/100,000) and almost six times higher than that of Asians (about 12/100,000). Various hypotheses, including genetic predisposition, tumor initiation or progression mechanisms, dietary factors, testosterone levels, and cultural barriers, have been suggested to explain these disparities. However, there is no clear data supporting any single hypothesis, indicating a likely multifactorial explanation for the observed differences in incidence and mortality (Sung et al., 2021).

Autopsy-based studies suggest that microscopic PCa lesions occur in approximately 30% of men in their forties, 50% in their sixties, and over 75% in men over 85 (Haas et al., 2008).

Approximately 1 in 6 men will develop PCa in their lifetime. Age is also a factor in PCa mortality rates. The lowest mortality rate is observed in patients aged 45-50 (about 3/100,000), increasing to about 30/100,000 in patients aged 60-65, and reaching a maximum of 400-500/100,000 in those aged 80 and older (L. Wang et al., 2022). Between the mid-1970s and 1991, there was a notable rise in PCa mortality rates, which

subsequently experienced a consistent decline. Intriguingly, this decline occurred despite an uptick in diagnoses. Experts attribute this trend to factors such as the aging population worldwide and advancements in diagnostic technologies (Sung et al., 2021).

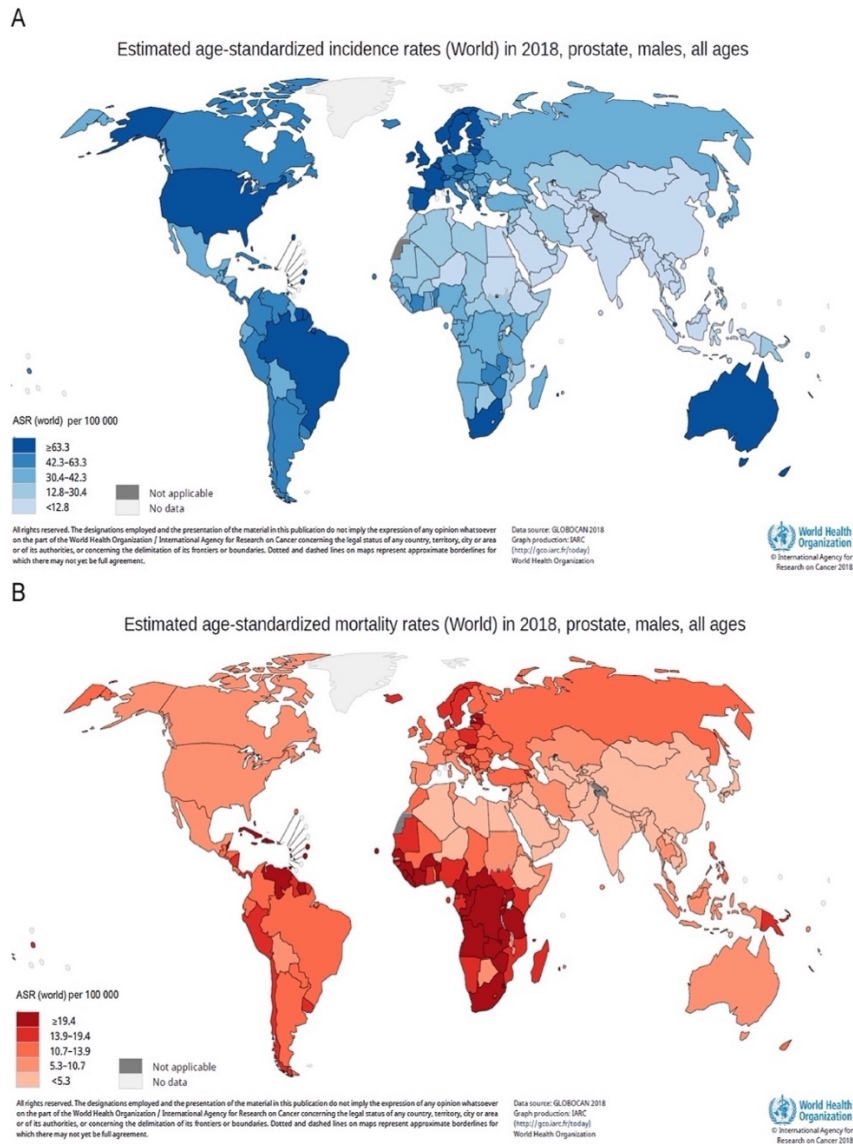


Figure 1. Prostate cancer incidence and mortality rate. A) Variation in age-standardized prostate cancer (PCa) incidence rates. B) Variation in age-standardized PCa mortality rates. Incidence: PCa is most prevalent in developed countries, particularly in North America, Europe, and Oceania. Incidence rates tend to be lower in Asian and African countries. The variation in incidence rates can be attributed to differences in genetic predisposition, lifestyle factors, access to healthcare, and screening practices. Mortality: Mortality rates from PCa also exhibit regional disparities, with higher rates observed in developed countries. Mortality rates tend to be lower in Asian and African countries compared to North America and Europe. Mortality rates have been declining in several developed countries due to advancements in early detection, treatment modalities, and improvements in healthcare infrastructure. Adapted from Culp et al. *Eur Urol* 2020.

3.2 Risk Factors

Family History

A higher incidence of PCa is linked to family history and ethnic background, indicating a potential genetic predisposition (Hemminki, 2012). Men of African descent living in Western countries experience less favorable outcomes, influenced by a combination of biological, environmental, social, and healthcare factors (Nyame et al., 2022). This group is more prone to being diagnosed with advanced disease, and post-prostatectomy upgrades occur more frequently compared to Caucasian men (49% vs. 26%) (Sanchez-Ortiz et al., 2006).

Hereditary Cancer

A small subset of individuals with PCa exhibits true hereditary disease, defined by criteria such as having more than three cases within the same family, PCa occurring in three successive generations, or more than two men being diagnosed with PCa before the age of 55. This hereditary form of PCa is characterized by an earlier onset of the disease by six to seven years, although there doesn't appear to be any discernible difference in disease aggressiveness or clinical course (Randazzo et al., 2016).

In a comprehensive USA population database, where 2.18% of participants reported hereditary disease, the relative risk (RR) was notably elevated. Specifically, the RR for the diagnosis of any PCa was 2.30, for early-onset PCa it was 3.93, for lethal PCa it was 2.21, and for clinically significant PCa (csPCa) it was 2.32 (Beebe-Dimmer et al., 2020). These increased risks with hereditary PCa surpassed those associated with familial PCa (defined as having more than two first- or second-degree relatives with PCa on the same side of the family tree) or familial syndromes like hereditary breast and ovarian cancer and Lynch syndrome.

In a study conducted within a Swedish population, when a father and two brothers were diagnosed with PCa, the likelihood of developing high-risk PCa by the age of 65 rose to 11.4%, significantly higher than the general population risk of 1.4%. Similarly, the probability of being diagnosed with any form of PCa increased to 43.9%, contrasting sharply with the population risk of 4.8% (Bratt et al., 2016).

Germline Mutations

The risk of PCa is influenced by more than 100 common susceptibility loci, as revealed by genome-wide association studies, particularly the aggressive form (Amin Al Olama et al., 2015; Eeles et al., 2013). Other studies indicate that 15% to 17% of cases carry germline mutations independently of their disease stage (Giri et al., 2019; Nicolosi et al., 2019). A genomic evaluation in PCa patients revealed that 15.6% of men with PCa have pathogenic variants in tested genes (BRCA1, BRCA2, HOXB13, MLH1, MSH2, PMS2, MSH6, EPCAM, ATM, CHEK2, NBN, and TP53), and 10.9% have germline pathogenic variants in DNA repair genes.

The most commonly identified pathogenic variants were in BRCA2 (4.5%), CHEK2 (2.2%), ATM (1.8%), and BRCA1 (1.1%).

An observational study tracking male carriers of BRCA1 and BRCA2 genes confirmed the correlation between BRCA2 mutations and aggressive forms of PCa (Nyberg et al., 2020). An outcomes analysis of 2,019 PCa patients (18 BRCA1 carriers, 61 BRCA2 carriers, and 1,940 non-carriers) revealed that PCa with germline BRCA1/2 mutations was more frequently associated with ISUP > 4, T3/T4 stage, nodal involvement, and metastases at diagnosis than PCa in non-carriers (E. Castro et al., 2013). A retrospective analysis was conducted on a cohort comprising 313 individuals who succumbed to PCa and 486 patients diagnosed with low-risk localized PCa (Na et al., 2017). The combined carrier rate of BRCA1/2 and ATM mutations was significantly higher in lethal PCa patients (6.07%) compared to localized PCa patients (1.44%).

3.3 Prostate Anatomy

The prostate is a small, walnut-shaped gland that is a part of the male reproductive system. It is located just below the bladder and in front of the rectum. The prostate surrounds the urethra, which is the tube that carries urine from the bladder and semen from the reproductive system out through the penis.

Here's a detailed breakdown of the anatomy of the prostate (see Figure 1):

1. **Lobes:** The prostate gland is divided into several lobes, typically referred to as anterior, posterior, lateral, and medial lobes. These divisions help in describing the location of various structures within the gland.

2. **Capsule:** The prostate is enclosed in a dense outer layer called the prostatic capsule. This capsule is important for maintaining the integrity and shape of the gland.
3. **Zones:** The prostate is further divided into zones based on its anatomy, which helps in understanding the distribution of various structures and potential areas of concern during medical examinations.
 - **Peripheral Zone:** This is the outermost region and constitutes about 70-80% of the gland. It is the most common location for PCa
 - **Central Zone:** This zone surrounds the ejaculatory ducts and is responsible for about 20% of ejaculatory fluid. It is less commonly affected by PCa.
 - **Transition Zone:** This is the innermost region surrounding the urethra. It is the area that enlarges with age, leading to conditions like benign prostatic hyperplasia (BPH), which can cause urinary symptoms.
4. **Ductal System:** The prostate gland has a complex ductal system that produces prostatic fluid, a major component of semen. The ducts converge into the prostatic urethra, and during ejaculation, the muscles of the prostate help propel the prostatic fluid into the urethra.
5. **Vasculature and Nerves:** The prostate has an extensive network of blood vessels and nerves. Blood supply comes from branches of the internal iliac artery, and nerve fibers control the gland's functions, including its role in ejaculation.
6. **Seminal Vesicles:** While not part of the prostate itself, the seminal vesicles are adjacent structures that contribute seminal fluid to semen. The ducts from the seminal vesicles join the duct from the prostate to form the ejaculatory ducts, which empty into the urethra

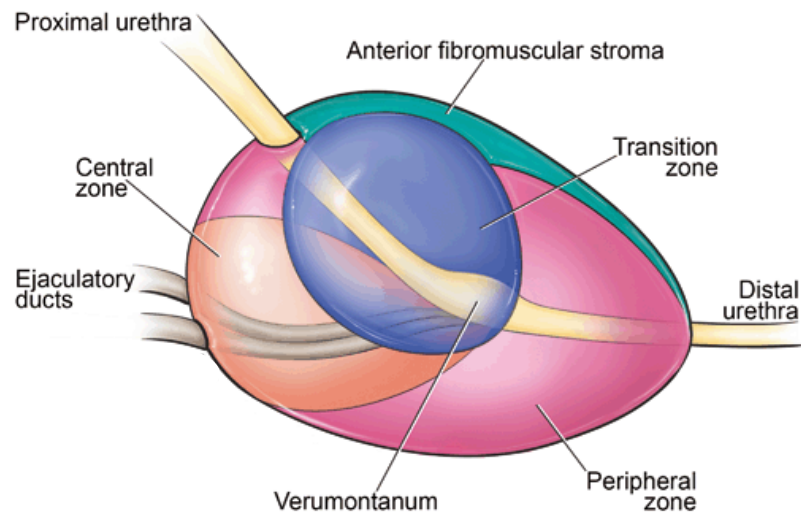


Figure 2. Prostate Anatomy and relations of different glandular zones. *Peripheral Zone: The peripheral zone is the largest and most accessible region of the prostate. It surrounds the distal urethra and is located at the back of the gland, adjacent to the rectum. This zone is where the majority of PCa originate, making it a primary focus for diagnostic evaluation and treatment. Transition Zone: The transition zone lies centrally within the prostate gland and surrounds the proximal urethra. It is characterized by the presence of glandular tissue and is responsible for producing prostatic fluid that contributes to semen. Benign prostatic hyperplasia (BPH), a non-cancerous enlargement of the prostate, typically originates in the transition zone. Central Zone: The central zone is situated between the transition zone and the peripheral zone. It accounts for a smaller portion of the prostate gland and primarily contains ejaculatory ducts. Unlike the transition zone, the central zone is less commonly affected by PCa or BPH. Anterior Fibromuscular Stroma: The anterior fibromuscular stroma is a non-glandular region located at the front of the prostate gland, anterior to the urethra. It consists mainly of fibrous and muscular tissue and serves a supportive role in maintaining the structural integrity of the prostate. Adapted from (Fine & Reuter, 2012)*

3.4 Prostatic Carcinoma Histotypes

Approximately 85% of prostate tumors are situated in the peripheral region of the gland, while the remainder are predominantly found in the transition zone (i.e., around the urethra or anteriorly) (Byar & Mostofi, 1972b; Epstein et al., 1994). PCa is classified as multifocal in over 85% of cases (Byar & Mostofi, 1972a). Interestingly, tumors initially appearing unilateral during digital rectal examination are bilateral in around 70% of cases upon final pathological examination. However, in many multifocal cases, the additional tumors are small, low-grade, and clinically insignificant.

Histologically, over 95% of PCa are adenocarcinomas. Transitional cell carcinomas account for 90% of the remaining 5%, with the remainder being neuroendocrine ("small cell") carcinomas or sarcomas. Adenocarcinomas typically exhibit hyperchromatic,

enlarged nuclei with prominent nucleoli. The diagnosis of adenocarcinoma primarily relies on architectural characteristics, with neoplastic glands being smaller and lacking branching compared to benign glands. Mucinous adenocarcinoma is a morphologic variant known for its aggressive behavior (Sciarra et al., 2011).

Primary transitional cell carcinoma, comprising 1% to 4% of all prostate carcinomas (Sawczuk et al., 1985), tends to infiltrate the bladder neck and surrounding tissues, resulting in locally advanced disease at diagnosis in over 50% of patients. Additionally, 20% of individuals with primary transitional cell carcinoma present with distant metastases, most commonly in the bone, lung, or liver. Survival is heavily influenced by the stage at presentation, with localized disease having better long-term outcomes compared to locally invasive disease.

Transitional cell carcinoma of the prostate is more common in patients with a history of flat transitional cell carcinoma in situ of the bladder, often after intravesical topical chemotherapy. (Arista-Nasr et al., 2016; H. Matzkin, M. S. Soloway, 1992; Mahadevia et al., 1986; Schellhammer et al., 1977; Wood et al., 1989).

Neuroendocrine carcinomas, also known as small cell carcinomas, resemble those found in the lung and are associated with poor survival (Têtu et al., 1987). Pure primary squamous carcinoma (Parwani et al., 2004) is rare and has a poor prognosis, while prostatic sarcomas are even rarer (Sexton et al., 2001). Hematological malignancies account for a very small percentage of prostatic tumors.

3.5 Grading of Prostatic Adenocarcinoma

Different grading systems have been proposed to evaluate adenocarcinoma, but the most widely accepted of all is the one introduced by Donald F. Gleason in 1966 (Gleason & Mellinger, 1974). Several current prediction models in PCa incorporate Gleason score (GS) as one of the foremost independent predictors of several endpoints in patients with PCa, such as pathologic stage, lymph node invasion status, and cancer control outcomes (Montironi et al., 2010).

3.5.1 Gleason System

Gleason's grading system is based solely on the architectural pattern of the tumor. Unlike the case of grading in other tumors, cytologic features play no role in grading PCa. This system uses a 5-point scale to characterize the degree of glandular differentiation identified at relatively low magnification. Instead of attributing the carcinoma grade based on the worst characteristics, our approach involves identifying and grading the two most representative areas of the tumor: the primary (most predominant) and secondary (second most prevalent) architectural patterns. These patterns are then assigned a grade on a scale of 1 to 5, with 1 indicating the highest level of differentiation and 5 representing the least differentiated state.

The Gleason score is determined by adding together these two patterns (Montironi et al., 2010). Gleason score ranges from 2, which is representative of a well-differentiated lesion, to 10, which is consistent with a totally undifferentiated tumor. Primary and secondary patterns are given the same grade in case of tumor that presents only one histologic pattern.

Tumors classified as Gleason pattern 1 and pattern 2 are characterized by well-defined nodules comprising uniform, individual, and closely packed medium-sized glands (Figure 2A). On the other hand, Gleason pattern 3 tumors infiltrate the non-neoplastic prostate, displaying noticeable irregularities in gland size and shape, with smaller glands compared to those in Gleason pattern 1 or pattern 2 (Figure 2B). When glands are no longer single and separate as in patterns 1 to 3, they meet the criteria for Gleason pattern 4. In Gleason pattern 4, it is possible to observe large, irregular cribriform glands, contrasting with the smaller, well-defined nodules typical of cribriform Gleason pattern 3 (Figure 2C). Tumors with Gleason pattern 4 have a significantly worse prognosis than tumors with only Gleason pattern 3 (Epstein et al., 1993; McNeal et al., 1990). Lastly, Gleason pattern 5 tumors have little or no differentiation into glands and are composed of solid sheets, cords, single cells, or tumor with central comedonecrosis (Figure 2D).

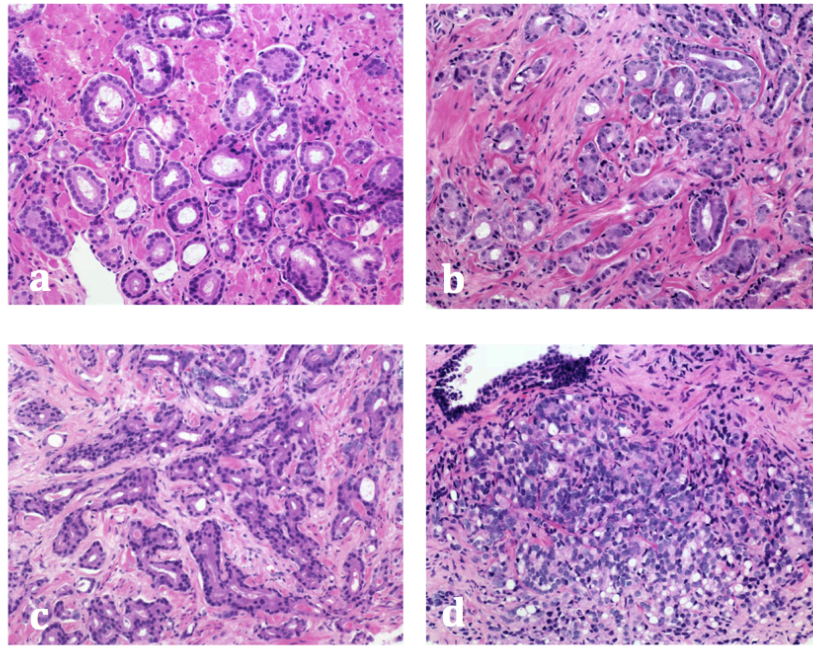


Figure 2. Pathological classification of PCa according to Gleason Score System. A) Gleason Patter 2, B) Gleason pattern 3, C) Gleason pattern 4, D) Gleason pattern 5.

a) Gleason Pattern 2: This pattern consists of well-differentiated glandular structures resembling normal prostate tissue. The tumor cells appear uniform and organized, with minimal disruption of glandular architecture. b) Gleason Pattern 3: This pattern is characterized by moderately differentiated glandular structures with some loss of organization. While the tumor cells retain some resemblance to normal prostate tissue, there is evidence of architectural disarray and cellular proliferation. c) Gleason Pattern 4: In this pattern, the tumor cells become less differentiated, with increased cellular proliferation and architectural disruption. Glandular structures may be irregularly shaped, and there is a higher degree of cellular atypia compared to Gleason pattern 3. d) Gleason Pattern 5: This pattern represents the most aggressive form of PCa, characterized by poorly differentiated glandular structures with minimal resemblance to normal tissue. The tumor cells are highly disorganized, with marked cellular atypia and extensive proliferation. Adpated from (Epstein et al., 1994).

3.5.2 International Society of Urological Pathology (ISUP) Grading System

The ISUP grading system, introduced in 2013, builds upon the modified Gleason system and categorizes tumors into 5 distinct prognostic grade groups. Grade group 1, representing the lowest grade tumor, offers an excellent prognosis according to a comprehensive multi-institutional study, with no risk of lymph node metastases (Ross et al., 2012b). Patients diagnosed with a grade group 1 tumor on biopsy can be reassured, often eligible for active surveillance. However, continued monitoring is essential, as approximately 20% of cases may harbor higher-grade cancer not sampled during biopsy (Epstein et al., 2012). Determining candidacy for surveillance involves a nuanced

evaluation, considering various clinical factors alongside biopsy grade and serum PSA levels. Grade group 2, indicating a slightly higher risk than grade 1, still boasts a very favorable prognosis with infrequent metastases. Conversely, grade group 3 presents a notably worse outlook compared to grade 2, akin to Gleason score 7's combination of 3+4 and 4+3 patterns.

Although grade group 4 falls short of the highest grade designation, it significantly outperforms grade group 5, which corresponds to Gleason scores 9 to 10. Notably, grade group 5 simplifies distinctions between Gleason scores 4+5, 5+4, and 5+5, similar to how grade group 1 renders differences between Gleason scores 2+2, 2+3, 3+2, and 3+3 irrelevant.

<p>Grade Group 1 (Gleason score ≤ 6) – Only individual discrete well-formed glands</p> <p>Grade Group 2 (Gleason score $3+4 = 7$) – Predominantly well-formed glands with lesser component of poorly- formed/fused/cribriform glands</p> <p>Grade Group 3 (Gleason score $4+3 = 7$) – Predominantly poorly-formed/fused/cribriform glands with lesser component of well-formed glands[†]</p> <p>Grade Group 4 (Gleason score $4+4 = 8$; $3+5 = 8$; $5+3 = 8$) Only poorly-formed/fused/cribriform glands <i>or</i> Predominantly well-formed glands and lesser component lacking glands^{††} <i>or</i> Predominantly lacking glands and lesser component of well-formed glands^{††}</p> <p>Grade Group 5 (Gleason scores 9-10) – Lacks gland formation (or with necrosis) with or w/o poorly formed/fused/cribriform glands[†]</p> <hr/> <p>[†]For cases with > 95% poorly-formed/fused/cribriform glands or lack of glands on a core or at RP, the component of < 5% well-formed glands is not factored into the grade.</p> <p>^{††}Poorly-formed/fused/cribriform glands can be a more minor component.</p>
--

Table 1. Histological definition of ISUP Grading System. *Grade Groups: The ISUP Grading System categorizes PCa into five Grade Groups, ranging from Grade Group 1 to Grade Group 5. Each Grade Group corresponds to a different level of tumor aggressiveness, with Grade Group 1 representing the least aggressive tumors and Grade Group 5 representing the most aggressive tumors. Gleason Score Correlation: The ISUP Grade Groups are closely aligned with the traditional Gleason score system, which assigns scores based on the architectural patterns observed in PCa tissue. Grade Group 1 corresponds to Gleason score 6 (or less), Grade Group 2 to Gleason score $3+4=7$, Grade Group 3 to Gleason score $4+3=7$, Grade Group 4 to Gleason score 8, and Grade Group 5 to Gleason scores 9-10. Adapted from (Epstein et al., 2015)*

3.5 Risk Group Classification

The European association of Urology (EAU) risk group classification, derived from D'Amico's system for categorizing PCa, integrates clinical information regarding tumor extent, PSA, and pathology (Table 2). Acknowledging the varied clinical characteristics within the intermediate-risk group, there is a clear call for a refined stratification system to better guide the management of these patients (Zumsteg et al., 2017). Notably, the National Cancer Center Network (NCCN) Guidelines go a step further by subdividing intermediate-risk disease into favorable intermediate-risk and unfavorable intermediate-risk categories. Unfavorable features encompass ISUP grade 3, > 50% positive biopsy cores, and/or a presence of at least two intermediate-risk factors (Schaeffer et al., 2023). Despite these efforts, the optimal stratification and treatment approach for this subgroup remain contentious.

Definition			
Low-risk	Intermediate-risk	High-risk	
PSA < 10 ng/mL and GS < 7 (ISUP grade 1) and cT1-2a*	PSA 10–20 ng/mL or GS 7 (ISUP grade 2/3) or cT2b*	PSA > 20 ng/mL or GS > 7 (ISUP grade 4/5) or cT2c*	any PSA any GS (any ISUP grade) cT3-4* or cN+**
Localised			Locally advanced

GS = Gleason score; ISUP = International Society for Urological Pathology; PSA = prostate-specific antigen.

* Based on digital rectal examination.

** Based on CT/bone scan.

Table 2: European Association of Urology (EAU) risk groups for localized and advanced disease. *Localized Disease: Low-Risk Group: This group includes patients with tumors that are confined to the prostate gland, have a low Gleason score (usually 6 or lower), and have low PSA levels (typically less than 10 ng/mL). These tumors are considered low risk for progression and are often managed with active surveillance or focal therapy. Intermediate-Risk Group: Patients in this group have tumors that are slightly more aggressive, with a higher Gleason score (usually 7) and/or higher PSA levels (between 10 and 20 ng/mL). While these tumors have a higher risk of progression than low-risk tumors, they are still confined to the prostate gland and may be treated with radical prostatectomy (RP), radiation therapy, or active surveillance depending on individual factors. High-Risk Group: This group includes patients with tumors that have a high Gleason score (usually 8-10) and/or PSA levels above 20 ng/mL. These tumors are more likely to spread beyond the prostate gland and require more aggressive treatment approaches such as RP combined with adjuvant therapy, radiation therapy with hormone therapy, or systemic therapy. Advanced Disease: Metastatic Hormone-Sensitive Disease: Patients with metastatic PCa that is still responsive to hormone therapy (androgen deprivation therapy) fall into this category. Treatment options may include hormone therapy alone or in combination with chemotherapy, targeted therapy, or immunotherapy. Metastatic Castration-Resistant Disease: This group includes patients with metastatic PCa that has progressed despite hormone therapy. Treatment options may include novel hormonal therapies, chemotherapy, targeted therapy, immunotherapy, or radionuclide therapy.*

3.5.1 Clinically Significant Prostate Cancer

The term "clinically significant" is frequently employed to distinguish PCa variants that pose a risk of morbidity or mortality in a particular patient from those that do not. This differentiation holds crucial significance, especially considering the prevalence of insignificant PCa that poses no harm (Bell et al., 2015). Failing to make this crucial distinction puts such cancers at risk of being overly treated, potentially subjecting patients to unnecessary side effects. The excessive treatment of insignificant PCas has been criticized as a major downside of PSA testing and early detection (Moyer & U.S. Preventive Services Task Force, 2012). While pathological factors are often utilized to delineate between significant and insignificant PCa, determining significance involves a delicate balance between tumor characteristics and patient-specific factors. Generally, high-risk PCa is deemed significant in most cases, except when life expectancy is limited, whereas low-risk PCa is considered insignificant in nearly all instances. From a pathological standpoint, large-scale studies of RP specimens with only ISUP grade 1 disease have shown rare occurrences of extraprostatic extension (EPE) and biochemical recurrence (3.5%), with no instances of seminal vesicle (SV) invasion or lymph node (LN) metastasis (Anderson et al., 2017; Ross et al., 2012a). It's important to note that these studies demonstrating the absence of metastasis were conducted on RP specimens; biopsies showing ISUP grade 1 are often linked with a minimal risk of metastasis and disease-specific mortality, potentially because they might not capture a higher-grade component.

Modifications in PCa grading, MRI techniques, and targeted biopsies over the past decade have resulted in a grade shift. For example, the introduction of the ISUP 2005 criteria led to 20% of pre-ISUP 2005 GS 6 tumors being upgraded to GS 7 or higher. This historical context must be considered when interpreting older studies (Zareba et al., 2009). While current standard practices such as MRI-targeted and template biopsies have reduced diagnostic inaccuracies (Goel et al., 2020), sampling errors may still occur, potentially missing higher-grade cancer.

An additional challenge in characterizing non-threatening cancer lies in the possibility of ISUP grade 1 progressing to higher grades over time, potentially becoming clinically relevant in subsequent biopsies. Hence, although ISUP grade 1 may initially be deemed clinically inconsequential, it's essential to take into account factors such as age,

pre-biopsy imaging, and the adequacy of core sampling. When combined with low-risk clinical factors, ISUP grade 1 represents low-risk PCa, with active surveillance or watchful waiting being the preferred management options (Preisser et al., 2020). Nevertheless, designating ISUP grade 1 as non-significant cancer does not signify it should be dismissed; instead, it warrants careful monitoring.

Epidemiological studies and postmortem analyses indicate that some ISUP grade 2 prostate cancers might go undetected throughout an individual's lifetime, posing a risk of overtreatment (Van der Kwast & Roobol, 2013). While deferred treatment may be an option for select patients with intermediate-risk PCa according to current guidelines, clear evidence for appropriate selection criteria is lacking (Overland et al., 2019). Recent studies have presented differing definitions of clinically significant cancer, often using ISUP grade 2 and above or even ISUP grade 3 and above, highlighting the lack of consensus and the evolving nature of its definition (Ahmed et al., 2017). Given the insufficient data linking modern histological grading to concrete clinical endpoints, it's crucial for authors to clearly define what they consider clinically significant PCa and how the disease was diagnosed in their studies.

3.6 Diagnosis and Staging

3.6.1 Clinical Presentation

PCa is rarely symptomatic at early stages, since in most cases the disease arises from the periphery of gland, far from the urethra. Systemic symptoms, such as bone pain, renal failure or anemia, suggest locally advanced or metastatic disease. Direct invasion of anatomical structures around the prostate can lead to different symptoms. Should the cancer grow into the urethra or the bladder neck, the patient may present with obstructive (e.g., hesitancy, reduction in urine stream, intermittency) and irritative symptoms (e.g., frequency, urgency, urge incontinence, nocturia). If the tumor invades the trigone of the bladder, it can lead to ureteral obstruction, which could lead to renal failure if both ureters are involved. Invasion of the ejaculatory ducts can lead to haemospermia and a decrease of ejaculate volume. Another symptom caused by local invasion of nearby structure is erectile dysfunction due to the spread of the cancer outside the prostatic capsule and into

the neurovascular bundles containing the nerves responsible for erection. This however is a rare finding in the PSA era.

When the disease is metastatic, symptoms are a result of the structures involved in the metastatic process. Lesions to the skeleton can cause bone pain due to microfractures or anemia from replacement of the bone marrow. Compression of the lymphatic vessels or of the iliac veins by metastatic pelvic lymph nodes may lead to lower extremity edema. Further rare symptoms of systemic involvement include malignant retroperitoneal fibrosis resulting from dissemination of metastatic cells along the peri-ureteral lymphatics, paraneoplastic syndromes from ectopic hormone synthesis, and disseminated intravascular coagulation (DIC).

Although PCa may present with different symptoms, the vast majority of patients (over 80%) lack symptoms suggestive of malignant disease and are diagnosed with PCa on the basis of an anomalous findings during a digital rectal examination (DRE) and/or an increase in serum PSA levels. The introduction of PSA testing in the late 1980s has led to screening and earlier detection of PCa, therefore reducing the number of patients diagnosed due to symptoms of advanced disease. It is indeed known that the introduction of PSA testing has brought a decline of 50-70% in the incidence of distant stage disease at diagnosis between 1986 and 1999(Chu et al., 2003).

3.6.2 Methods of Diagnosis

The primary diagnostic methods for identifying PCa include digital rectal examination (DRE), measuring serum PSA levels, and transrectal ultrasonography (TRUS). However, the conclusive diagnosis of PCa relies on histological analysis of biopsy or surgical samples. Additionally, histopathological examination plays a critical role in grading the tumor and assessing its extent.

3.6.2.1 Digital Rectal Examination (DRE)

Given that the majority of PCa are situated in the outer regions of the prostate gland, a digital rectal examination (DRE) can identify them once they reach a volume of 0.2 mL or greater. A positive finding during a DRE, characterized by the detection of a palpable nodule, warrants an immediate prostate biopsy. Interestingly, around 18% of PCa cases are discovered solely through a positive DRE, regardless of the PSA level (Richie et al.,

1993). For individuals with a PSA level of up to 2 ng/mL, the positive predictive value of a positive DRE typically ranges between 5% and 30% (Carvalho et al., 1999).

3.6.2.2 Prostate-Specific Antigen (PSA)

PCa detection has been revolutionized by the introduction of serum PSA testing (Stamey et al., 1987). PSA is a serine protease similar to kallikrein, primarily synthesized by the epithelial cells within the prostate gland. However, it's important to note that PSA is specific to the prostate organ rather than indicative of cancer alone. Elevated levels of PSA can occur in benign conditions such as benign prostatic hyperplasia (BPH), prostatitis, and various other non-cancerous conditions. Nonetheless, if we consider PSA as an independent variable, it performs better than DRE or TRUS findings in predicting PCa (Catalona et al., 1994).

There isn't a universally agreed-upon threshold or ceiling for serum PSA levels. PSA is instead viewed as a continuous variable (Table 3), meaning that as the value increases, the likelihood of PCa being present also increases (Thompson et al., 2004). The data in the table emphasizes how even at low levels of serum PSA, there is a considerable number of men harboring PCa. Therefore, when taking into consideration a hypothetical PSA threshold, it is crucial to determine how to avoid detecting insignificant PCa that is unlikely to be life-threatening (Stamey et al., 1993).

PSA level (ng/mL)	Risk of PCa
0-0.5	6.6%
0.6-1	10.1%
1.1-2	17.0%
2.1-3	23.9%
3.1-4	26.9%

Table 3. Rate of Prostate Cancer diagnosed in relation to serum PSA. Analysis performed on 2950 men (Thompson et al., 2004)

In efforts to enhance the accuracy of PSA testing for early PCa detection, various modifications to the PSA test have been proposed. These include measures like PSA density, age-specific reference ranges, and different molecular isoforms of PSA such as cPSA and proPSA. However, their practical utility in routine clinical practice remains somewhat limited at present.

3.6.2.3 Transrectal Ultrasonography and Prostatic Biopsies

The role of Transrectal Ultrasonography (TRUS) in diagnosing PCa is to ensure accurate wide-area sampling of prostate tissue in men at higher risk for harboring PCa based on DRE and PSA. Several studies have confirmed the inability of TRUS to localize early PCa (Ellis et al., 1994; Flanigan et al., 1994; Rifkin et al., 1990). Indeed, the conventional depiction of a hypoechoic region in the peripheral zone of the prostate may not consistently manifest (F. Lee et al., 1989). Conventional gray-scale TRUS lacks sufficient reliability in detecting PCa areas. Hence, it is not advisable to substitute systematic biopsies with targeted biopsies of suspicious regions. Nonetheless, performing additional biopsies of suspect areas may offer some utility. Performing prostate biopsies guided by ultrasound is now considered the standard of care. While transrectal biopsy is the standard approach for most prostate biopsies, certain urologists opt for a perineal approach. Interestingly, the cancer detection rates achieved through perineal prostate biopsies are similar to those obtained via transrectal biopsies (Hara et al., 2008; Takenaka et al., 2008). Decisions regarding prostate biopsies should be guided by PSA levels and/or abnormalities detected during a digital rectal examination (DRE).

3.6.2.4 MRI and MRI-guided Biopsy

The integration of multiparametric magnetic resonance imaging (mpMRI), incorporating T2-weighted imaging along with at least one functional imaging modality (such as DWI, DCE, or H1-spectroscopy), is increasingly utilized in clinical settings. This approach demonstrates high sensitivity in detecting and pinpointing clinically significant prostate cancer (CSPCa), which encompasses cancers graded ISUP grade ≥ 2 . Several studies were performed with the aim of evaluating the benefits of MRI-target

biopsy (TBx) compared to systematic biopsy, both in biopsy-naïve patients and in patients undergoing repeat biopsy. Findings from an extensive meta-analysis (Drost et al., 2019) reveal that MRI-targeted biopsy (MRI-TBx) exhibits superior performance over systematic biopsy in identifying CSPCa among individuals with a history of negative systematic biopsy. However, this advantage is not observed in men undergoing biopsy for the first time. Limiting the analysis to individuals who have not undergone biopsy previously, three randomized trials conducted across multiple centers are under scrutiny: the PRECISION trial (Taneja, 2018), MRI FIRST trial (Rouvière et al., 2019) and 4M (Met Prostaat MRI Meer Mans) study (van der Leest et al., 2019). In the initial approach, patients with a positive multiparametric MRI (mpMRI) solely undergo MRI-targeted biopsy (MRI-TBx), while those with negative mpMRI are not subjected to any biopsy procedure. Conversely, the subsequent studies adopted the 'combined pathway', wherein patients with a positive mpMRI undergo both systematic and targeted biopsy, while those with negative mpMRI solely undergo systematic biopsy.

Even though results have shown that MRI-TBx did not significantly outperform systematic biopsies in all series, they nonetheless confirmed its diagnostic value. Moreover, MRI-TBx causes a significant reduction in the overdiagnosis of noncsPCa, as compared to systematic biopsy. Setting a PI-RADS threshold for the biopsy indications allows the evaluation of how many invasive procedures could be avoided with the employment of the MR pathway. Setting a threshold of ≥ 3 could have prevented 30% of all biopsy procedures, albeit at the cost of overlooking 11% of all identified ISUP grade ≥ 2 cancers, according to research by Drost et al. in 2019 (Drost et al., 2019). By increasing the threshold to ≥ 4 , 59% of all biopsy procedures could have been avoided, though this would result in missing 28% of all detected ISUP grade 2 cancers. The misdiagnosis of clinically significant CSPCa often stems from MRI failure, such as when the cancer is not visible or misinterpreted by the reader, or targeting failure, such as when the target is missed or inadequately sampled during MRI-targeted biopsy.

Hence, the implementation of the magnetic resonance (MR) pathway holds promise in potentially minimizing the need for biopsy procedures. This approach aims to decrease the identification of low-grade PCa while concurrently maintaining, or even enhancing, the detection of CS PCa compared to the traditional systematic biopsy method.

3.7 Clinical and Pathological Staging

Information gathered during staging is crucial for determining the scope of the disease. The TNM (tumor, node, metastasis) system, established by the International Union Against Cancer and the American Joint Committee on Cancer (AJCC), stands as the most commonly utilized staging system. This classification method is based on anatomy, wherein the tumor is categorized by the size of the primary lesion (T1-4, with higher numbers denoting larger tumors), the presence of nodal involvement (N0 indicating no involvement and N1 indicating involvement), and the identification of metastatic disease (M0 indicating no metastases and M1 indicating metastases). These various combinations of T, N, and M scores, and tumor histologic grade G, are then grouped into stages typically denoted by numbers I-IV. The 2009 TNM classification for PCa is shown in Table 4.

PCa clinical staging involves using pre-treatment factors to anticipate the actual scope of the disease. The objectives of cancer staging include evaluating prognosis and aiding informed decision-making on treatment choices. An precise evaluation of disease extent holds significant importance for men newly diagnosed with PCa, as the pathological stage serves as a dependable predictor of treatment outcomes for men with cancer localized clinically (Pound et al., 1997). PCa's primary extension evaluation typically involves digital rectal examination (DRE), PSA measurement, and bone scan, complemented by computed tomography (CT) or magnetic resonance imaging (MRI). Additionally, chest X-rays may be employed in certain contexts.

T - Primary tumor		
Tx		Primary tumor cannot be assessed
T0		No evidence of primary tumor
T1		
	T1a	Tumor incidental histological finding in 5% or less of tissue resected
	T1b	Tumor incidental histological finding in more than 5% of tissue resected
	T1c	Tumor identified by needle biopsy (e.g. because of elevated PSA level)
T2		Tumor confined within the prostate ¹
	T2a	Tumor involves one half of one lobe or less

	T2b	Tumor involves more than half of one lobe, but not both lobes
	T2c	Tumor involves both lobes
T3		Tumor extends through the prostatic capsule ²
	T3a	Extracapsular extension (unilateral or bilateral) including microscopic bladder neck involvement
	T3b	Tumor invades seminal vesicle(s)
T4		Tumor is fixed or invades adjacent structures other than seminal vesicles: external sphincter, rectum, levator muscles, and/or pelvic wall
N - Regional lymph nodes³		
NX		Regional lymph nodes cannot be assessed
N0		No regional lymph node metastasis
N1		Regional lymph node metastasis
M - Distant metastasis⁴		
MX		Distant metastasis cannot be assessed
M0		No distant metastasis
M1		Distant metastasis
	M1a	Non-regional lymph node(s)
	M1b	Bone(s)
	M1c	Other site(s)
¹ Tumor found in one or both lobes by needle biopsy, but not palpable or visible by imaging, is classified as T1c.		
² Invasion into the prostatic apex, or into (but not beyond) the prostate capsule, is not classified as pT3, but as pT2.		
³ Metastasis no larger than 0.2 cm can be designated pN.		
⁴ When more than one site of metastasis is present, the most advanced category should be used.		

Table 4. The 2009 TNM (Tumor Node Metastasis) classification for PCa

3.8 Management of prostate cancer patients

To effectively manage patients with PCa, clinicians must consider a multitude of factors to tailor treatment plans that are both risk-adapted and patient-centric. These factors encompass diverse clinical profiles across different disease stages (ranging from localized to metastatic stages, and distinguishing between castration-sensitive and castration-resistant statuses), as well as histopathological and molecular attributes (such as neuroendocrine, cribriform, or intraductal patterns, and DNA repair alterations).

Additionally, patient-specific characteristics, including life expectancy, overall health, familial history, and individual preferences, further influence the decision-making process.

Usually, in instances of localized non-metastatic disease (cT1–2 cN0 M0), patients have the option of active monitoring or local intervention such as radical prostatectomy (RP) or radiotherapy. Sometimes, hormonal therapy may also be administered. The decision on treatment is guided by the likelihood of biochemical relapse (BCR), which is assessed based on factors like initial PSA level, Gleason score, or more specifically, ISUP grade, and clinical T stage. As defined before, men affected by PCa are categorized into low-risk, intermediate-risk, or high-risk groups, each associated with corresponding 5-year BCR rates exceeding 25%, falling within the range of 25–50%, and surpassing 50%, respectively (D’Amico et al., 1998)

The intermediate-risk category encompasses a wide range of patients with varying prognoses. Further stratification into low intermediate (ISUP grade 2) and high intermediate (ISUP grade 3) risk groups allows for a more refined and accurate assessment of risk (Epstein et al., 2016; Kane et al., 2017).

For cases of locally advanced PCa (classified as cT3–4) and/or the presence of metastases in pelvic lymph nodes (N1), treatment strategies often involve a combination of the aforementioned options utilizing multimodal approaches.

In the past decade, there have been significant advancements in the treatment approach for metastatic PCa. Current guidelines recommend initiating androgen deprivation therapy (ADT) using luteinizing hormone-releasing hormone (LHRH) analogues for mCSPC until disease progression. Subsequently, for metastatic castration-resistant prostate cancer (mCRPC), the treatment regimen typically involves the addition of docetaxel and prednisolone alongside continued ADT (Tannock et al., 2004). Since that time, several novel classes of medications have been introduced, such as next-generation androgen receptor (AR) signaling inhibitors (ARSIs) like abiraterone acetate, enzalutamide, apalutamide, and darolutamide, as well as radionuclides like radium-223, chemotherapy/taxanes, and poly(ADP-ribose) polymerase inhibitors (PARPi). These advancements continuously reshape the treatment paradigm, with their utilization transitioning from standalone therapies to combination regimens and from late-stage

castration-resistant prostate cancer (CRPC) to earlier castration-sensitive prostate cancer (CSPC) treatment scenarios (Gillesen et al., 2022).

Reducing the production of gonadal androgens to levels akin to castration triggers cell death in PCa and results in a temporary remission of symptoms. This is evidenced by a decrease in PSA levels and/or a shrinkage of tumors on radiographic scans in most patients with metastatic castration-sensitive prostate cancer (CSPC). Standard androgen deprivation therapy (ADT) involves the use of luteinizing hormone-releasing hormone (LHRH) analogs, including LHRH agonists such as goserelin, leuprorelin, and buserelin, as well as LHRH antagonists like degarelix. Additionally, first-generation androgen receptor signaling inhibitors (ARSIs) such as bicalutamide and flutamide are utilized. LHRH agonists initially activate the LHRH receptor in the pituitary gland, leading to a temporary increase in luteinizing hormone (LH) release, followed by its suppression (Schally et al., 2017). Conversely, LHRH antagonists prevent LHRH from binding to its pituitary receptor, directly inhibiting LH secretion. The resultant decrease in LH halts testicular testosterone production, achieving medical castration. In patients with metastases, initiating LHRH agonist treatment can induce tumor flare, causing a temporary exacerbation of cancer-related symptoms (Vis et al., 2015).

The significant involvement of continuous AR signaling in advancing the progression of CRPC, even in the presence of low testosterone levels post-castration, has led to the development of innovative agents like C17,20-lyase (CYP17A1) inhibitors. These compounds specifically target the synthesis of androgenic steroids, addressing the acquired capability to convert precursor steroids into testosterone (Attard et al., 2005).

CYP17A1 is present in the testes, adrenal glands, and prostate tissue, where it facilitates the conversion of glucocorticoids and cholesterol into DHT. Abiraterone acetate acts on the androgen signaling pathway by inhibiting both CYP17A1-mediated androgen synthesis and directly blocking AR activity (Z. Li et al., 2015).

Abiraterone, when combined with low-dose prednisolone, is employed to counteract the potential mineralocorticoid excess induced by abiraterone treatment. Prednisolone itself possesses some limited antiproliferative effects on PCa cells. On the other hand, the next-generation ARSIs like enzalutamide, darolutamide, and apalutamide operate by directly impeding AR activation. Unlike first-generation AR blockers such as bicalutamide, these

newer ARSIs not only block AR nuclear translocation but also inhibit AR transcription factor activity, enhancing their therapeutic efficacy (Schalken & Fitzpatrick, 2016).

3.9 Tumor Microenvironment (TME) of Prostate cancer

PCa is often considered a "cold tumor" due to its characteristic lack of immune cell infiltration within the tumor microenvironment. Unlike "hot tumors," which have high levels of immune cell infiltration and are more responsive to immunotherapy, cold tumors like PCa typically exhibit minimal immune activity. This immune evasion is thought to contribute to the cancer's ability to proliferate and resist immune-mediated destruction. PCa's classification as a "cold tumor" stems from several factors related to its unique biology and immune microenvironment (Figure 3).

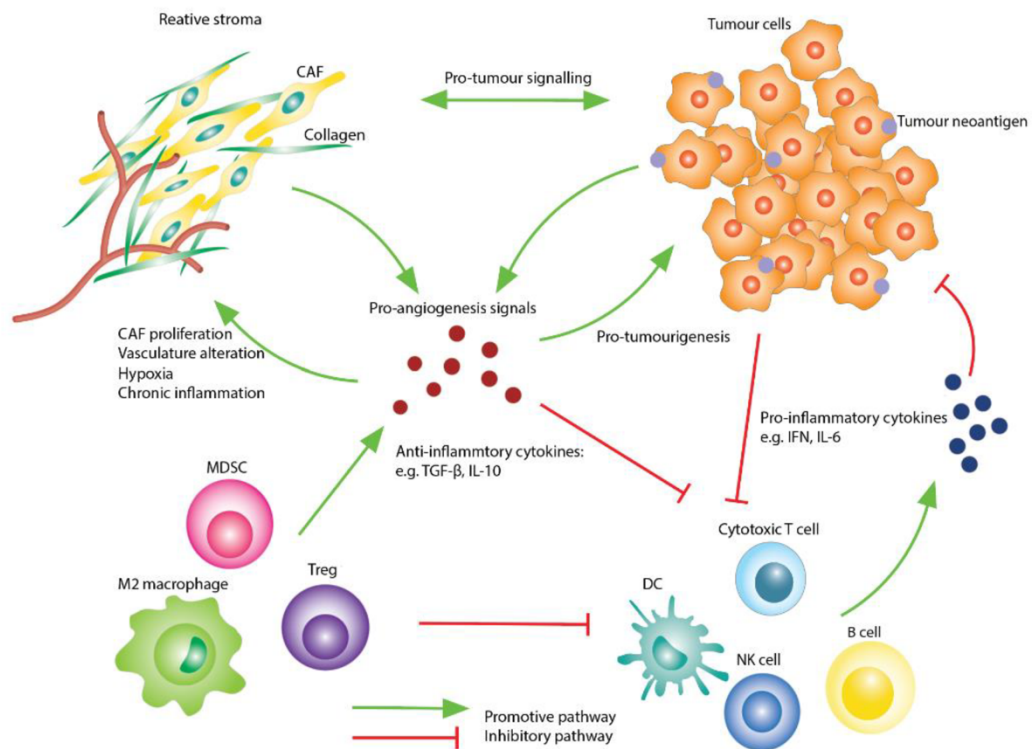


Figure 3. The Tumor Immune Microenvironment (TME) in Prostate Cancer. TME comprises stromal elements, tumor cells, and various immune cell populations. Interactions between stromal components and tumor cells foster a hypoxic and pro-tumor milieu through cytokine secretion and pro-inflammatory signaling. As immune cells infiltrate the tumor microenvironment, immunosuppressive cell types such as regulatory T cells (Tregs), myeloid-derived suppressor cells (MDSCs), and M2 macrophages inhibit the anti-tumor activity of dendritic cells (DCs), cytotoxic T cells, natural killer (NK) cells, and B cells, collectively fostering an immunosuppressive milieu. Figure adapted from (Zhang et al., 2022).

3.9.1 Low Mutational Burden and Genomic alterations

PCa frequently exhibits intricate and severe structural rearrangements in DNA, leading to the loss of tumor suppressor genes, amplifications, changes in copy numbers, translocations, and the formation of gene fusions. These events contribute to the destabilization of the genome (Barbieri & Rubin, 2015).

The emergence of gene fusions such as TMPRSS2-ERG plays a significant role in the initiation and advancement of PCa. These gene fusions are typically classified into two groups: those within the ETS gene family, which account for approximately 50% of fusions linked to PCa, and non-ETS fusions. Although less common, non-ETS gene fusions can play pivotal roles in driving tumorigenesis. The structural rearrangements underlying these fusions often stem from genomic instability triggered by transcription, particularly androgen-induced transcription, which is associated with ETS fusion and predisposition to TMPRSS2-ERG fusion. TMPRSS2-ERG fusion is often linked to poorer clinical outcomes, yet further investigation is needed to fully understand the biological mechanisms driving the adverse effects of structural rearrangements on patient outcomes (Barbieri & Rubin, 2015). In PCa, genomic rearrangements also lead to the amplification of oncogenes such as MYC and AR, as well as the deletion of tumor suppressor genes including PTEN, RB1, TP53, and NKX3.1.

Mutations in these genes are associated with unfavorable traits in both hormone-sensitive and hormone-resistant prostate cancer (PCa). Concurrent loss of PTEN, RB1, and TP53 results in genetic instability, facilitating the transition of castration-resistant prostate cancer (CRPC) into a more aggressive subtype known as neuroendocrine PCa. Co-occurring mutations in PTEN, RB1, and TP53 promote lineage plasticity, enabling cancer cells to transition into diverse cell types, potentially driving therapy resistance and metastasis of PCa to distant locations. In vivo studies have elucidated the critical role of intact PTEN, TP53, and RB1 function as genetic determinants influencing treatment resistance and cancer metastasis. Simultaneous inactivation of PTEN/TP53, PTEN/RB1, or PTEN/RB1/TP53 leads to the development of prostate tumors with molecular characteristics associated with aggressive phenotypes like those seen in advanced mCRPC in humans. Additionally, these studies underscore the importance of histone-modifying enzymes such as EZH2, DOT1L, DNMT1, and DNMT3A in regulating the epigenetic control of target genes, as well as the significance of SOX2, a key driver of

lineage plasticity and stem cell-like properties (Ku et al., 2017; Mu et al., 2017; Qu et al., 2013).

Genetic variations in genes related to DNA damage and repair (DDR), both in germline and somatic contexts, have been associated with Prostate Cancer (PCa), contributing to alterations in DNA (Mateo et al., 2017). Abnormalities in DDR genes, specifically BRCA1 and BRCA2, are prevalent in both localized and Castration-Resistant Prostate Cancer (CRPC) (Venkitaraman, 2002).

DDR, functioning as tumor suppressors, play crucial roles in DNA repair processes, such as homologous recombination and nonhomologous end-joining pathways. Mutations in mismatch repair genes, particularly MutS homolog 2 and 6 (MSH2 and MSH6), have also been linked to PCa (Dowty et al., 2013). Disruptions in the DDR pathway result in a phenotype deficient in DNA repair, increasing susceptibility to aggressive disease. While DDR defects are observed in localized primary PCa, the frequencies of alterations in DDR genes are higher in metastatic CRPC. Targeting PCa with DDR defects and a lethal phenotype can be achieved using Poly (ADP-ribose) polymerase (PARP) inhibitors (Mateo et al., 2020).

DDR pathway defects lead to the accumulation of neoantigens, potentially triggering a more robust response to Checkpoint Inhibitors (CPIs). Therefore, a combination therapy involving PARP inhibitors and immune CPIs shows promise for enhanced therapeutic responses. Additionally, preclinical models suggest that significant DNA damage activates stimulator of interferon genes, releasing type I interferons and initiating a T-cell response against immunogenic tumors (Crisuolo et al., 2019).

Despite the interesting data, targeting DDR genes in primary PCa tumors poses challenges due to their limited detection rates and the intricate molecular mechanisms governing their biology.

Despite its low mutation burden, PCa is prone to genomic instabilities such as chromothripsis and kataegis. Chromothripsis manifests as abnormal breakages and rearrangements of chromosomal fragments within cancer genomes, often coinciding with kataegis, where numerous mutations cluster within a confined region of the genome. These mutations primarily involve dinucleotide substitutions catalyzed by the APOBEC3A/B family of enzymes. Several cellular dysregulations contribute to the occurrence of chromothripsis and kataegis, including P53 loss, aberrant cell cycle

progression, failure of DNA repair mechanisms, and telomere shortening and fusion (E. Wang, 2013)

Approximately 40% of men with PCa display extensive chromothripsis and kataegis in their genome (Alexandrov et al., 2013; Kovtun et al., 2015). Some types of PCa, such as those involving the TMRSS2 gene (ETS+ tumors), exhibit a phenomenon known as "chromoplexy." Unlike chromothripsis, where genomic rearrangements occur primarily in 1 or 2 chromosomes, chromoplexy involves a series of intrachromosomal gene rearrangements spanning multiple chromosomes. Bioinformatic analysis indicates that chromoplexy simultaneously disrupts the transcription of important genes for survival, and giving rise to fusion events that promote tumor growth. It is hypothesized that chromothripsis and chromoplexy in PCa cells represent a single clonal event occurring during tumor initiation rather than tumor promotion (Baca et al., 2013; Kass et al., 2016). In contrast, kataegis is believed to represent the emergence of distinct clonal subsets within a clone, each containing regions of hypermutations. These mutations may enable particular clones to proliferate during advanced stages of cancer development, thereby heightening the likelihood of relapse in aggressive disease (Espiritu et al., 2018).

3.9.2 Adaptive immune cells

The involvement of tumor-infiltrating lymphocytes (TILs) in PCa progression is not fully understood, as they impact the disease through various mechanisms that remain to be clearly defined.

T lymphocytes, encompassing both CD4+ and CD8+ subsets, are integral constituents of the adaptive immune system and are observed to infiltrate the prostate glands.

CD8+ T cells

The prognostic significance of CD8+ TIL infiltration in PCa is a topic of debate, with conflicting observations. For instance, Ness et al. found that a high density of CD8+ TILs in primary PCa specimens is independently associated with a negative prognosis for biochemical failure-free survival. Similarly, high levels of CD8+ TILs and PD-L1 expression by tumor cells have been linked to an increased risk of clinical progression in men with node-positive PCa (Petitprez et al., 2019b).

On the contrary, contrasting findings indicate that a heightened presence of CD8+ Tumor-Infiltrating Lymphocytes (TILs) post-surgery is independently associated with enhanced survival in the majority of high-risk Prostate Cancer (PCa) patients. Other studies have noted that heightened PD-L1 levels and diminished density of CD8+ TILs serve as indicators for unfavorable prognoses, alongside potential markers for biochemical and metastatic relapse in PCa (Cecile Vicier, 2019; Yuanquan Yang, 2018). Consequently, factors beyond CD8+ TILs seem to play a pivotal role in prognosis. Indeed, the efficacy of CD8+ effector T cells in facilitating tumor regression largely depends on their cytokine secretion profile and self-renewal capabilities. Recent evidence suggests that the Tumor Microenvironment (TME) can trigger the emergence of dysfunctional CD8+ T cells with limited cytotoxic functionality. Furthermore, various phenotypes of CD8+ T cells, including senescent, regulatory, and dysfunctional stem-cell-like memory cells, may coexist, lacking anti-tumor activity (Tsaur et al., 2021).

CD4 T cells

Among TILs, a significant contributor to cancer progression is the T-regulatory cell (Treg). These CD4+ T cells play a crucial role by inhibiting the activity of T effector cells. The definition of Tregs based on cell surface markers is continuously evolving due to the diverse nature of the Treg population. This ongoing refinement of the Treg phenotype presents a challenge in interpreting scientific literature, requiring a discernment of how Tregs are characterized in each publication. Typically, Tregs are associated with dampening anti-tumor responses rather than directly stimulating the growth of tumor cells. Supporting the significance of Tregs in PCa, studies have shown an increase in Tregs (CD4+CD25+) with immunosuppressive function in PCa tissues compared to non-cancerous prostate tissues (Sfanos et al., 2008). Furthermore, in efforts to characterize the phenotype of TILs, a research team conducted multiple prostate biopsies and utilized flow cytometry to determine the phenotypes of the collected cells.

Their research uncovered that within the TME, CD4+ T cells displayed a propensity towards Treg (FoxP3) and T helper 17 (Th17) types, rather than the Th2 profile. This trend was also evident in peripheral blood samples. Tregs (CD4+CD25+) were notably higher in peripheral blood of PCa patients compared to healthy individuals (Sfanos et al., 2008). Also CD8+ FoxP3+ cells (defined as Tregs) predominantly hindered the

proliferation of naive T cells through a mechanism reliant on direct cell-to-cell interaction (Sfanos et al., 2008). Other researchers conducted an assessment on the levels of Tregs (CD4+CD25 FoxP3+) in blood samples of healthy individuals and PCa patients using flow cytometry. Their findings revealed that while there were no notable differences in the quantity of Tregs in the blood samples, Tregs isolated from PCa patients exhibited significantly heightened suppressive activity compared to those from healthy donors (Yokokawa et al., 2008).

Another subset of CD4+ T cells known as Th17 cells has emerged as a potential influencer of PCa biology and responses to immunotherapy. Th17 cells are effector T cells that produce interleukin-17 (IL-17), a pro-inflammatory cytokine known to recruit and activate granulocytes and monocytes (Rakebrandt et al., 2016). However, the role of Th17 cells in cancer remains contentious, as they have been reported to exhibit both inhibitory and promotional effects on tumor growth. Researchers investigated the levels of Th17 cells and Tregs in the blood of PCa patients who were about to undergo immunotherapy. They found that patients with lower levels of Th17 cells tended to have a longer time before their disease progressed. Those who responded well to the treatment by showing a significant drop in prostate-specific antigen (PSA) had Th17 cell levels similar to healthy people, while those who didn't respond had different Th17 cell levels compared to both responders and healthy individuals (Derhovanessian et al., 2009). They observed an inverse correlation between the frequency of Th17 cells and the time to disease progression. Additionally, patients who responded to immunotherapy with substantial reductions in PSA exhibited a Th17 phenotype similar to that of healthy men, whereas non-responders had significantly different Th17 profiles.

On the other hand, although PCa patients had more Tregs in their blood compared to healthy individuals of the same age, there was no difference between responders and non-responders. These results imply that Th17 cells could predict how well someone responds to whole-cell vaccine treatment. However, whether Th17 cells slow down or speed up PCa growth might depend on the tumor stage (Derhovanessian et al., 2009).

3.9.3 Immune Checkpoint Expression

The expression of PD-L1 has been found to be significantly increased in prostate cancer (PCa) tissues when compared to corresponding normal tissues. A majority of the examined cases displayed moderate to elevated levels of PD-L1 expression. Interestingly, this heightened expression correlated positively with pathological status and AR level in men with aggressive forms of the disease. PD-L1 expression emerged also as an independent factor for biochemical recurrence (BCR) (Gevensleben et al., 2016).

Furthermore, in high-risk prostate cancer patients, PD-L1 was found to be highly expressed, indicating an unfavorable prognosis for those undergoing adjuvant hormonal therapy (H. Li et al., 2019). Tissue microarrays from radical prostatectomy patients were used to investigate the relationship between PD-1/PD-L1 expression and clinicopathologic features. PD-L1 expression was more common in tumor cells from cases with advanced tumors or nodal metastasis, while PD-1 expression in tumor cells did not correlate with tumors (Y. Xu et al., 2021). PD-L1 expression was associated with poorer oncological outcomes and was found higher in cases with high Gleason scores still expressing AR. However, factors such as age, pathological stage, nodal status, and PSA levels did not significantly correlate with PD-L1 expression (Y. Xu et al., 2021).

PD-L1-positive tumors had nearly four times higher risk of distant metastasis compared to PD-L1-negative and that the expression of PD-L1 was associated with an higher frequency of CD8⁺ T cell. Interestingly, PD-L1 expression in tumor cells and a high density of CD8⁺ T cells in tumors were linked to increased risk of clinical progression in men with lymph node-positive PCa (Petitprez et al., 2019b). PD-L1 expression was not confined to cancer cells but also observed in prostate circulating tumor cells in all PCa patients (Schott et al., 2017). Regarding the number of tumors with a positive staining of PD-L1, a study found a positivity in only 7.7% of primary prostate acinar adenocarcinoma cases, while significantly higher proportions were observed in small cell carcinomas of the prostate and mCRPCs (Haffner et al., 2018; Schott et al., 2017).

CTLA-4 serves as a prominent immune checkpoint within PCa. Normally, it's found on activated T cells and regulatory T cells, and its increased presence on exhausted T cells further dampens immune activity. CTLA-4 has a strong affinity for CD80 and CD86, which are molecules involved in activating T cells, and by binding to them, it

prevents T-cell activation (Schildberg et al., 2016) (Seidel et al., 2018). This interaction typically occurs under physiological circumstances. In PCa, cancer cells exploit CTLA-4 to their advantage, leading to a state of anergy. CTLA-4 binding to CD80 or CD86 on DCs inhibits PI3K activation in T cells, disrupting the usual signaling triggered by the T-cell receptor. The inhibition of PI3K reduced several activities and function of T-cells, such as cytokine secretion (e.g. IL-2 and TNF α) (Schildberg et al., 2016)

3.9.4 Immunosuppressive Cell Types

NK cells

As a crucial component of the innate immune system, natural killer (NK) cells play a vital role in immune surveillance, exhibiting cytotoxic activity and cytokine production to combat infections and tumors. Existing evidence suggests a correlation between highly effective NK cells and prolonged castration response, as well as improved prognosis in patients with metastatic PCa (Cortesi et al., 2018).

Cortesi et al. (2018) demonstrated that CD1d-restricted invariant natural killer (iNKT) cells directly interacted with macrophages within the tumor microenvironment (TME). This interaction sustained a proinflammatory M1-like phenotype in macrophages, ultimately inhibiting tumor advancements. Moreover, aggressive human PCa cases exhibited a significant decrease in intratumoral iNKT cells, alongside an increase in M2-like macrophages. These findings underscore the fact that the TME in PCa is partly attributed to immature NK cells with diminished cytolytic function.

This phenomenon might partially contribute to the heightened secretion of TGF- β by prostate cancer (PCa) cells, which could induce a state of tolerance towards natural killer (NK) cells, potentially facilitating disease progression (Pasero et al., 2016).

Numerous mechanisms are employed by cancer cells to evade assaults from NK cells. NKG2D, an activating immunoreceptor belonging to the lectin-like type-2 transmembrane family, is chiefly found on NK cells. The interplay between NKG2D and its ligands acts as a robust trigger for NK cell activation, while also delivering a co-stimulatory cue for the activation of CD8⁺ T cells (Raulet, 2003).

The tumor cells' suppression of NKG2D ligands could potentially result in the tumor evading the immune system. Notably, a previous investigation underscored that prostate cancer (PCa) cells employ the release of NKG2D ligands as a tactic to evade

detection by both NK cells and T cells. Additionally, another research team unveiled that PCa cells control PD-L1/NKG2D ligand levels inversely through the JAK/STAT3 signaling pathway by secreting IL-6. This effectively reduces the vulnerability of tumor cells to the effects of NK cells (L. Xu et al., 2018).

Myeloid-derived suppressor cells (MDSCs)

MDSCs, acknowledged for their role in promoting tumor growth through immunosuppression, are key players in PCa, contributing significantly to its spread, metastasis, and resistance to therapy. Calcinotto et al demonstrated that MDSCs produce IL-23, initiating the activation of the AR pathway. This cascade promotes the survival and growth of PCa. In clinical observations, increased levels of IL-23 and infiltration of MDSCs in the TME have been noted in patients diagnosed with castration-resistant prostate cancer (CRPC) (Calcinotto et al., 2018). Furthermore, there is additional clinical evidence indicating a connection between MDSCs and the advancement of metastatic disease. Elevated levels of MDSCs have been observed to correspond with more advanced tumor stages and a diminished survival of PCa subjects. The immunosuppressive effects exerted by MDSCs involve diverse mechanisms, such as indirect communication through paracrine and endocrine signaling, along with direct interactions with other cells present in PCa microenvironment. For example, the presence of MDSCs has been linked to heightened levels of IL-6 and IL-8 in individuals with PCa. Significantly, both IL-6 and IL-8 possess the ability to activate multiple oncogenic pathways, thereby fostering the proliferation, invasion, and chemoresistance of prostate cancer cells (Araki et al., 2007; Chi et al., 2014; Nguyen et al., 2014). Additionally, it has been documented that MDSCs release reactive nitrogen species, which lead to the tyrosine nitration of LCK, known as a lymphocyte-specific protein tyrosine kinase. This process culminates in CD4 and CD8 exhaustion attributed to diminished IL-2 production (Feng et al., 2018).

Although these discoveries shed light on certain aspects, there is still a lack of comprehensive understanding regarding the exact molecular mechanisms that drive the recruitment and expansion of MDSCs during prostate carcinogenesis. Consequently, further investigation is necessary to elucidate these processes.

Macrophages

In the context of PCa progression and aggressiveness, Tumor Associated Macrophages (TAMs) play a crucial role as connectors bridging inflammation and immunosuppression.

Various functional phenotypes have been attributed to TAMs, spanning from M1-like macrophages, which are classically activated and possess proinflammatory and antitumor attributes, to M2-like macrophages, characterized by alternative activation and demonstrating anti-inflammatory and protumor traits (Martinez & Gordon, 2014).

TAMs play a crucial role in promoting tumor advancement through diverse pathways, such as aiding tumor cell proliferation, fostering angiogenesis, promoting cell migration, and aiding in evasion of immune detection. Particularly noteworthy is a recent investigation revealing that TAMs facilitate the metastasis of PCa by transmitting CCL2, resulting in the upregulation of CCL22 and CCR4 within PCa cells (Maolake et al., 2017).

The inflammatory TME surrounding PCa cells can trigger an increase in cytokines and chemokines, encouraging the development of an M2-like phenotype. For instance, studies have shown that CXCL2 effectively shifts infiltrating TAMs towards a pro-tumor phenotype, thereby facilitating PCa progression (Di Mitri et al., 2019a).

While the presence of macrophages can exacerbate tumorigenesis, the interaction is complex, suggesting the need for future studies to unravel the reciprocal influence between macrophages and tumor cells for the development of novel therapeutic strategies. A recent finding demonstrated that androgen deprivation therapy (ADT), achieved through MDV3100 or castration treatment, induces the secretion of colony-stimulating factor 1 (CSF1) and other cytokines from tumor cells (Escamilla et al., 2015). As a result, this process encourages the development of a pro-tumorigenic M2 phenotype within TAMs. Consequently, M2-like macrophages release factors such as VEGF-A, MMP-9, and ARG-1, which play a role in resistance to conventional therapy (ADT) and the advancement of cancer. The inhibition of CSF1-CSF1R pathway showed potential for enhancing effectiveness and maintaining a lasting response to hormonal therapy in PCa.

3.9.5 Stromal Influence

The TME comprises fibroblasts, smooth muscle cells, immune cells, cancer cells, and an extracellular matrix composed of collagen, elastin, and other proteins.

Within the prostate, the stromal component is comprised of smooth muscle cells. These cells engage in interactions with the epithelial layer to control the proliferation, and migration of epithelial cells, thereby contributing to the overall maintenance of homeostasis (Karlou et al., 2010).

The dynamic interplay between smooth muscle and epithelial cells is vital for maintaining the structural integrity and optimal function of the prostate gland. However, genetic damage to the epithelium can disrupt signaling within the epithelial cells, affecting the smooth muscle as well. Anomalies in multiple signaling pathways play a role in the development of PCa cancer, disrupting the intricate equilibrium between smooth muscle layers and the epithelial compartment (Cunha et al., 1996). The disturbance caused by this phenomenon results in the loss of cellular differentiation and the unchecked tumor advancement.

Fibroblast growth factors (FGF) orchestrate communication between the prostate epithelium and stroma. The altered expression of FGF-related stromal-epithelial receptors is implicated in the establishment and progression of PCa, leading to enhanced proliferation, inhibited apoptosis, and angiogenesis (Wu et al., 2003). Targeting FGF receptors and their signaling pathways holds promise not only for directly eliminating tumor cells but also for preventing angiogenesis through cytokines like TGF- β , which possesses antiproliferative and pro-apoptotic properties. Traditionally, TGF- β plays a role in inhibiting proliferation, promoting apoptosis, and facilitating prostatic epithelial cell differentiation (Tang et al., 1999). However, despite the presence of high levels of TGF- β in the tumor microenvironment, its inhibitory effects are diminished due to decreased expression of TGF- β receptors and other influencing factors. Notably, TGF- β assumes a tumor-promoting role primarily when interacting with stromal cells (Ao et al., 2006). In cancer-associated stroma, TGF- β plays a crucial role in epithelial differentiation (Massagué et al., 2000).

TGF- β acts as a facilitator of tumor growth by promoting angiogenesis and inhibiting immune surveillance mechanisms. Moreover, it is implicated in conferring

resistance to androgens and plays a role in mediating the spread of cancer to the bone (Zhu et al., 2008).

The efficacy of targeting TGF- β in cancer treatment depends on the particular stage of the disease, considering its notable impact on tumor progression across different stages. Cancer cells, which precede invasive carcinomas, are characterized by a pivotal process wherein cancer cells invade the stroma, altering the TME to support tumor development and advancement. This invasive behavior of tumor cells within the stroma triggers several responses, including the activation of fibroblasts, recruitment of inflammatory cells, alteration of the extracellular matrix (ECM), promotion of angiogenesis, and release of growth factors bound to the ECM (Winkler et al., 2020). As the influence of stromal activity intensifies and the myofibroblast population grows, there is a corresponding rise in the Gleason score, which serves as a critical marker of aggressiveness in PCa.. The stromal reaction serves as a significant indicator of adverse clinicopathological parameters and the likelihood of cancer recurrence (Ayala et al., 2003). Recent research has provided further insights into how a stromogenic environment fuels the progression of PCa (Yanagisawa et al., 2008).

3.10 Immunotherapy in Prostate Cancer

Immunotherapy and precision medicine have increasingly integrated into oncological treatment, ushering in novel therapeutic strategies in recent times. These innovative approaches have demonstrated encouraging results in managing aggressive cancers, potentially leading to prolonged remission for patients. Immunotherapy continues to be a significant aspect of PCa management, presenting an attractive avenue for enhancing disease control. Despite it has demonstrated success in treating other types of cancer, its effectiveness against PCa has yielded varied results.

The approval of the first PCa vaccine in 2010 named Sipuleucel-T offered advanced PCa patients a promising treatment option to enhance disease outcomes. Nevertheless, the efficacy of the prostate vaccine has only resulted in partial improvements in survival rates.

In addressing the inhibitory TME, ongoing immunotherapy investigations focus on addressing T cell infiltration, the mutational burden of PCa cells, and the synergistic effectiveness of treatment (Bilusic et al., 2017).

Notably, within a specific subset of patients characterized by elevated PD-L1 tumor expression, CDK12 mutations, or heightened microsatellite instability (MSI) and mismatch repair deficiency (dMMR), immune checkpoint inhibitors (ICIs) may play a crucial role in eliciting responses to combination therapy.

Currently, there are just three immunotherapy options endorsed by the FDA for men diagnosed with PCa. Sipuleucel-T, a vaccine crafted from stimulated immune cells derived from patients. This vaccine targets the prostatic acid phosphatase (PAP) protein and is specifically approved for a subset of patients with advanced PCa. The remaining two options are immunomodulatory treatments, namely dostarlimab and pembrolizumab. Both of these drugs are immune checkpoint inhibitors designed to act on the PD-1/PD-L1 pathways. These drugs are approved for use in patients with specific genetic characteristics such as microsatellite instability (MSI-H), DNA mismatch repair deficiency (dMMR), or high mutational burden (TMB-H). Significantly, since 2017, the FDA has approved six drugs for the treatment of metastatic castration-resistant prostate cancer (mCRPC), irrespective of tumor histology. These approved medications encompass pembrolizumab designed for patients with dMMR or high MSI, entrectinib and larotrectinib targeting tumors with neurotrophic tyrosine receptor kinase fusions, dostarlimab for tumors exhibiting deficient DNA mismatch repair, and trametinib in combination with dabrafenib indicated for tumors with a specific mutation of BRAF (V600E) (Rehman et al., 2023).

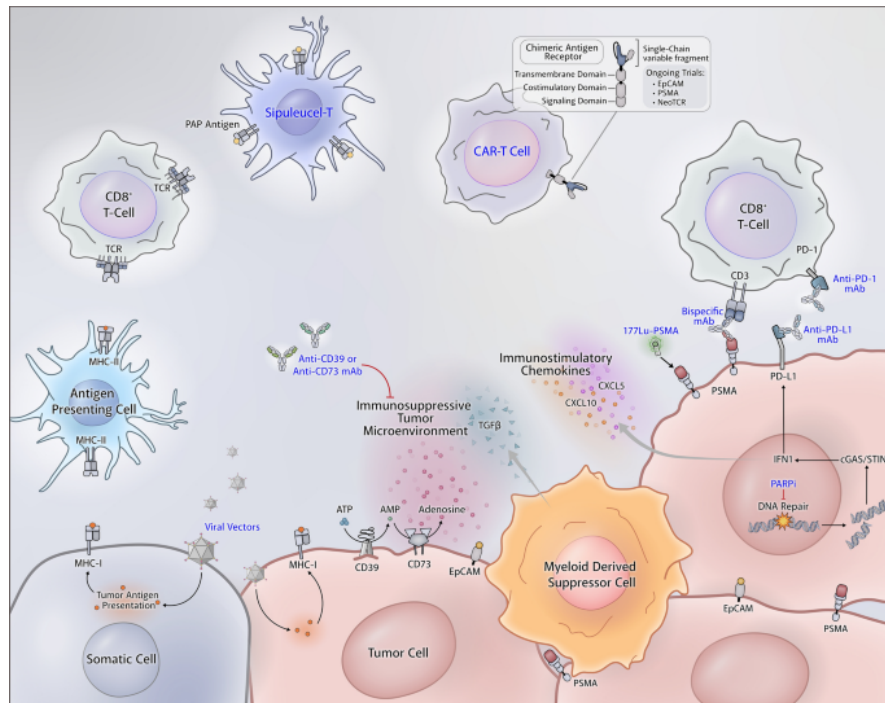


Figure 4. Comprehensive examination of immune system pathways and targets in prostate cancer. Tumor-specific antigens, delivered through viral vectors like PROSTVAC, are presented on major histocompatibility complexes (MHCs), facilitating recognition by immune cells. Additionally, PCa cells often exhibit distinct markers such as PSMA, making them susceptible to targeting by chimeric antigen receptor T cells (CAR-Ts). Custom neoantigens unique to individual patients can also serve as potential targets, with tailored neoantigen T-cell receptors (NeoTCRs) offering a personalized approach. Furthermore, cell-mediated therapies like Sipuleucel-T leverage PCa-specific antigen-presenting cells that showcase prostatic acid phosphatase (PAP), thereby stimulating the immune system's anti-tumor response. However, the efficacy of these immune responses can be hindered by factors like increased levels of extracellular adenosine and myeloid-derived suppressor cells, as well as immune checkpoints such as PD-1/PD-L1. Nevertheless, monoclonal antibodies targeting these checkpoints present promising opportunities for immune modulation. Adpated from (Rathi et al., 2021)

3.10.1 Immune checkpoint inhibitors

Directing attention to the co-inhibitory pathways of T cells, known as T cell checkpoints, triggers an anti-tumor response by rebalancing the inhibition imposed by co-inhibitory molecules such as LAG-3, PD-1, TIM-3, and CTLA-4. This shift creates a pro-inflammatory environment that hinders tumor growth.

Immunotherapy for solid tumors primarily involves the use of inhibitors targeting programmed cell death-1 (PD-1)/programmed cell death ligand-1 (PD-L1) and cytotoxic T lymphocyte antigen-4 (CTLA-4), collectively referred to as immune checkpoint blockade (ICB) (Rebuzzi et al., 2022). Among the monoclonal antibodies commonly employed in ICB, nivolumab blocks PD-1, and ipilimumab targets CTLA-4. Nevertheless, a clinical trial assessing nivolumab in mCRPC patients did not demonstrate significant objective response rates. Subsequent clinical investigations of pembrolizumab, another anti-PD-1 monoclonal antibody, in mCRPC patients proved ineffective, highlighting that the use of PD-1 inhibitors as standalone treatments and relying on PD-L1 expression as a marker for PD-1 blockade therapy sensitivity may be insufficient for advanced PCa treatment (Antonarakis et al., 2020a). A phase II clinical trial combining ipilimumab with radiotherapy in mCRPC patients and a phase III trial involving patients with prior chemotherapy showed no discernible differences in objective response rates between placebo and ipilimumab (Fizazi et al., 2020).

mCRPC patients exhibiting a high intratumoral CD8⁺ T cell density displayed favorable responses to CTLA-4-targeting antibodies, suggesting that augmenting CD8⁺ activation could yield clinical benefits (Subudhi et al., 2020). Remarkably, an extended examination of mCRPC patients who underwent ipilimumab treatment showcased substantially superior overall survival rates in comparison to those in the control cohort. This underscores the enduring advantages of immunotherapy for these individuals. Given the limited effectiveness of single-agent checkpoint inhibition in patients, there's a growing consensus for combination therapies. One notable effort to enhance the benefits of immunotherapy is the CheckMate 650 clinical trial, which explores dual checkpoint blockade. This trial compares two dosing regimens of ipilimumab/nivolumab against single-agent ipilimumab and the standard chemotherapy cabazitaxel in a randomized, controlled trial.

Findings from the study revealed that patients who underwent treatment with a combination of ipilimumab and nivolumab demonstrated the most substantial overall response rate (19.5% compared to 12.2% with cabazitaxel) as well as a higher complete response rate (4.9% compared to 0% with cabazitaxel). Moreover, individuals receiving this combined therapy exhibited an extended duration of radiographic response (6.5

months compared to non-responders), highlighting its considerable clinical efficacy (P. Sharma et al., 2023).

3.10.2 Dendritic cell vaccines: Sipuleucel T

Sipuleucel-T emerges as an exceptional dendritic cell vaccine, distinguished by its fusion of PAP with granulocyte-macrophage colony-stimulating factor. It currently holds the distinction of being the only approved active cellular immunotherapy for mCRPC (Kantoff et al., 2010). Administering Sipuleucel-T to patients pre-prostatectomy has shown to stimulate sustained immune responses involving both T and B cells, leading to reduced PSA levels and enhanced overall survival rates (Fong et al., 2014). Ongoing studies explore various combinations and clinical contexts, including pairing Sipuleucel-T with approved mCRPC medications, antibodies, or radiation therapy. In a recent randomized phase II trial, the combination of Sipuleucel-T with or without interleukin-7 (IL-7), a homeostatic cytokine, was investigated (Pachynski et al., 2021). The findings suggested a notable increase in lymphocyte populations and enhanced immune reactions, coupled with a decrease in PSA levels among patients who received the combination treatment in contrast to those solely administered Sipuleucel-T. This suggests that utilizing combination approaches holds significant promise for enhancing clinical effectiveness in treating mCRPC.

3.10.2 Prostate Specific Membran Antigen (PSMA) CAR T therapy

The prostate, known for its minimal mutational burden, has prompted extensive exploration of PCa antigens such as PSCA, PSMA, and EpCAM for potential application in CAR T therapy (Milowsky et al., 2007). The development of Anti-PSMA CAR T cell therapy builds upon prior monoclonal antibody studies and has progressed into clinical trials. A phase I clinical trial involving an armored PSMA CAR, expressing a dominant-negative receptor for the immunosuppressive cytokine TGF- β , includes 13 patients across four dose levels (Narayan et al., 2022).

Promisingly, the trial has documented significant expansion of T cells, with one participant demonstrating a remarkable decrease of over 98% in PSA levels, while three

others displayed partial responses characterized by more than a 30% reduction in PSA levels. In a distinct phase I clinical investigation targeting PSMA in a cohort of nine patients, three individuals witnessed a decline in PSA levels exceeding 50%, coupled with notable enhancements in PSMA positron emission tomography (PET) imaging. Nevertheless, one participant in this trial encountered a severe grade 5 adverse event linked to hepatic failure and potential macrophage-activation syndrome attributed to the medication (Slovin et al., 2013). Other in vivo study, utilizing a second-generation PSMA-targeting CAR T therapy in combination with chemotherapy, demonstrated the elimination of tumor cells in mice. An ongoing clinical trial explores the integration of anti-PSMA CAR T therapy with PD-1 blockade in treating mCRPC (NCT04768608). This development introduces novel treatment paradigms, positioning CAR T cell therapy as a promising alternative for the management of PCa.

3.10.3 Bi-specific T cell engagement (BiTE)

A different treatment strategy involves using bi-specific T cell engagement (BiTE), which utilizes monoclonal antibodies with dual targeting capabilities (Runcie et al., 2018). One hook is designed to target proteins outside tumor cells, while the second hook is directed at the CD3, a typical T cell receptor. The BiTE construct facilitates the interaction between these two cell types. Currently, acapatamab is undergoing investigation in Phase I trials, demonstrating response rates nearing 33%. This modality is being explored in combination with PD1 blockers and hormone therapy to enhance its efficacy (Giraudet et al., 2021).

Despite its potential benefits, a notable drawback of BiTE therapy is the occurrence of cytokine storm syndrome, presenting a double-edged sword in immunotherapeutic treatment. To address this challenge, novel molecules with reduced affinity for CD3 are being explored as potential solutions to mitigate the cytokine storm among patients (Singh et al., 2021). These advancements aim to strike a balance, optimizing the therapeutic benefits while minimizing adverse events associated with BiTE therapy.

4 AIM OF THE WORK

The primary objective of this project is to elucidate and characterize the immunological factors associated with the aggressiveness of PCa. PCa exhibits a spectrum of clinical phenotypes, ranging from indolent forms that can be managed through active surveillance to aggressive variants with a high risk of mortality. In recent decades, significant progress has been made in uncovering the genomic heterogeneity that underlies these distinct clinical presentations.

Researchers have identified specific molecular subtypes of PCa and exploited their uniqueness to predict clinical outcomes, develop novel biomarkers for diagnosis, and devise innovative treatment strategies. Molecular biomarkers and genomic profiling hold promise for enhancing risk stratification and enabling personalized treatment approaches tailored to individual patients. In addition to genetically defined markers, the role of tumor-infiltrating immune cells such as CD8 and CD4 as crucial prognostic indicators in PCa has been increasingly recognized.

These immune cells play a pivotal role in the tumor microenvironment, influencing the immune landscape within the tumor. Despite extensive research, the biological mechanisms and clinical implications underlying the variable infiltration of immune cells into PCa tumors remain poorly understood.

The primary objectives of this project are as follows:

- To characterize the composition of immune cells in both healthy prostate tissue and tumor samples obtained from patients undergoing radical prostatectomy.
- To analyze immune cell populations in tissue and blood samples collected from PCa patients, with the aim of identifying potential biomarkers and elucidating their clinical relevance.
- To investigate the spatial distribution and genomic features of the immune microenvironment within prostate tumors.

5 RESULTS

5.1 Unveiling Prostate Immune Cell Composition

5.1.1 Patient Cohort and Tissue Retrieval

Understanding the immune infiltrate landscape of the TME is essential in elucidating the mechanisms driving PCa progression, devising effective immunotherapeutic strategies, and finding potential correlations between immunological signatures and features of the prostate tumor. Therefore, in the initial phase of our research, we focused on studying and identifying the key immune cell populations in RP samples.

For that, we analyzed 3 prostate samples (Figure 5 A) from high-risk PCa patients who underwent robotic RP. After the surgical procedure, an immediate histopathological evaluation was performed. Following confirmation of negative surgical margins, two different areas (Tumoral vs. Healthy) of the peripheral zone were manually dissected (Figure 5 B-C). The surgical samples were then processed taking advantage of ad hoc-designed digestion protocol (Vitek et al., 2022) to obtain a single-cell suspension suitable for further analyses. The selected patients were matched for PSA values, age, preoperative clinical characteristics, and pathological grade assessed at RP (Gleason Score 8 or 9). In one out of the three selected patients a localized nodal disease was identified.

A

ID	Age (years)	PSA ng/mL	Gleason Score	pStage	Surgical Margin	LNI
#1	67	12,40	4+4	pT3a	R0	N1
#2	59	9,28	4+5	pT3b	R0	N0
#3	74	7,50	4+4	pT3a	R0	N0

B



C

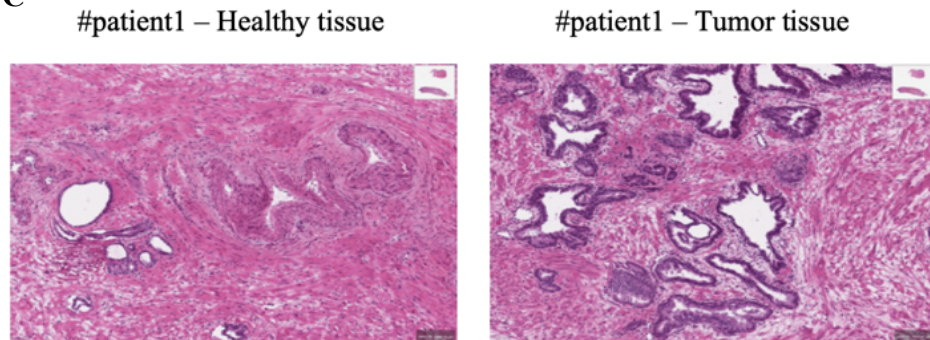


Figure 5. Composition and tissues retrieval pipeline of samples from study cohort of patients. (A) Composition and characteristics of analyzed cohort of patients. (B) Pathological and methodological evaluation protocol of samples retrieval pipeline. (C) Representative histological micrographs of healthy (left) and tumor (right) tissue obtained and analyzed from indicated patient.

5.1.2 Flow cytometry – t-SNE analysis on fresh prostate samples

We took advantage of spectral multiparametric high-dimensional flow cytometry to comprehensively profile the immune cell populations within the prostate. Single-cell suspensions underwent thorough analysis to identify key immune cell types, such as T cells, B cells, monocytes, macrophages, neutrophils, and dendritic cells. To gain deeper insights into the composition of both healthy and tumor tissues within prostate samples, we conducted non-linear dimensional reduction analysis using the t-SNE algorithm on total CD45⁺ leukocytes (Figure 6A).

Based on the expression of surface proteins, we were able to identify 10 primary main cells clusters (Figure 6 A-B). Notably, our analysis allowed us to distinguish two distinct clusters of CD8⁺ and CD4⁺ T cells based on the differential expression of CD103 and HLA-DR. Indeed, cluster 1 identified a population of CD4⁺ T cells expressing both CD103 and HLA-DR, indicative of a tissue-resident identity (Webb et al., 2014). In contrast, cluster 2 mainly comprised CD4⁺ T cells lacking expression of these surface markers, suggesting their belonging to a conventional/non-activated repertoire.

CD8⁺ T cells were segregated into clusters 3 and 4, with the former positive for the molecule CD103, associated with the tissue-resident phenotype (Duhon et al., 2018). Cluster 7, defined by the presence of CD19⁺ HLA-DR⁺ cells, was designated as B cells. In contrast, Cluster 6 comprised cells expressing CD14, CD16, and HLA-DR, were assigned as dendritic cell lineage. Additionally, Clusters 5 and 8, characterized by cells expressing CD16 and CD56, respectively, were annotated as neutrophils and NK cells. Interestingly, we found cluster 2 and cluster 3 to be the two major populations that were, beside not statistically significant, differently represented between healthy and tumor samples. Indeed, we found cluster 2 to be slightly enriched in tumor samples unlike cluster 3, that appeared to be less represented.

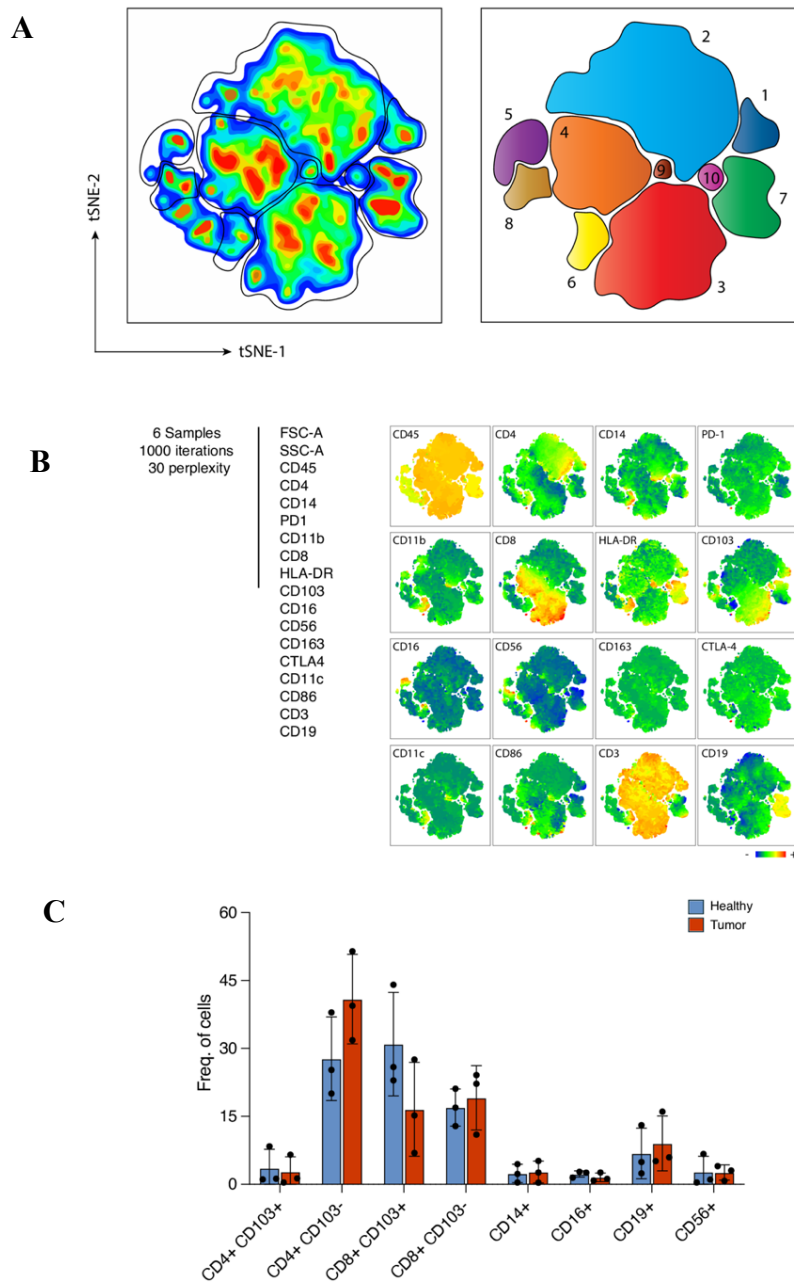


Figure 6. *t*-Distributed Stochastic Neighbor Embedding (tSNE) analysis of CD45⁺T cells in healthy and tumoral prostate tissue. (A) (left) Two-dimensional map showing clustering results of all 60,000 cells from all six samples via t-SNE visualization. (right) representative rendering of identified clusters in tSNE analysis with relative enumeration. (B) Heatmap from tSNE analysis showing the co-expression of markers shown in indicated panel (left) in equally concatenated CD45⁺ cells in healthy and tumoral prostate tissue samples from 3 analyzed patients. Analysis was performed on 10,000 events per sample, 1000 iterations, 30 perplexity. (C) Histogram showing the relative frequency of indicated cell populations in healthy (blue) and tumoral (red) samples of specified cohort of patients. Dots represent individual samples. Data are expressed as mean \pm SEM.

The annotation of cellular clusters identified through unsupervised analysis of flow cytometry data has laid the groundwork for comprehending the heterogeneity of immune cells within prostatic tissue. In particular, T cells (including CD4 and CD8 subsets) constitute the predominant intra-prostatic leukocytes, indicating their potential immunological role in tumor control and tissue homeostasis maintenance. Through quantifying cell frequencies within each cluster, we aimed to delineate signatures/differences in the composition of immune cells between tumor and healthy tissue.

5.1.3 PD-1 and CTLA4 analysis on prostate tissues

Many studies have shown that both CD4⁺ and CD8⁺ T cells can acquire a dysfunctional phenotype in diverse tumor microenvironments. Indeed, T cells have been reported to enter a dysfunctional or exhausted state, often characterized by sustained expression of inhibitory receptors, and contributing to tumor progression. Among negative regulators that can mediate T cell dysfunction, PD-1 and CTLA-4 have been pointed out as key players (Buchbinder & Desai, 2016)

In our experimental setup, CD4⁺ and CD8⁺T cells appeared to be among the most abundant populations, both in tumor and healthy tissue. However, no significant differences were found between the two study groups (tumor vs. healthy tissue) (all p value > 0.3). Since no differences were found in terms of frequency, we measured the surface expression of CTLA4 and PD-1, well-known markers of dysfunction and exhaustion, in the most represented clusters (T cells, CD4⁺, and CD8⁺) (Figure 7). Interestingly, we did not identify significant differences in the expression of immune checkpoint (IC) molecules on CD4⁺ and CD8⁺ T cells in patients with high-risk prostate disease compared to healthy tissues (p value >0.1), in contrast to findings reported in other tumor microenvironments (Jhunjhunwala et al., 2021)

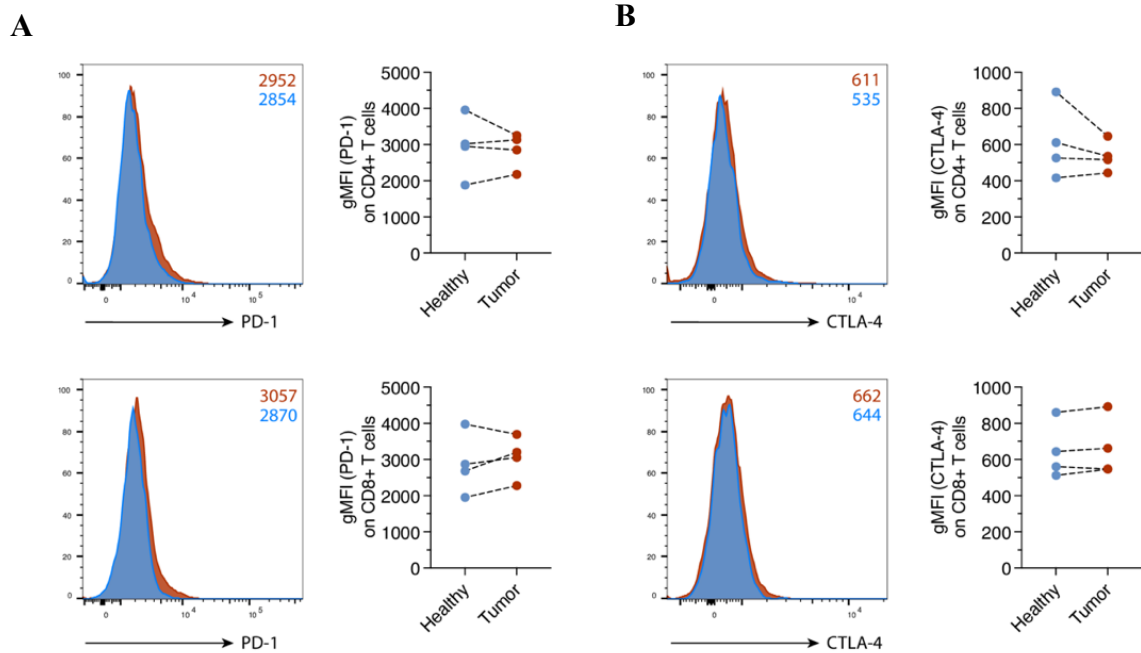


Figure 7. PD-1 and CTLA-4 surface expression on CD4⁺ and CD8⁺ T cells do not correlate with high-risk prostate cancer disease. (A) (left) MFI representative modal expression of PD-1 on CD4⁺T cells (top) and CD8⁺T cells (bottom). Blue lines and values represent PD-1 MFI on CD8⁺ and CD4⁺ T cells in healthy donor tissues. Red lines and values refer to PD-1 MFI on CD8⁺ and CD4⁺ T cells in tumoral donor tissues. Numerical values within the plot refer to mean MFI of indicated group. (right) Histograms of the MFIs of PD-1 on CD8⁺ and CD4⁺ T cells in healthy (blue full dots) or tumoral analyzed tissue samples (red full dots). Dotted lines connect values belonging to same analyzed sample. (B) (left) MFI representative modal expression of CTLA-4 on CD4⁺T cells (top) and CD8⁺T cells (bottom). Blue lines and values represent CTLA-4 MFI on CD8⁺ and CD4⁺ T cells in healthy donor tissues. Red lines and values refer to CTLA-4 MFI on CD8⁺ and CD4⁺ T cells in tumoral donor tissues. Numerical values within the plot refer to mean MFI of indicated group. (right) Histograms of the MFIs of CTLA-4 on CD8⁺ and CD4⁺ T cells in healthy (blue full dots) or tumoral analyzed tissue samples (red full dots). Dotted lines connect values belonging to same analyzed sample.

5.1.4 Multiplex Immunohistochemical Phenotyping

To explore the spatial distribution of the most abundant infiltrating immune cell types identified in previous experiments, we conducted multiplex immunofluorescence on a sizable cohort of patients affected by localized PCa who underwent surgery, with or without lymph nodal dissection. Our analysis encompassed 40 patients treated at San Raffaele Hospital, as detailed in Figure 8.

A

Risk Group	N of Patients	Age	PSA Ng/ml	Glaeason Score	Positive Margin	Positive Nodes
Low Risk	10	71,4	12,66	GS 6	0	0
Intermediate Risk	10	69,8	9,74	GS 7	1	1
High Risk	20	70,6	10,33	GS 8-10	6	10

B

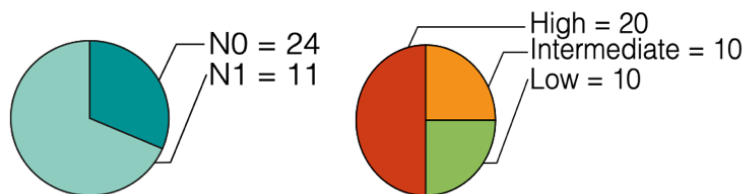


Figure 8. Composition and characteristics of study cohort of patients for multiplex immunohistochemical phenotyping. (A) Composition and characteristics of analyzed cohort of patients. (B) (left) Proportions of N0 and N1 classified patients in study cohort of PCa patients based on lymph node invasion (LNI). (right) Proportions of cases in study cohort of PCa patients basing on relative level of risk disease (green, low-risk disease; orange, intermediate-risk disease; red, high-risk disease).

The presence of each immune cell type in the stromal (peritumoral) and epithelial (intratumoral) compartment (Figure 9) was determined in PCa tissue samples by using Ventana Discovery Ultra (See section 8.7 Multiplex Ventana phenotyping and Table 9).

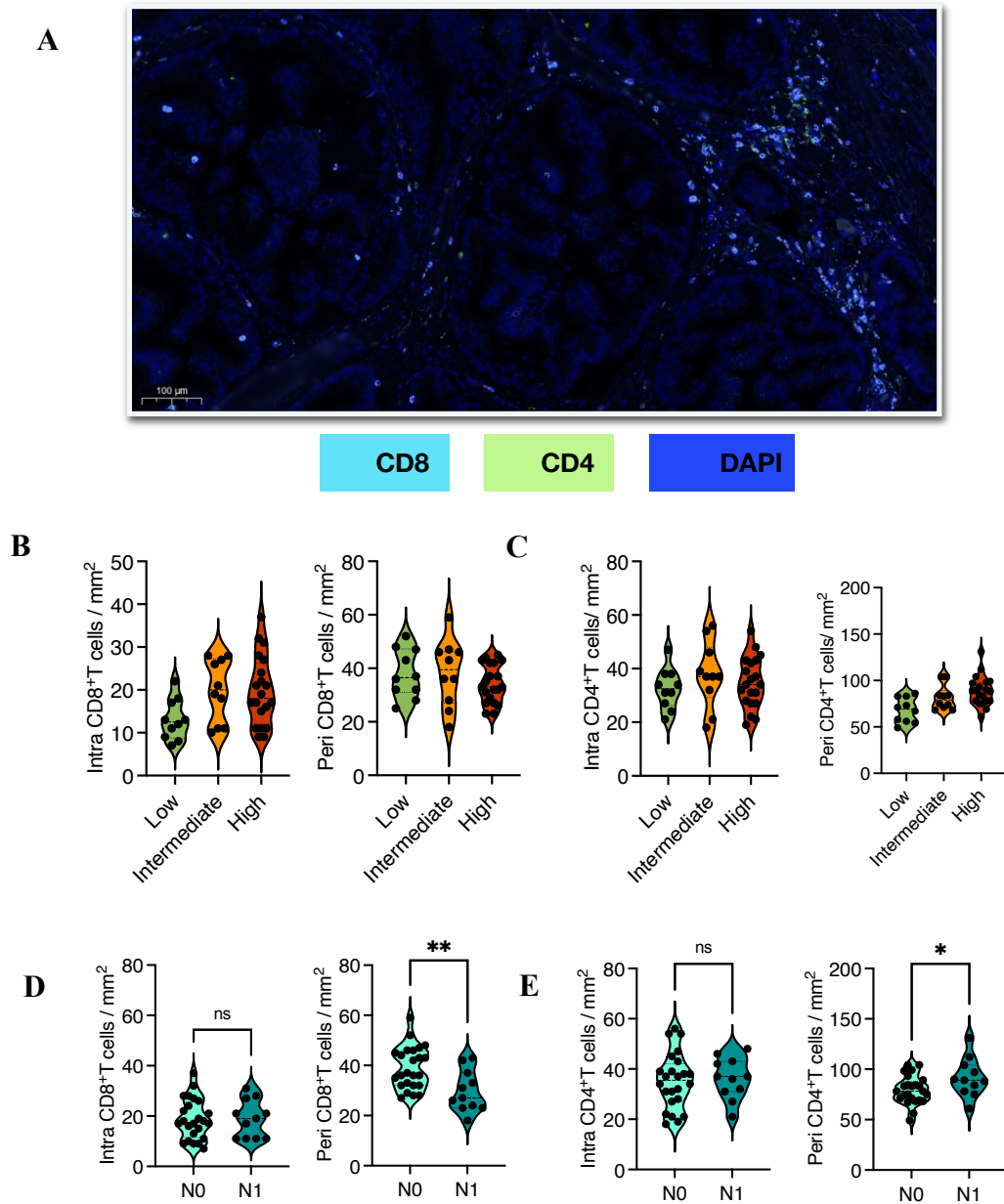


Figure 9. CD4⁺ and CD8⁺T cell infiltration evaluation on patients affected by localized prostate cancer. (A) Immunofluorescence representative micrographs of prostate sections from recruited cohort of patients of high-risk disease group. The micrograph shows the distribution of CD8⁺T cells (light blue) and CD4⁺T cells (light green) in prostate tissue. Cell nuclei are highlighted by DAPI staining (dark blue). Scale bar represents 100 µm. (B) Violin plots showing of CD8⁺T cells numbers in intratumoral and peritumoral zone of analyzed tissues basing on relative level of risk disease

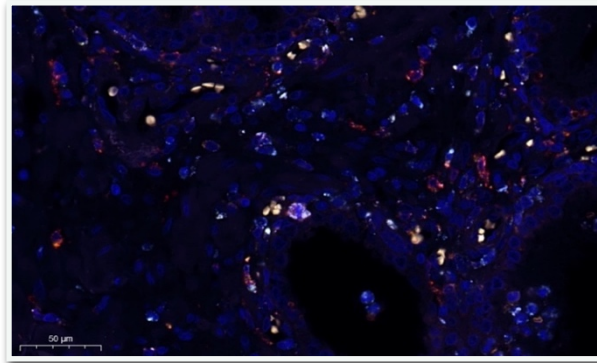
(green, low-risk disease; orange, intermediate-risk disease; red, high-risk disease). Dots represent individual samples. (C) Violin plots showing of CD4⁺T cells numbers in intratumoral and peritumoral zone of analyzed tissues basing on relative level of risk disease (green, low-risk disease; orange, intermediate-risk disease; red, high-risk disease). Dots represent individual samples. (D) Violin plots showing of CD8⁺T cells numbers in intratumoral and peritumoral zone of analyzed tissues basing on lymph node invasion (LNI) of analyzed patients. Dots represent individual samples. (E) Violin plots showing of CD4⁺T cells numbers in intratumoral and peritumoral zone of analyzed tissues basing on lymph node invasion (LNI) of analyzed patients. Dots represent individual samples. Data are expressed as mean \pm SEM. Statistics: Man-Whitney nonparametric unpaired t-test, ns p -value > 0.05 * p -value ≤ 0.05 , ** p -value ≤ 0.01 .

In the epithelial compartment, we found no significant disparities in terms of T cell infiltration across PCa risk groups based on nodal status post-surgery (all p values >0.1). Within the stromal compartment, no differences were noted in terms of T cells/mm², although CD4⁺ infiltration appeared elevated in aggressive disease, albeit marginally significant ($p = 0.071$). Examining the status of lymph node involvement (LNI), a decrease in the number of CD8⁺ T cells was noted ($p > 0.01$), alongside a significant increase in terms of CD4⁺ T cell preponderance ($p < 0.05$).

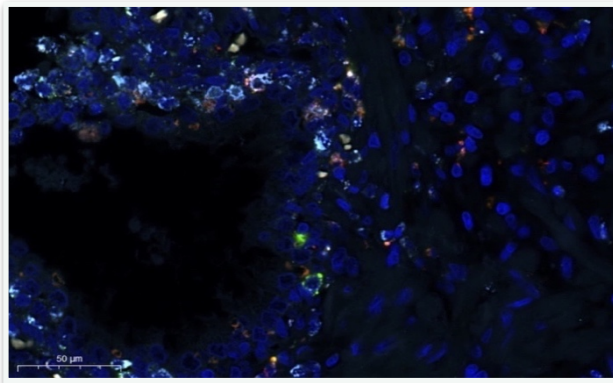
The relationship between T cells and macrophages in PCa is well known to be complex and multifaceted and therefore, the balance and relative distribution of T cells and macrophages within the TME is critical in determining the outcome of PCa progression (Larionova et al., 2020). We then analyzed, in the same Formalin Fixed Paraffin Embedded (FFPE) samples, the eventual abundance of two distinct macrophage cell populations which may exhibit varying degrees of anti-tumoral functionality based on their polarization states (Figure 10). We assessed the presence of M2 (identified as CD68⁺CD63⁺) and M1 macrophages (identified as CD68⁺ CD86⁺), with the former recognized for its role in promoting tumor growth and metastasis through immune response suppression, while the latter known to exert anti-tumoral effects by enhancing T cell activation and cytotoxicity (Pan et al., 2020).

A

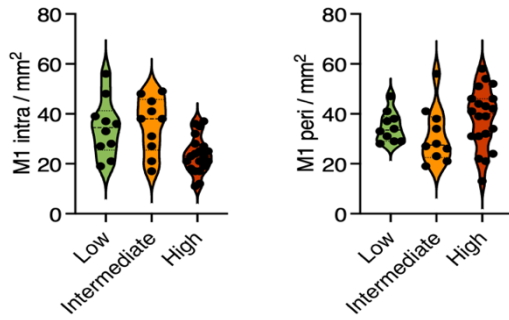
CD68+ CD86+ (M1-



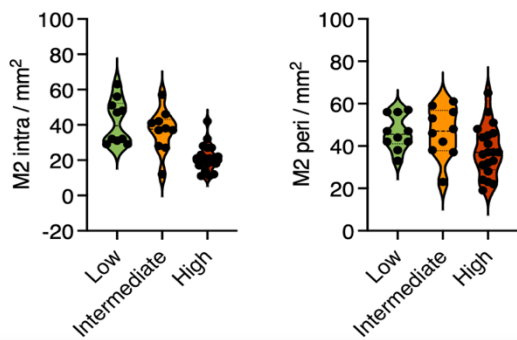
CD68+ CD63+ (M2-



B



C



D

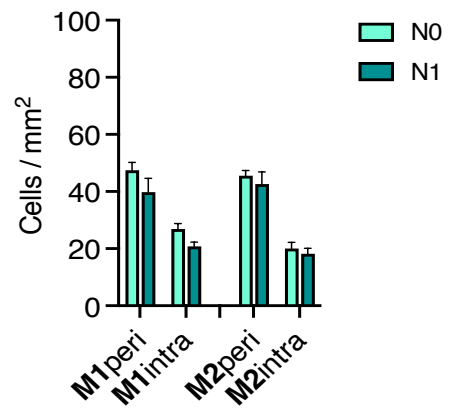


Figure 10. M1 and M2 infiltration evaluation on patients affected by localized prostate cancer. (A) Immunofluorescence representative micrographs of prostate sections from recruited cohort of patients of high-risk disease group. The micrograph shows the distribution of CD68⁺ CD86⁺ cells (aqua and red) and CD68⁺ CD63⁺ (red and green) in prostate tissue. Cell nuclei are highlighted by DAPI staining (dark blue). Scale bar represents 50 μ m. (B) Violin plots showing of CD68⁺ CD86⁺ cells numbers in intratumoral and peritumoral zone of analyzed tissues basing on relative level of risk disease (green, low-risk disease; orange, intermediate-risk disease; red, high-risk disease). Dots represent individual samples. (C) Violin plots showing of CD68⁺ CD63⁺ cells numbers in intratumoral and peritumoral zone of analyzed tissues basing on relative level of risk disease (green, low-risk disease; orange, intermediate-risk disease; red, high-risk disease). Dots represent individual samples. (D) Bar plots showing of M1 and M2 cells in intratumoral and peritumoral zone of analyzed tissues basing on lymph node invasion (LNI) of analyzed patients. Dots represent individual samples. Data are expressed as mean \pm SEM. Statistics: Man-Whitney nonparametric unpaired t-test, ns p-value > 0.05 * p-value \leq 0.05, ** p-value \leq 0.01.

No significant changes in macrophage subsets frequency were identified among the study groups (all p value >0.05). Therefore, based on our clinical setting, we excluded the percentage of macrophages subsets to be considered a prognostic factor for stratifying our patients in the three risk groups (low, intermediate, and high). However, we did notice a negative trend in the number of M1 and M2 macrophages in patients with locally advanced disease (N1). This result could be framed within a broader context of prostate tumor inhibition in recruiting cells from the immune system (immune evasion mechanisms) (Erlandsson et al., 2019)

5.1.5 Fresh tissue analysis for the identification of Immune Biomarkers

After testing our flow cytometry panel (Figure 6B) and identifying populations of interest, we wanted to understand whether the immune cell infiltrate profile could be a predictive tool for stratifying PCa risk. With this aim, we included in the study a larger cohort of patients (32 patients) all of which underwent surgery. For each included patient, a tissue prostate sample and a pre-surgical blood sample were collected and analyzed. We included in our analysis 15 samples from healthy tissue (patients affected by BPH), 5 from patients with low-risk, 7 with intermediate-risk, and 5 with high-risk disease (Table 5).

N 32 patients	Age	PSA (ng/ml)	Gleason Score	Risk Group
5	66,4	6,44	6	Low-Risk
7	68,3	6,10	7	Intermediate-Risk
5	72,5	7,34	8-10	High-Risk
15	67,9	7,75	BPH	Negative

Table 5 Study cohort of patients for identification of immune cells in tissue and blood samples. Composition and characteristics of analyzed cohort of patients.

We performed unsupervised clustering analysis (t-SNE) on CD45+ cells in prostate samples, by which we were able to identify 9 main cell clusters (Figure 11A). With this analysis, we were able to identify comparable cellular populations that we previously described in initial experiments. Indeed, CD8+ and CD4+ T cell clusters were the most represented ones. Within both immune populations, t-SNE analysis revealed two distinct subsets, one of which expresses the surface marker CD103 while the other does not. Despite the larger sample size, we were unable to identify a significant difference between tumor and healthy tissue or within the different risk classes (all p value >0.05). However, it is noteworthy that a trend emerged in the CD8+ CD103+ subset population. Specifically, we observed a decrease in the CD103+CD8+ T cell population concurrent with the progression of prostate disease grade (Figure 10B). Aggressive tumors with a high risk of lymph node metastasis, in fact, exhibit the lowest percentage of this cellular subtype. Moreover, we analyzed the CD4/CD8 ratio, an indicator of the immune status within the TME (Cerqueira et al., 2020). The CD4/CD8 ratio was not able to discriminate between the populations. The bar plot only suggests an abundance of CD4+ T cells relative to CD8+ T cells, which could indicate a more regulatory or suppressive immune environment (Figure 11C).

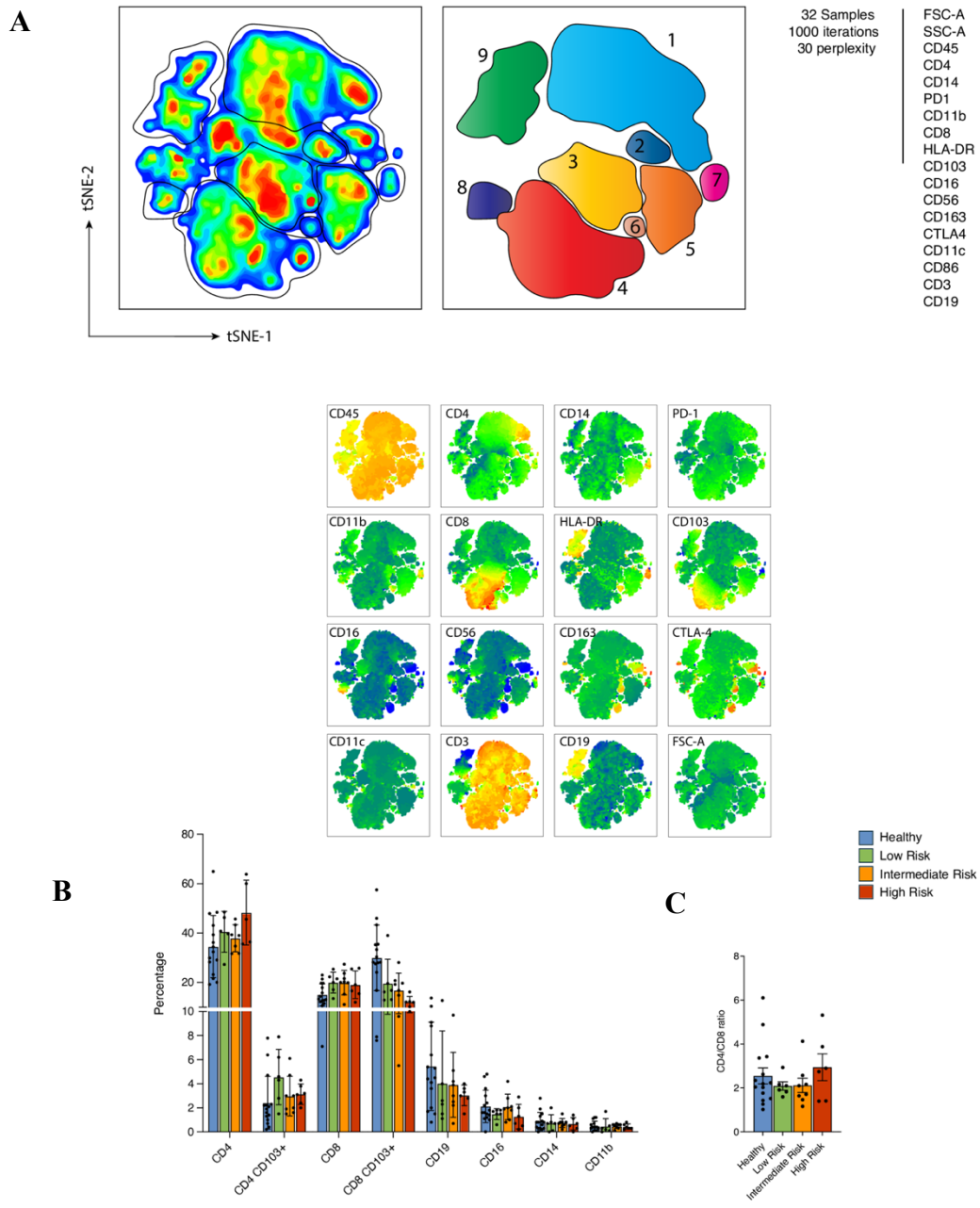


Figure 11. tSNE analysis of CD45⁺T cells in tissue prostate samples from stratified low, intermediate and high-risk disease patients. (A) (left) Two-dimensional map showing clustering results of all 80,000 cells from all 32 samples via t-SNE visualization. (right) representative illustration of identified clusters in tSNE analysis with relative enumeration and annotation. Analysis was performed on 3,000 events per sample, 1000 iterations, 30 perplexity. (B) Histogram showing the relative frequency of indicated cell populations in healthy (blue), low-(green), intermediate- (orange) and high- (red) risk disease patient samples. Dots represent individual samples. Data are expressed as mean \pm SEM. (C) Histogram showing the CD4⁺/CD8⁺T cell ratio values in healthy (blue), low- (green), intermediate- (orange) and high- (red) risk disease patient samples. Dots represent individual samples. Data are expressed as mean \pm SEM.

A logistic regression model was then employed in order to explore the eventual impact of this cell population on clinically significant disease prediction (defined as Gleason Score ≥ 7). At the univariate analysis (Figure 12A), the relative abundance of CD103⁺CD8⁺ T cell population emerged as an independent predictor of clinically significant PCa (p=0.05) or PCa disease (p=0.01). This trend is depicted by the Locally Weighted Scatterplot Smoothing curve for the probability of clinically significant cancer (Figure 12B). However, due to a limited number of events (patients with Intermediate or high-risk disease), we excluded multivariate regression as suitable analysis.

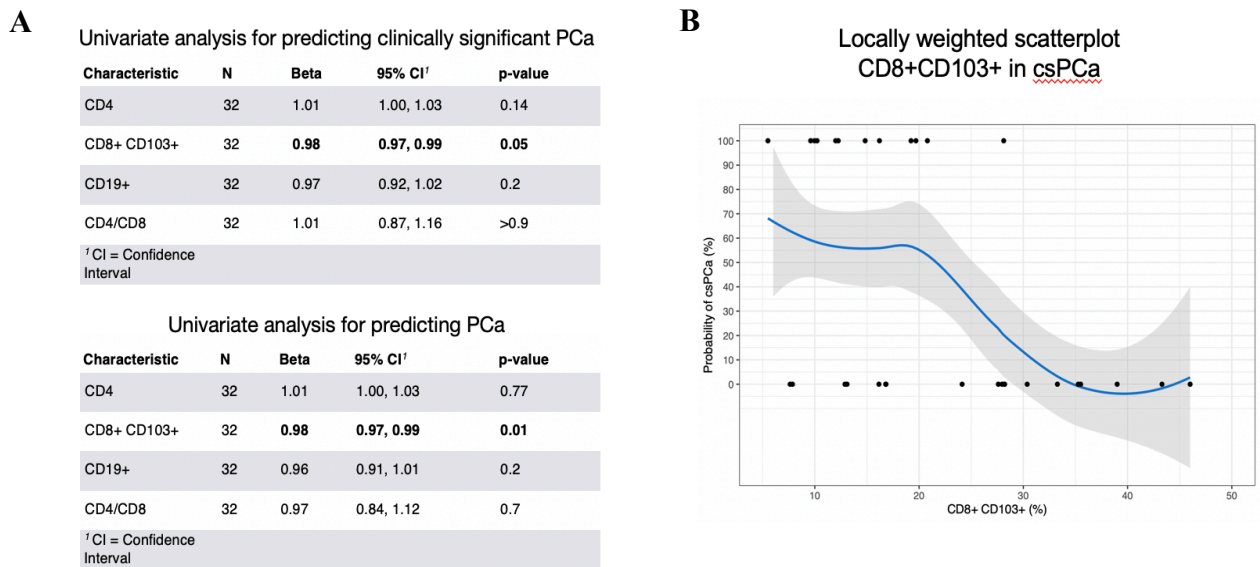


Figure 12. CD103⁺CD8⁺ T cell population as an independent predictor of clinically significant PCa. (A) Univariate logistic regression measuring predictive performance of variables. (B) Locally weighted scatter plot analysis of CD103⁺ CD8⁺ T cells in clinically significant PCa.

5.1.6 Peripheral Blood Samples as a source of Immune biomarkers

One of the aims of our study was to ultimately identify blood biomarkers with the potential to aid in the diagnosis or prognosis of patients with prostate neoplasia. The introduction of PSA into clinical practice has had a profound impact on patient prognosis by improving the detection of prostate cancer and identifying metastatic disease at earlier stages (Carlsson & Vickers, 2020). Despite these achievements, PSA unfortunately remains a nonspecific biomarker, underscore the pressing need for more effective alternatives.

In our study, we also aimed to explore immunological signatures capable of not only identifying prostate diseases but also aiding in the stratification of patients across various risk classes. We included in our analysis the same cohort population described in Table 5.

Before starting the surgical procedure, all patients who had signed informed consent underwent a blood draw of approximately 5 ml of whole blood. All samples were immediately processed and analyzed using the same antibody panel used for prostate tissue analysis (Figure 6B). This analysis revealed the presence of different cellular clusters expressed differently in terms of percentages compared to prostatic tissue (Figure 13A). As expected, the predominantly present population consists of neutrophils (cluster 9, CD16+), immediately followed by T cells (CD4 and CD8, cluster 2 and 3,4 respectively). (Figure 13B)

We did not observe any significant differences (all p value >0.05) on overall abundance of these clusters in our study group samples (Figure 13C). However, the number of CD4⁺T cells in patients with clinically significant prostate disease (Gleason Score 7 to 10) was observed to be increased compared to control or low-risk disease patients (Gleason Score 6).

Although peripheral blood immunological parameters have been attempted to be used as PCa biomarkers, we did not consider this approach, with the tested tools, to be suitable for our clinical study. Indeed, patient heterogeneity can often be a challenging factor that does not easily allow to identify univocal parameters directly associated with established tumor diseases.

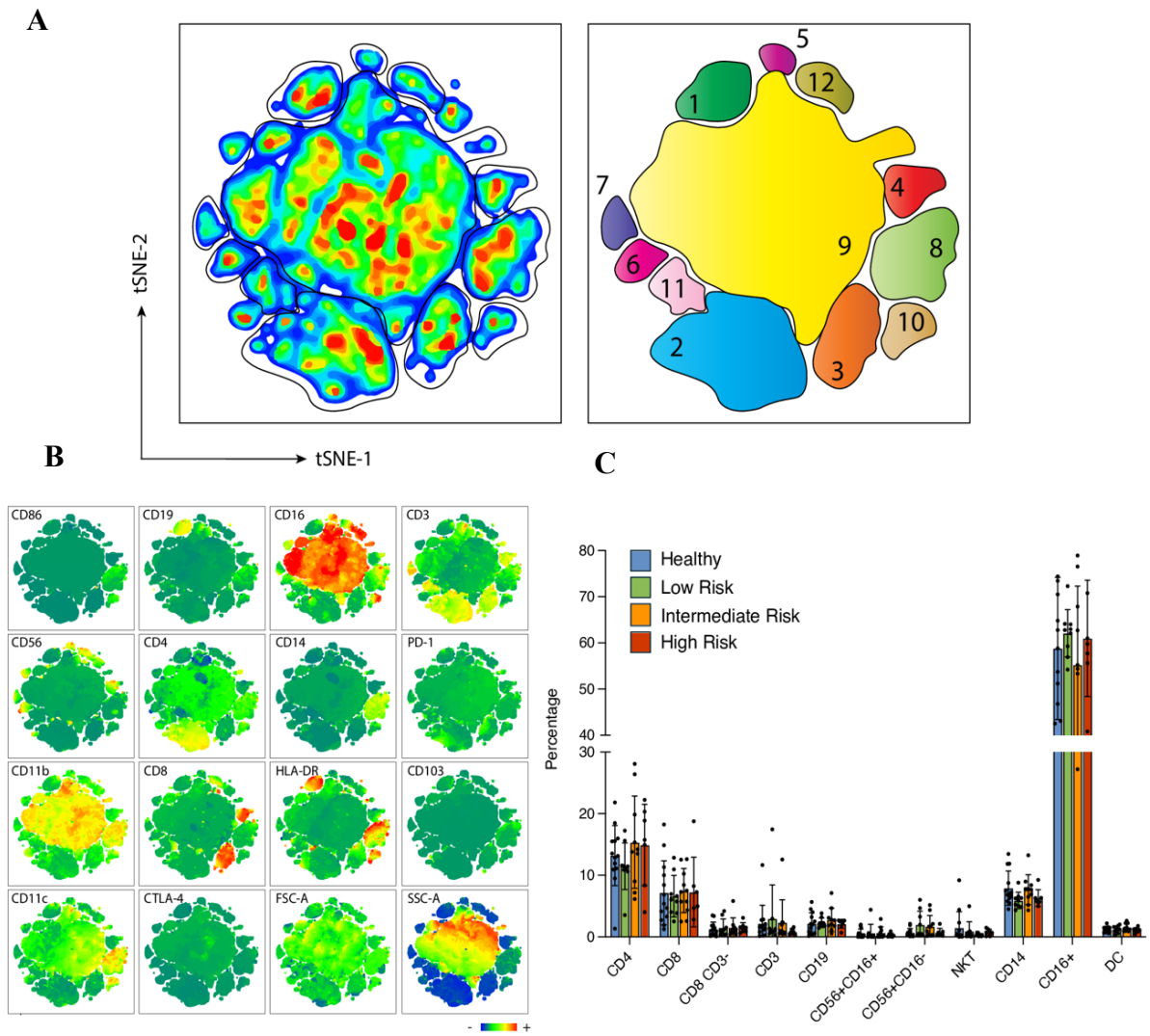


Figure 13. tSNE analysis of CD45⁺T cells in the blood of stratified low, intermediate and high-risk disease patients. (A) (left) Two-dimensional map showing clustering results of all 80,000 cells from all 32 samples via t-SNE visualization. (right) representative illustration of identified clusters in tSNE analysis with relative enumeration and annotation. Analysis was performed on 3,000 events per sample, 1000 iterations, 30 perplexity. (B) Heatmap from tSNE analysis showing the co-expression of markers shown in indicated panel (Figure. 8A) in equally concatenated CD45⁺ cells in blood samples from 32 analyzed patients. (C) Histogram showing the relative frequency of indicated cell populations in healthy (blue), low- (green), intermediate- (orange) and high- (red) risk disease patient samples. Dots represent individual samples. Data are expressed as mean \pm SEM.

5.2 Characterization of T Cells subsets in Healthy and Prostate Cancer tissue

We then decided to deeply analyze and characterized CD4+ and CD8+ T cell compartments as the main populations that showed the greatest degree of variability within our study group. To do so, we recruited 10 patients who underwent surgery (Table 6). These patients were categorized into 3 different clinically distinguished groups based on pathological characteristics. Specifically, 4 patients were assigned to the control group (patients affected by BPH), 3 patients to insignificant cancer (Gleason 6), and 3 patients to clinically significant diseases (3 men with Gleason 7 and 1 patient with Gleason 9).

N 10 patients	Age	PSA (ng/ml)	Gleason Score	Risk Group
3	68,4	7,11	6	Low-Risk
3	70,1	9,10	7	Intermediate-Risk
1	68	10,14	9	High-Risk
4	71,8	8,65	BPH	Negative

Table 6. Study cohort of patients for the characterization of T cells in tissue samples. Composition and characteristics of analyzed cohort of patients.

To further characterize the T cell populations, we designed a flow cytometry panel that included targets that define major cellular populations and several markers of activation, exhaustion, naive, memory, Treg, or cytotoxic cellular phenotype (CD127, CCR7 CD56, CD69; TCF1, TOX, CD39, TIGIT, Ki67, TCF1, Foxp3, PD1, TOX) (see Method, section 8.5, Flow cytometry analysis; Table 8).

The unsupervised t-SNE analysis conducted on the CD45+ population revealed the presence of 9 distinct cell clusters (Figure 14A). Once again, CD8+ and CD4+ T populations appeared to be the most represented in the analyzed samples, comprising approximately 35% and 40%, respectively, of the total CD45+ population. Although they did not reach statistical significance (Figure 14 B), we observed a correlation between the CD4+ and CD8+ T cell counts and disease aggressiveness (Clinically significant PCa) (Figure 14C). Comparing the cells between clinically significant tumors and the control sample, we observed differences in CD8+ and CD4+ T cell clusters (cluster 3 and 1, respectively). The difference lies not only in terms of the absolute frequency of cells but also, crucially, in terms of cellular composition. Therefore, we decided to focus our

attention on these two cell populations by further conducting a CD4- and CD8-specific unsupervised analysis.

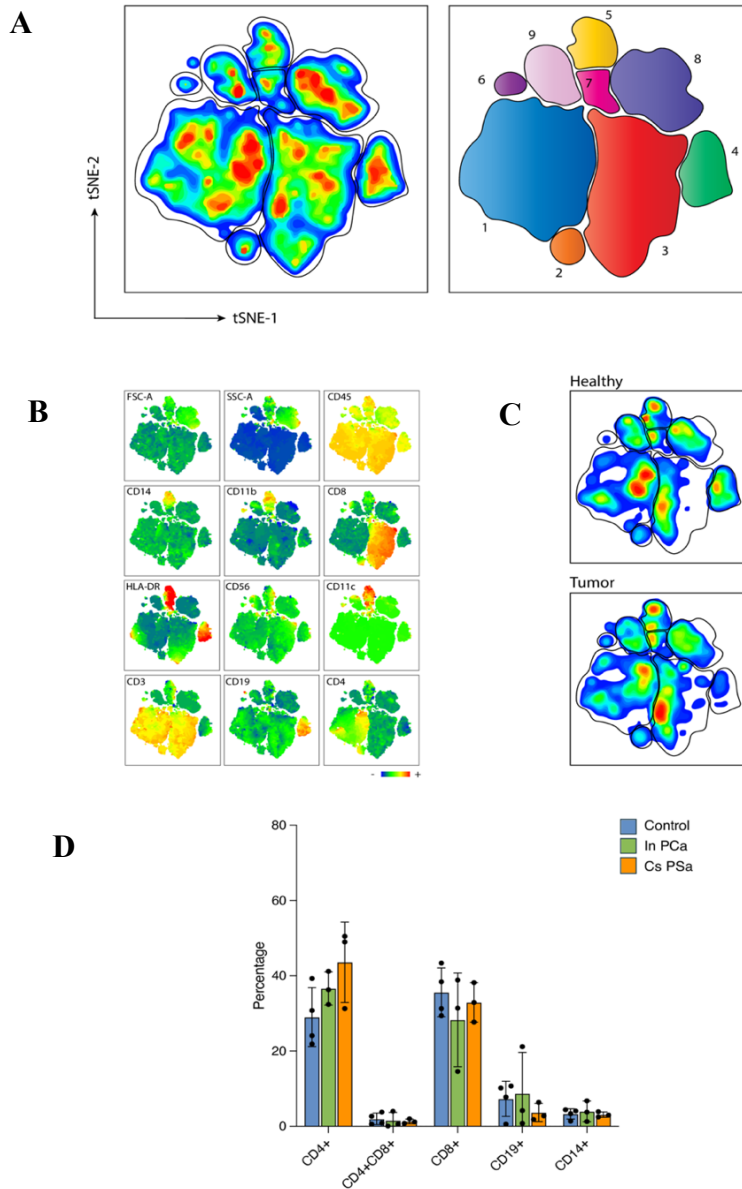


Figure 14. tSNE analysis of CD45⁺T cells in tissue samples of patients stratified as control, Insignificant and Clinically Significant patients. (A) (left) Two-dimensional map showing clustering results of all 60,000 cells from all 10 samples via t-SNE visualization. (right) representative illustration of identified clusters in tSNE analysis with relative enumeration and annotation. Analysis was performed on 2,000 events per sample, 1000 iterations, 30 perplexity. (B) Heatmap from tSNE analysis showing the co-expression of markers shown in indicated panel (Fig. 8A) in equally concatenated CD45⁺ cells in tissue samples from 10 analyzed patients. (C) Two-dimensional map showing the difference regarding Cluster 1 and 3 between Healthy and CS PCa patients via t-SNE visualization. (D) Histogram showing the relative frequency of indicated cell populations in healthy (blue), Insignificant- (green), Clinically Significant (orange) disease patient samples. Dots represent individual samples. Data are expressed as mean ± SEM.

5.2.1 Unsupervised analysis on CD4⁺ cells

A clustering analysis was performed within the CD4⁺ T cell cluster. The markers used for this purpose included CD45RA, CD69, HLA-DR, CD103, Foxp3, CD127, TOX, PD-1, CCR7, and CD39 (Figure 15 A-C). These markers might play a crucial role in identifying specific subsets or states of CD4⁺ T cells. In detail, CD45RA is a marker used to distinguish between naive and memory T cells. Naive CD4⁺ T cells typically express CD45RA, while memory T cells generally do not. CD69 is an early activation marker expressed on T cells shortly after activation. HLA-DR, a major histocompatibility complex class II (MHC-II) molecule is involved in antigen presentation. CD103 is an integrin expressed on tissue-resident T cells. Foxp3 is a transcription factor associated with regulatory T cells (Tregs). Tregs expressing Foxp3 are involved in immune tolerance and suppression of immune responses. CD127, also known as IL-7 receptor alpha chain, is a marker commonly used to identify memory T cells. CD39 is an ectonucleotidase enzyme expressed on regulatory T cells (Tregs). CCR7: CC chemokine receptor 7 (CCR7) is a chemokine receptor involved in T cell trafficking and homing to secondary lymphoid organs. It is expressed on naive and central memory T cells. PD-1 was finally used to identify T cell exhausted.

The bubble plot was performed to better identify, based on the level of Mean Fluorescence Intensity (MFI) values of the described markers, the different cellular subsets within the CD4 population (Figure 15 C).

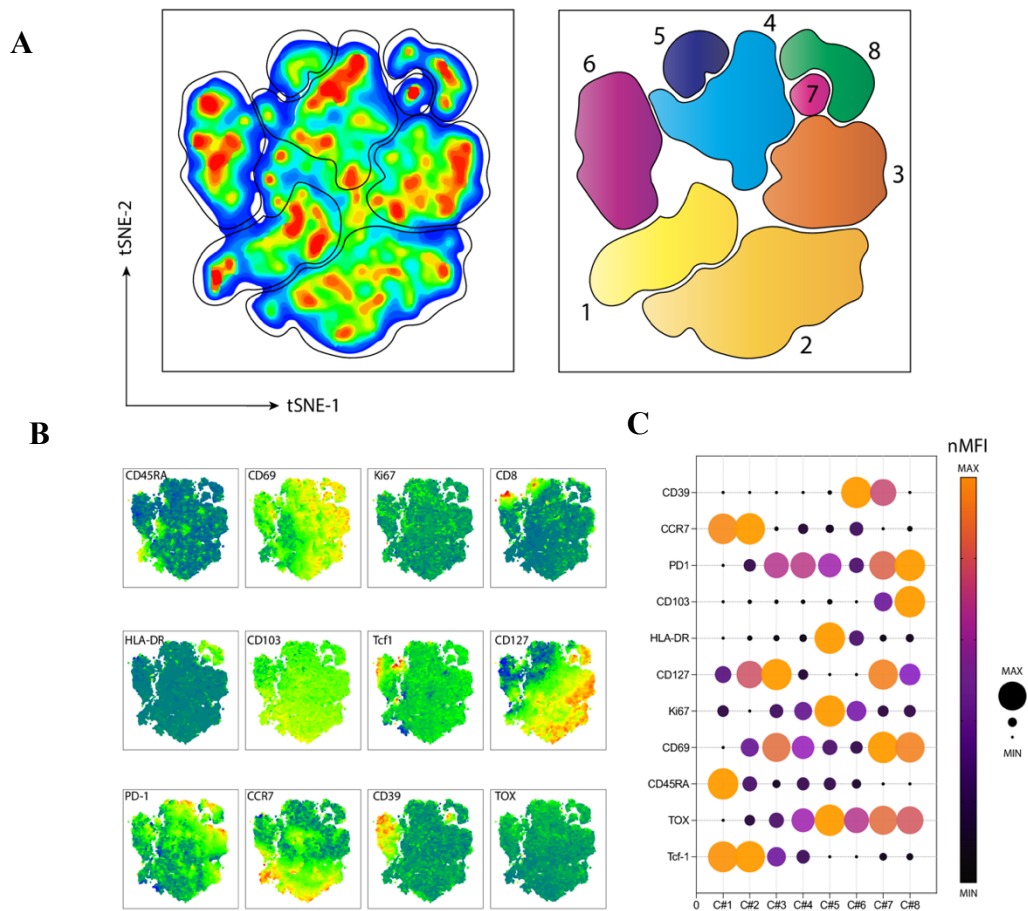


Figure 15. tSNE analysis of $CD4^+$ T cells in prostate tissue samples of patients affected by localized prostate cancer. (A) (left) Two-dimensional map showing clustering results of all 64,000 $CD8^+$ T cells from all 10 samples via t-SNE visualization. (right) representative illustration of identified $CD4^+$ T cells clusters in tSNE analysis with relative enumeration and annotation. Analysis was performed on 2,000 cells per sample, 750 iterations, 40 perplexity. (B) Heatmap from tSNE analysis showing the co-expression of selected markers shown in previously indicated panel (Figure 8A) in equally concatenated $CD4^+$ T cells in tissue samples from 10 analyzed patients. (C) Bubble plot showing the normalized value of the MFI of indicated markers in each identified and indicated cluster. Bubbles color gradient and size indicate the expression intensity in terms of MFI.

Eight clusters were identified, and the frequency of each cluster was calculated in the study populations (Figure 16). Among the eight clusters underlined, two of them exhibited differences in terms of frequencies between patients affected by clinically significant pathology or indolent disease (Figure 16B). The bubble plot enabled us to identify markers that could discriminate between patient groups within the clusters, regardless of frequency (Figure 16 C).

Cluster 1 was mainly composed by CCR7⁺CD45RA⁺Tcf-1⁺ CD4⁺ T cells with low surface expression of tissue-residency associated markers (CD103, CD69) and was found to be significantly reduced in tumoral samples compared to healthy ones. On the contrary, we found cluster 4 to be significantly enriched in tumoral samples and mainly comprised CD69⁺ CD4⁺T cells expressing exhaustion-associated markers (TOX, PD-1) and retaining proliferative capacities (Ki-67⁺). These data, while providing a partial insight into the actual composition of the CD4⁺T population within prostate tumors, highlight the importance and need for a deeper and extensive characterization of such populations in order to unveil their impact in the context of PCa.

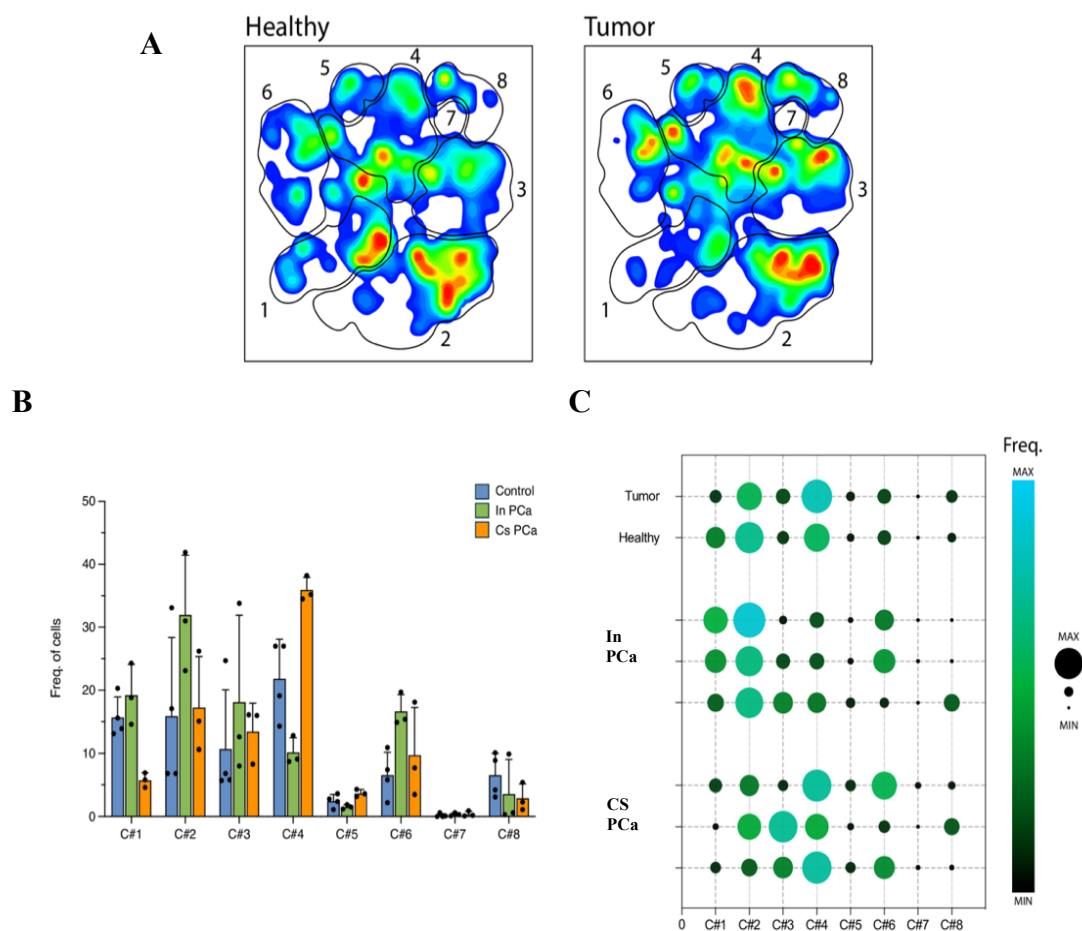


Figure 16. tSNE analysis of CD4⁺T cells in prostate tissue samples of insignificant and clinically significant PCa patients. (A) Representative two-dimensional plot of identified CD4⁺T cells clusters in tSNE analysis with relative enumeration and annotation in healthy (left) and tumor (right) tissue samples. (B) Histogram showing the relative frequency of indicated CD4⁺T cell cluster in healthy control (blue), insignificant PCa (green) and clinically significant PCa (orange) in analyzed prostate tissue samples. Dots represent individual samples. Data are expressed as mean \pm SEM. (C) Bubble plot showing the relative frequency of indicated clusters in each patients tissue sample analyzed. Bubbles color gradient and size indicate the expression intensity in terms of MFI.

5.2.2 Unsupervised analysis on CD8⁺ cells

As for what has been done for CD4⁺T cells, t-SNE analysis was then performed on the CD8⁺T. Markers used for the analysis included: CD45RA, CD69, HLA-DR, CD103, CD127, PD-1, CCR7, CD39, TCF1, Tox, and Ki67. Six distinct CD8⁺ T cell clusters were identified, characterized by different expression and/or activation profiles (Figure 17). Cluster 1 is primarily represented by cells highly expressing CCR7, CD127 and TCF1, while cluster 2 exhibits high expression of CD45RA and moderate expression of TCF1. Cluster 3 demonstrates high expression of HLA-DR, Ki67, and moderate expression of Tox. Cluster 4 exhibits high expression of PD1, CD103, and CD69. Cluster 5 is characterized by high expression of CD39, PD1, CD103, CD69, and Tox. Finally, cluster 6 is primarily characterized by the expression of Ki67, with moderate expression of Tox, TCF1, and CD39.

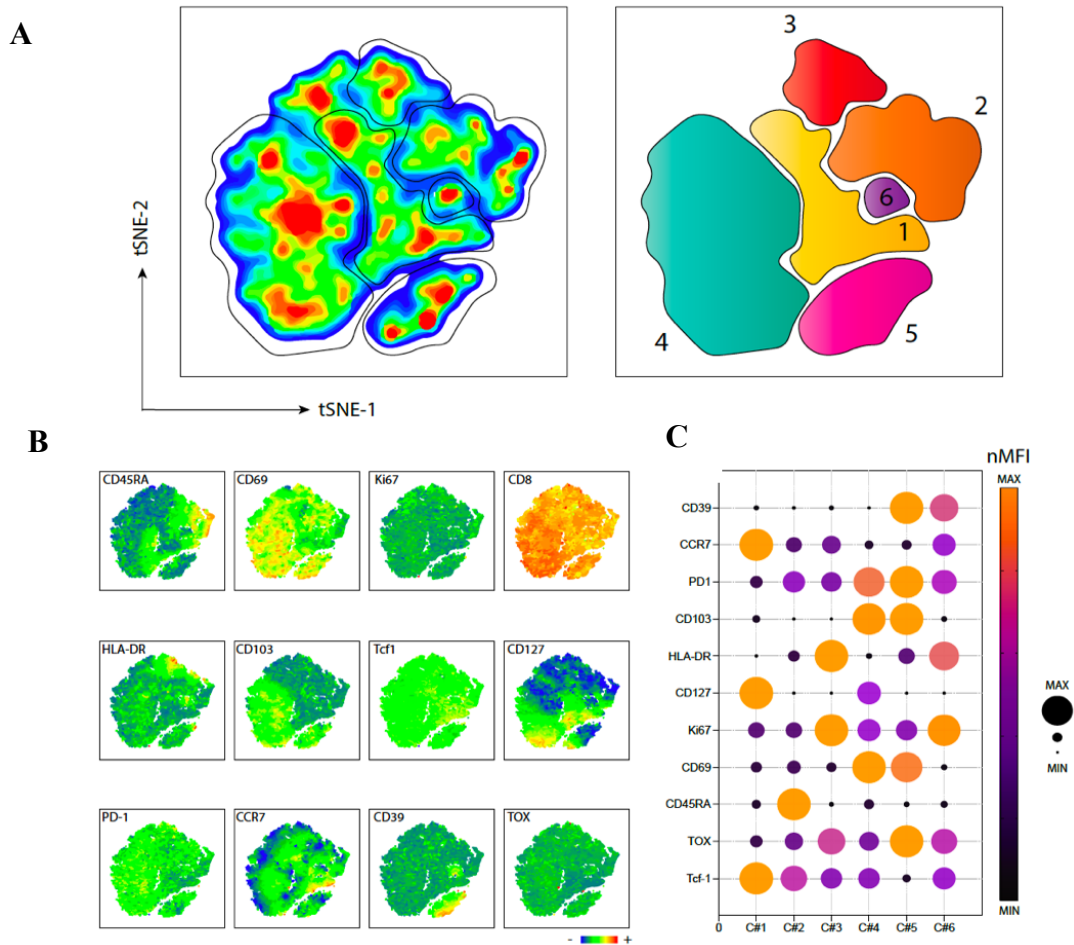


Figure 17. tSNE analysis of CD8⁺T cells in prostate tissue samples of patients affected by localized prostate cancer. (A) (left) Two-dimensional map showing clustering results of all 64,000 CD8⁺T cells from all 32 samples via t-SNE visualization. (right) representative illustration of identified CD8⁺T cells clusters in tSNE analysis with relative enumeration and annotation. Analysis was performed on 2,000 cells per sample, 750 iterations, 40 perplexity. (B) Heatmap from tSNE analysis showing the co-expression of selected markers shown in previously indicated panel in equally concatenated CD8⁺ T cells in blood samples from 32 analyzed patients. (C) Bubble plot showing the normalized value of the MFI of indicated markers in each identified and indicated cluster. Bubbles color gradient and size indicate the expression intensity in terms of MFI.

Interestingly, clusters 1 and 5 showed the most significant changes between control and clinically significant tumor clinical groups (Figure 18 B). Cluster 1, characterized by the expression of markers such as CCR7, CD127 and TCF1 was annotated as a naïve-like CD8⁺ T cell cluster and was found to be significantly reduced in patients with clinically significant aggressive disease. Cluster 5, on the other hand, which was characterized by the expression of CD103, CD69, PD1, and CD69, was attributed to a T resident memory-like CD8⁺T cell subpopulation and was found to be positively associated with both clinically significant or non-significant PCa patients. Of note, cluster 5 cells also expressed low levels of CD127, thus prompting out to a chronic activation phenotype.

Supervised flow cytometric analyses of CD103 and CD39 expression on CD8⁺ T cells revealed three primary cell populations: CD103⁻CD39⁻ double-negative T cells, CD103⁺CD39⁻ single-positive T cells, and CD103⁺CD39⁺ double-positive T cells (Figure 18 C). Although many other studies already reported the importance of a CD103⁺CD39⁺ CD8 T cell population as prognostic factor in terms of oncological outcomes or response to immunotherapy in various solid tumors (Duhon et al., 2018) , their role in PCa is still unclear. It therefore remains uncertain whether this specific subset of CD8⁺T cells could effectively correlate to PCa but remains of intriguing possibility the better characterization of this population within a specific clinical group in the context of PCa and immunotherapy.

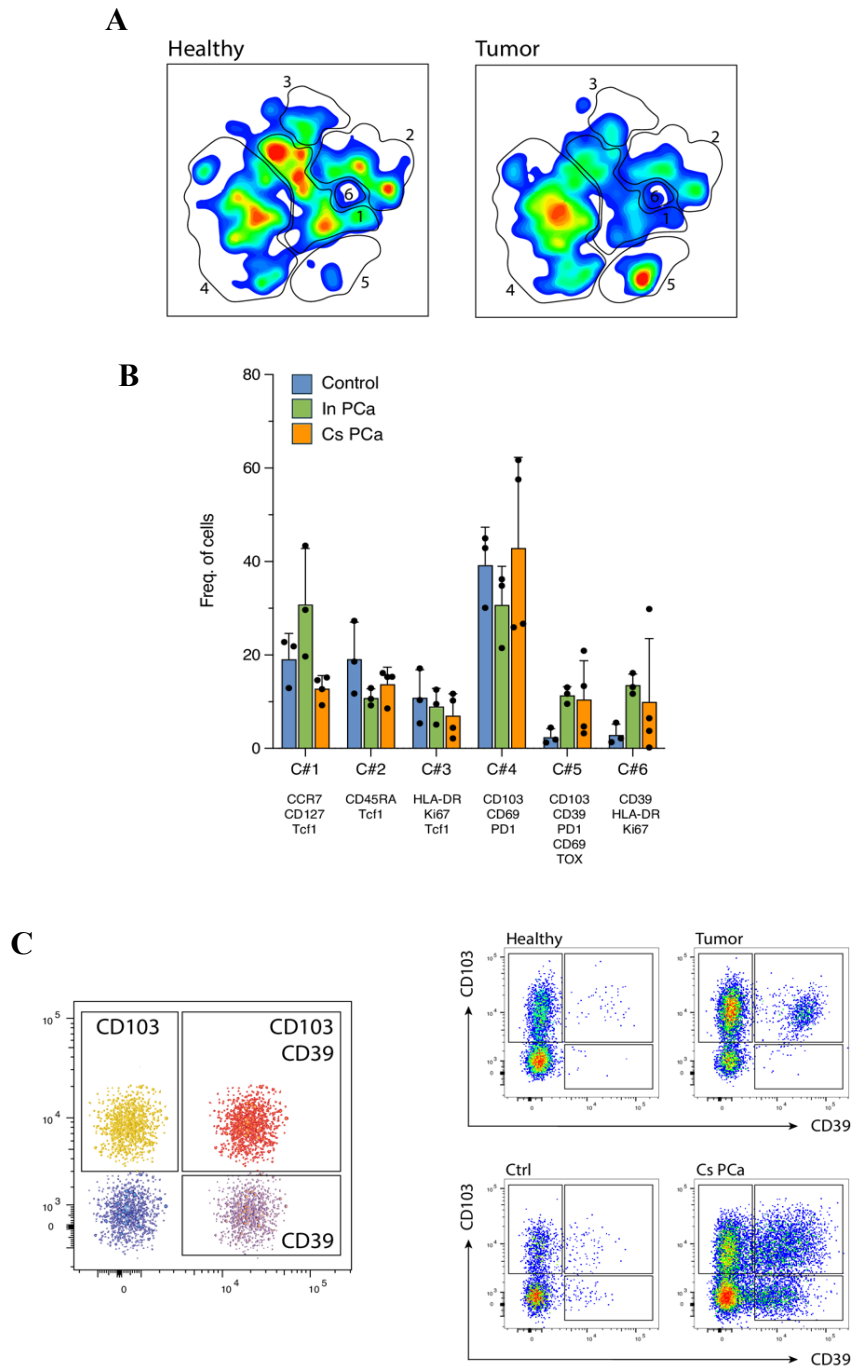


Figure 18. tSNE analysis of CD8+T cells and a supervised analysis on CD103+ CD8+ T cells. (A) Representative two-dimensional plot of identified CD8+T cells clusters in tSNE analysis with relative enumeration and annotation in healthy (left) and tumor (right) tissue samples. (B) Histogram showing the relative frequency of indicated CD8+T cell cluster in healthy control (blue), insignificant PCa (green) and clinically significant PCa (orange) in analyzed prostate tissue samples. Dots represent individual samples. Data are expressed as mean \pm SEM. (C) Representative FACS plot and gate strategy to visualize CD8+T cells expressing CD103 and CD39 in differential combination, in healthy (left plots) and tumor (right plots) tissue samples. Live, CD45+, CD4-, CD19-, CD8+ cells.

5.2.3 Spatial localization of T Cell Infiltration through Multiplex Analysis

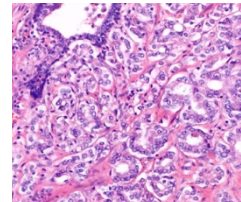
To validate the presence and spatial distribution of tissue-resident memory-like populations (double-positive CD8+ CD103+ or triple-positive CD8+ CD103+ CD39+), we conducted an immunofluorescence assessment of FFPE prostate samples obtained from individuals who underwent RP at San Raffaele Hospital, with a minimum of 5 years of follow-up. Our study included 27 patients: 12 with high-risk, 11 with intermediate-risk, and 4 with low-risk disease. There were no significant differences in PSA values, age, or other clinical variables among the groups. Lymph node metastases were detected in 7 out of the 27 patients at the time of surgery. Over time, 7 out of the 27 patients experienced biochemical recurrence (BCR) (Figure 19 A). Considering that PCa often exhibits diminished inflammatory infiltrates, we specifically selected patients with at least 10% neoplasia throughout the entire organ and confirmed inflammatory infiltrates by expert uro-pathologists (Figure 19 B).

A

Risk Group	Low	Intermediate	High
N patients 27	4	11	12
Age (median)	67,4	68,7	70,4
PSA (ng/mL)	11,5	8,94	7,43
Gleason Score	6	7	8-10
Positive Margin	0	2	5
Positive Nodes	0	3	7
Recurrence	0	2	7
CD8	77,5	80,63	88,25
CD4	131	122	127,25
CD8+CD103+	39,5	40	30,75
CD8+CD103+CD39+	1,9	2,54	4,41

B

Low immune cellular infiltration



High immune cellular infiltration

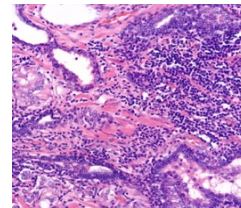


Figure 19. CD103+CD8⁺T cells in prostate tissue samples of insignificant and clinically significant PCa patients. (A) Composition and characteristics of analyzed cohort of patients. (B) Representative histological micrographs of low-infiltration (left) and high infiltration (right) tissue prostate samples of analyzed cohort of patients

We then quantified the presence of CD8+, CD4+, CD103+, and CD39+ cells in the different experimental groups (Figure 20). CD8+ and CD4+ T cells (Figure 20 C) did not significantly differ between the various risk classes, while a statistically significant difference ($p < 0.05$) was confirmed between the intermediate and high-risk groups regarding the frequency of CD8+ CD103+ cells (Figure 20D left). Triple-positive CD8+ CD103+ CD39+ cells showed a significant increase in high-risk samples compared to low and intermediate-risk tumors (p values < 0.01 and < 0.05 , respectively) (Figure 20 D right). The trend identified by these data confirms both the findings obtained from flow cytometry and the ability of tissue resident memory-like cells to stratify the different risk class

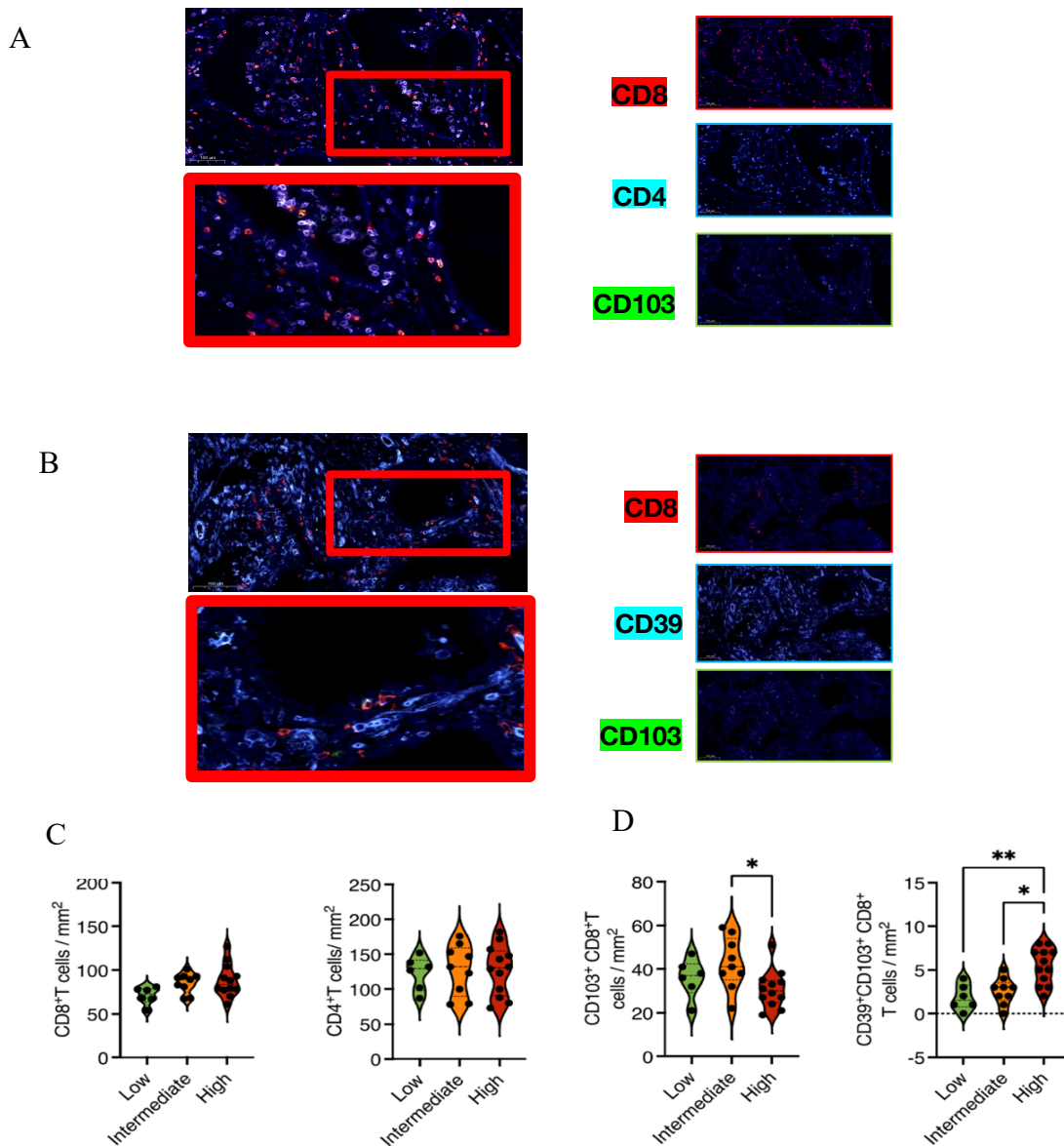


Figure 20. CD103+CD8⁺T cells infiltration and quantification in prostate tissue samples. (A) Immunofluorescence representative micrographs of prostate sections from recruited cohort of patients of high-risk disease group. The micrographs shows the distribution of CD8⁺T cells (red) and CD4⁺T cells (light blue) and CD103⁺ cells (green) in analyzed prostate tissue. On the right micrographs represent single markers staining: CD8⁺T cells (red), middle: CD4⁺T cells (light blue), right: CD103⁺ cells (green). Bottom Graph: zoom up of selected region. Scale bar represents 100 μ m. (B) Immunofluorescence representative micrographs of prostate sections from recruited cohort of patients of high-risk disease group. The micrographs show the distribution of CD8⁺T cells (red), CD39⁺ cells (light blue) and CD103⁺ cells (green) in analyzed prostate tissue. On the right, micrographs represent single markers staining. CD8⁺T cells (red), middle: CD39⁺ cells (light blue), right: CD103⁺ cells (green). (Bottom) zoom up of selected region. Scale bar represents 100 μ m. (C) Violin plots showing of CD8⁺T cells (left) and CD4⁺T cells (right) numbers in analyzed tissues basing on relative level of risk disease (green, low-risk disease; orange, intermediate-risk disease; red, high-risk disease). Dots represent individual samples. (D) Violin plots showing of CD103⁺CD8⁺T cells (left) and CD39⁺ CD103⁺CD8⁺T cells (right) numbers in analyzed tissues basing on relative level of risk disease (green, low-risk disease; orange, intermediate-risk disease; red, high-risk disease). Dots represent individual samples. Data are expressed as mean \pm SEM. Statistics: Man-Whitney nonparametric unpaired t-test, * p-value \leq 0.05, ** p-value \leq 0.01.

5.2.4 Correlation between Immune Cell Infiltration and Adverse Features in Prostate Cancer

We further evaluated the prognostic significance of infiltrating immune cell types in FFPE prostate samples. In our cohort, univariate logistic regression analysis revealed significant associations between Gleason Score (Gleason Score 8-10) and levels of infiltrating CD8⁺ CD103⁺ CD39⁺ cells (p: 0.027), with an AUC of 0.89. Additionally, our cells were identified as a prognostic factor for lymph node invasion (p: 0.032) with an AUC of 0.83 (Figure 21 A-C). Of note positive surgical margin status and high Gleason score (\geq 7) were predictors of lymph nodal invasion in our cohort.

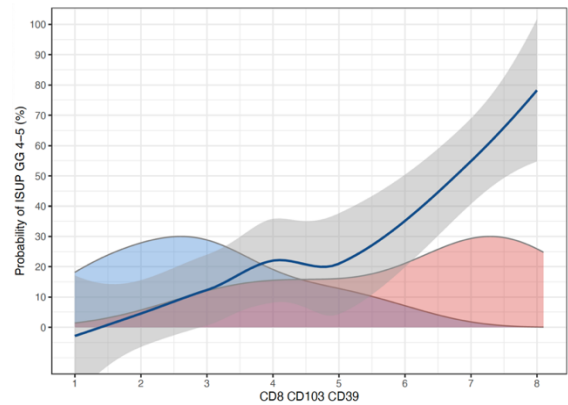
A locally weighted scatter plot analysis was conducted to assess the prognostic significance of CD39⁺ CD103⁺. The analysis plotted the presence of TRM cells against the likelihood of high-grade disease or nodal metastasis, allowing for the visualization of trends or correlations. In this study, the presence of CD39⁺ CD103⁺ cells was assessed as a potential prognostic factor for High-grade disease or Nodal metastasis (Figure 21 B-D).

A

GS 4-5 (AUC per CD8 CD103 CD39: 0.89)

Characteristic	N	Event N	OR ¹	95% CI ¹	p-value
CD4	27	8	0.99	0.96, 1.02	0.4
CD8	27	8	1.02	0.97, 1.08	0.4
CD8 CD103	27	8	0.93	0.83, 1.01	0.13
CD8 CD103 CD39	27	8	2.76	1.53, 7.26	0.027

¹OR = Odds Ratio, CI = Confidence Interval

B**C**

LNI (AUC per CD8 CD103 CD39: 0.83)

Characteristic	N	Event N	OR ¹	95% CI ¹	p-value
CD4	27	9	1.01	0.98, 1.03	0.6
CD8	27	9	1.06	1.00, 1.14	0.079
CD8 CD103	27	9	0.99	0.91, 1.07	0.4
CD8 CD103 CD39	27	9	1.84	1.20, 3.30	0.0032

¹OR = Odds Ratio, CI = Confidence Interval

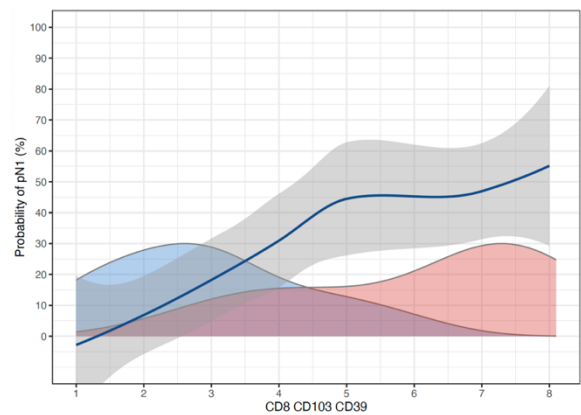
D

Figure 21. CD39⁺CD103⁺CD8⁺ T cell population as an independent predictor of high grade disease and lymph node invasion. (A,C) Univariate logistic regression measuring predictive performance of variables. (B,D) Locally weighted scatter plot analysis of CD39⁺CD103⁺ CD8⁺T cells in analyzed cohort of patients.

5.3 Transcriptional and Functional Profiling of CD8+CD103+ Cells

5.3.1 Gene expression profiling of prostate samples

To explore the diversity of cell types and transcriptional states found in localized PCa samples, we processed tissue specimens from RP procedures performed on individuals diagnosed with high-risk disease (three patients). Specifically, we obtained both tumor tissue and healthy adjacent tissue from each patient following the prostatectomy procedure, resulting in a total of six samples. A single-cell suspension was prepared using an in-house tissue digestion protocol. To enrich the sample for leukocytes, a purification step was employed. This involved labeling the single-cell suspension with PE Anti-Human CD45 antibody and isolating the CD45+ population using anti-PE Miltenyi beads (see Method Section). Following this procedure, we obtained a sample comprising more than 90% CD45+ cells. Subsequently, we employed the 10x Genomics Chromium Single Cell Gene Expression assay for scRNAseq analysis.

After completing this procedure, a combined total of 55,701 cells were obtained by integrating the datasets from each of the six samples (Figure 22). The differential gene expression analysis was performed among all clusters and the top 5 specific markers for each cluster were represented in a Dotplot (Figure 22 B). The UMAP visualization provided a comprehensive overview of cellular heterogeneity within the analyzed tissue, highlighting distinct cell populations. Heterogeneous cell populations were identified and grouped in 17 distinct clusters, each characterized by specific gene expression profiles (Figure 17A).

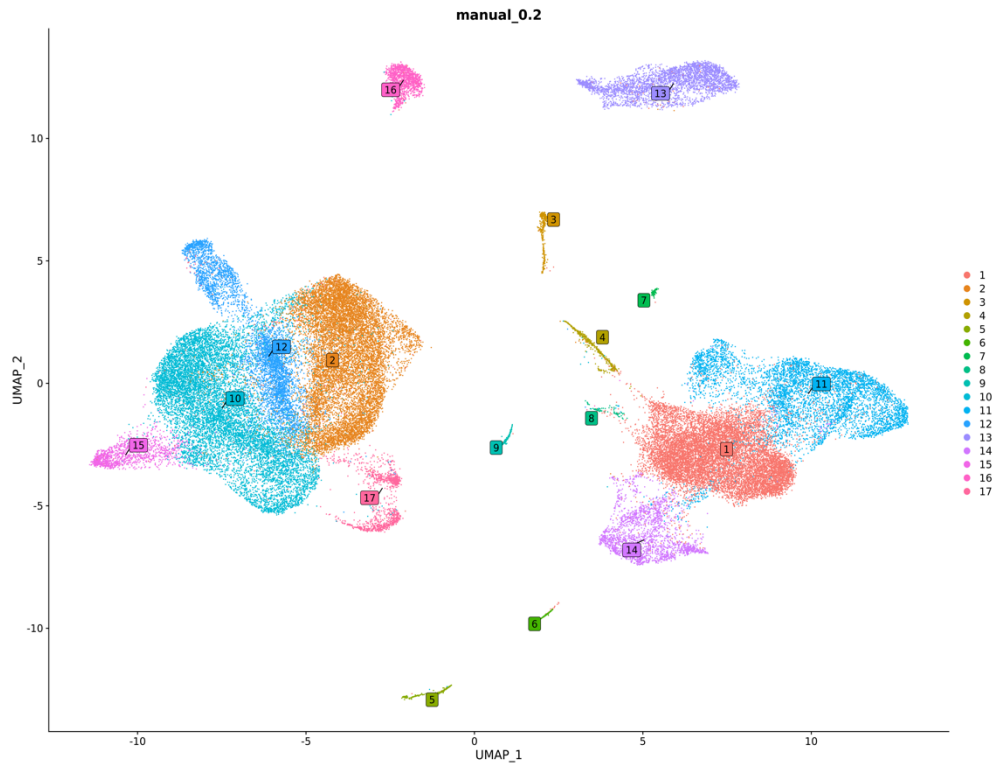
A**B**

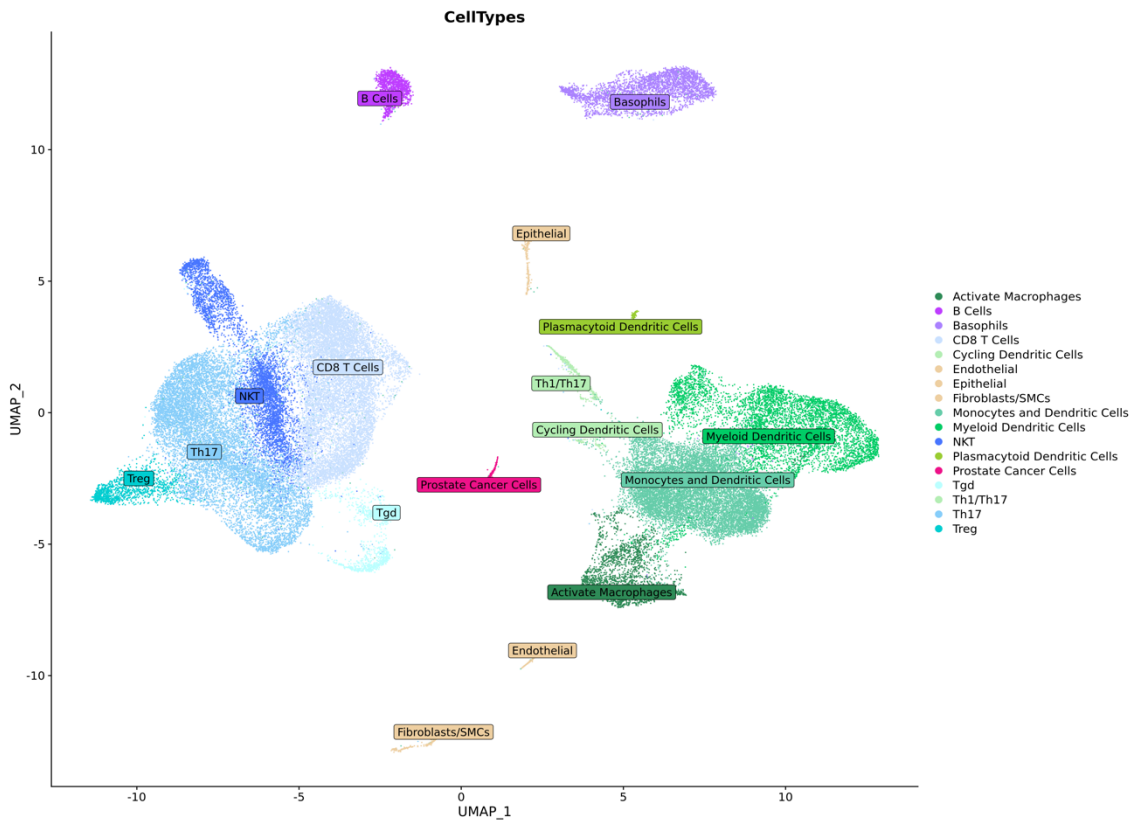
Figure 22. Single Cell RNA sequencing analysis on CD45+ cells. (A) Uniform Manifold Approximation and Projection (UMAP) visualization of single-cell RNA sequencing data. Each point represents an individual cell, colored by cell type or cluster identity determined through unsupervised clustering. **(B)** Dotplot describing the differential gene expression among all clusters. The top 5 specific markers for each cluster were represented.

Cells were annotated as Active Macrophages, B cells, Basophils, CD8 T cells, Dendritic Cells, Endothelial, Epithelial, Fibroblasts, Monocytes, Myeloid, NKT, Plasmacytoid cells, PCa cells, Tgs, Thq, Th17, and T reg based on established marker genes (Figure 23 A). PCa cells were distinguished by the expression of luminal epithelial (LE) markers KLK3, KLK2, and MSMB, consistent with LE cells being the predominant epithelial cell type in PCa samples. Endothelial cells were characterized by SPARCL1 and SELE expression, while fibroblasts expressed IGFBP5 and IGFBP7. T cell compartments were identified by high-level expression of IL7R, CD8A, and CD4, while the B cell cluster showed high expression levels of MS4A1 and CD79A.

Our cohort comprised three specimens of PCa tissue with matched benign tissue. We evaluated whether the tumor compartment and the healthy counterpart showed a similar distribution of different cell types across samples. As anticipated, major cell types were detected in each sample, with T cells (CD8+ and CD4+) constituting the most abundant population (Figure 23 B).

We noted a notable rise in the quantity of CD8+ and CD4+ cells within the healthy compartment, alongside elevated frequencies of monocyte and myeloid cells in tumor samples ($P < 0.05$, Mann–Whitney U test) (Figure 23 B). These results were predominantly influenced by one patient (#patient 2), where the tumor compartment exhibited a significant enrichment of monocyte cells.

A



B

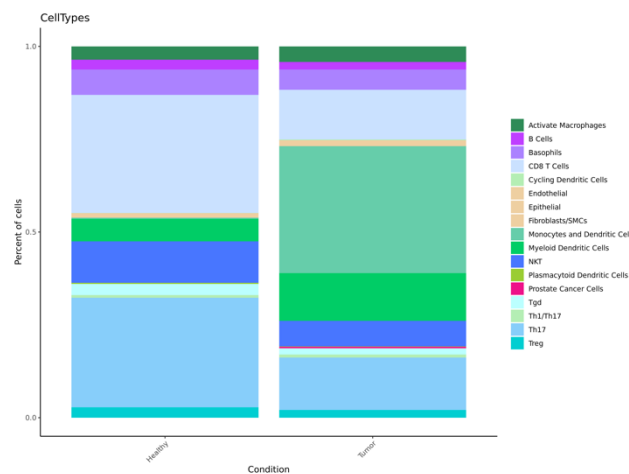


Figure 23. Characterization of immune populations in prostate samples by single cell RNA sequencing. A) Uniform Manifold Approximation and Projection (UMAP) plot illustrating the clustering of cells based on single-cell RNA sequencing data. Each point represents an individual cell, with colors indicating distinct clusters identified through unsupervised clustering algorithms. Cell clusters were annotated based on marker gene expression profiles and known cell type characteristics. (B) Bar plot illustrating the relative abundance of major cell populations identified in the RNA single-cell analysis. Left) Health Tissue and right) PCa Tissue. Each bar represents the percentage composition of different cell types within the analyzed sample. Cell populations are annotated based on known marker genes and biological functions

5.3.2 Intracluster Analysis of CD8B Gene-Expressing Cells in Prostate Tissue

To identify the transcriptional cell states of CD8⁺ cells associated with PCa, we focused on cells belonging to the T cell cluster which expressed the CD8B gene (Figure 24 A). The spatial arrangement of cells on the UMAP plot reflects the underlying transcriptional similarities, revealing a distinct cluster CD8 within the tissues. The integrated dataset was therefore subset to keep only these cells and a new integration was performed (Figure. 24 B).

The clustering on the CD8B⁺ cells subset revealed 7 distinct clusters representing CD8⁺ subpopulations within the prostate tissue. The spatial arrangement of cells on the UMAP plot (Figure 24 C) revealed a notable overlap between healthy and tumor samples across all clusters. Indeed, the analysis did not demonstrate populations that were significantly overrepresented by tumor samples compared to healthy tissues.

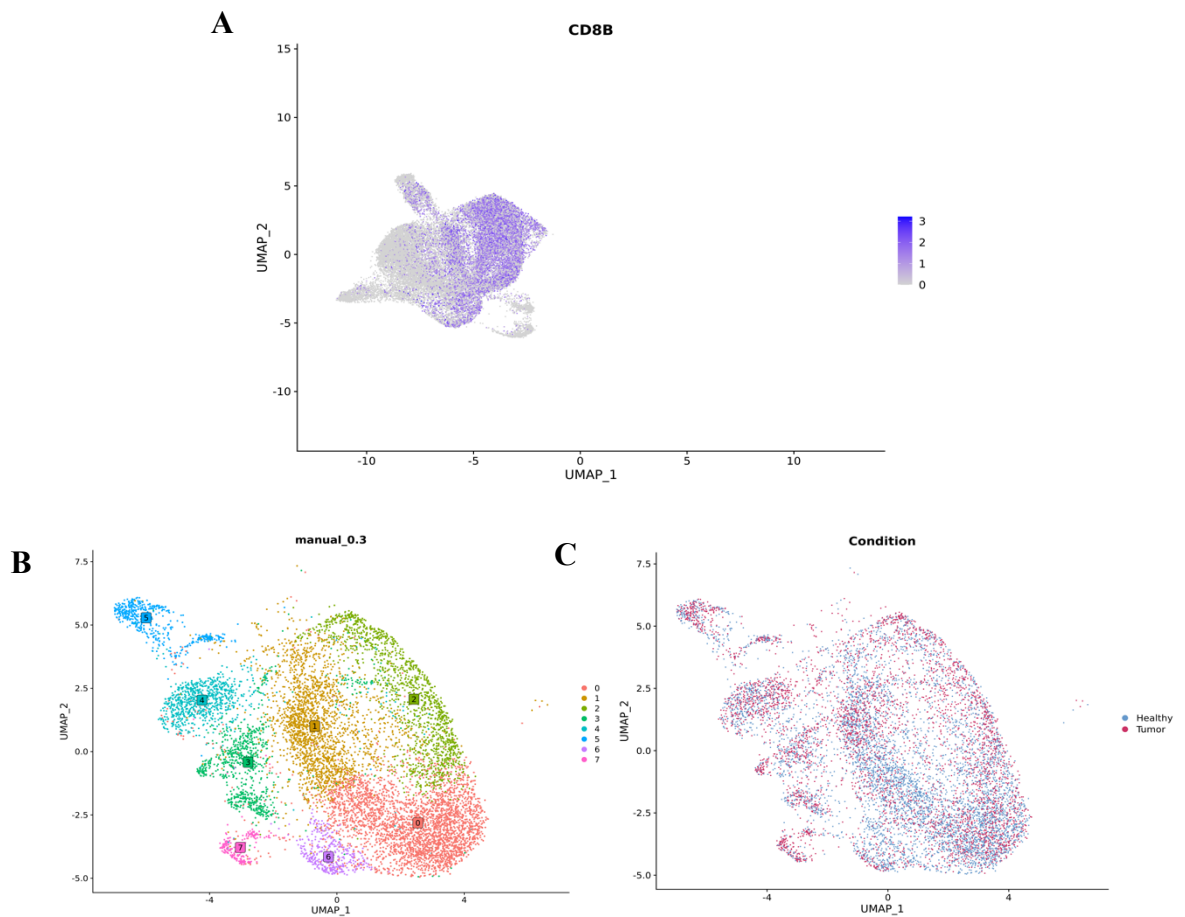


Figure 24. CD8B Gene Expression on CD45+ prostate populations. **A)** Uniform Manifold Approximation and Projection (UMAP) plot illustrating the cellular landscape of prostate tissue with a focus on CD8B gene expression-positive cells. Each point represents an individual cell, color-coded based on expression levels of CD8B. Cells expressing detectable levels of CD8B are highlighted in blue, while non-expressing cells are shown in grayscale. **B)** UMAP) plot illustrating the clusterization of CD8B expressing cells. Each point represents a single cell colored according to its assigned cluster. The UMAP visualization reveals 7 distinct clusters of CD8B expressing cells based on their transcriptional profiles. **C)** UMAP plot displaying the distribution of cells from healthy and tumor samples across distinct clusters. Each dot represents an individual cell, colored according to its sample origin (healthy in blue and tumor in red) and clustered based on gene expression profiles.

The top marker genes for each cluster were detected through the FindAllMarkers function of Seurat (Vandenbon & Diez, 2020) and plotted in a heatmap that shows a well-defined pattern of gene expression for all the clusters. A total of eight distinct T cell subpopulations were identified: a CD8+ naïve-like population, CD8+ NKT-like cells, activated T cells, GMZK+ effector memory cells, cytotoxic T cells, activated effector memory cells, tissue-resident effector memory cells, and regulatory T cells (Figure 25).

In detail, the CD8+ naïve-like subset was characterized by the presence of CCR7 and SELL, tissue-resident memory T cells (TRM) were distinguished by CXCR6 expression, activated T cells exhibited Heat Shock Proteins, activated effector memory cells showed CCL4, CCL3, IFNG, and XCL1 expression, GMZK effector memory T cells (TEM) were identified by GZMK and ENC1, NKT cells expressed FGFBP2, NKG7, and GLNY, cytotoxic T cells were marked by Metalloproteinases, ANXA, and XCL1, and regulatory CD8 T cells (HLA-DR+) were recognized by the presence of HLA-DR and CD74 (Figure 25 B). All clusters were evenly distributed between tumor and healthy counterparts (Figure 25 C).

It is noteworthy that there was exclusively a reduction in TRM cells in the tumor population. This finding aligns with the protein levels measured via flow cytometry in prior experiments. These experiments, confirming our previous observations, demonstrated that the decrease in this compartment serves as a promising prognostic indicator for high-grade PCa.

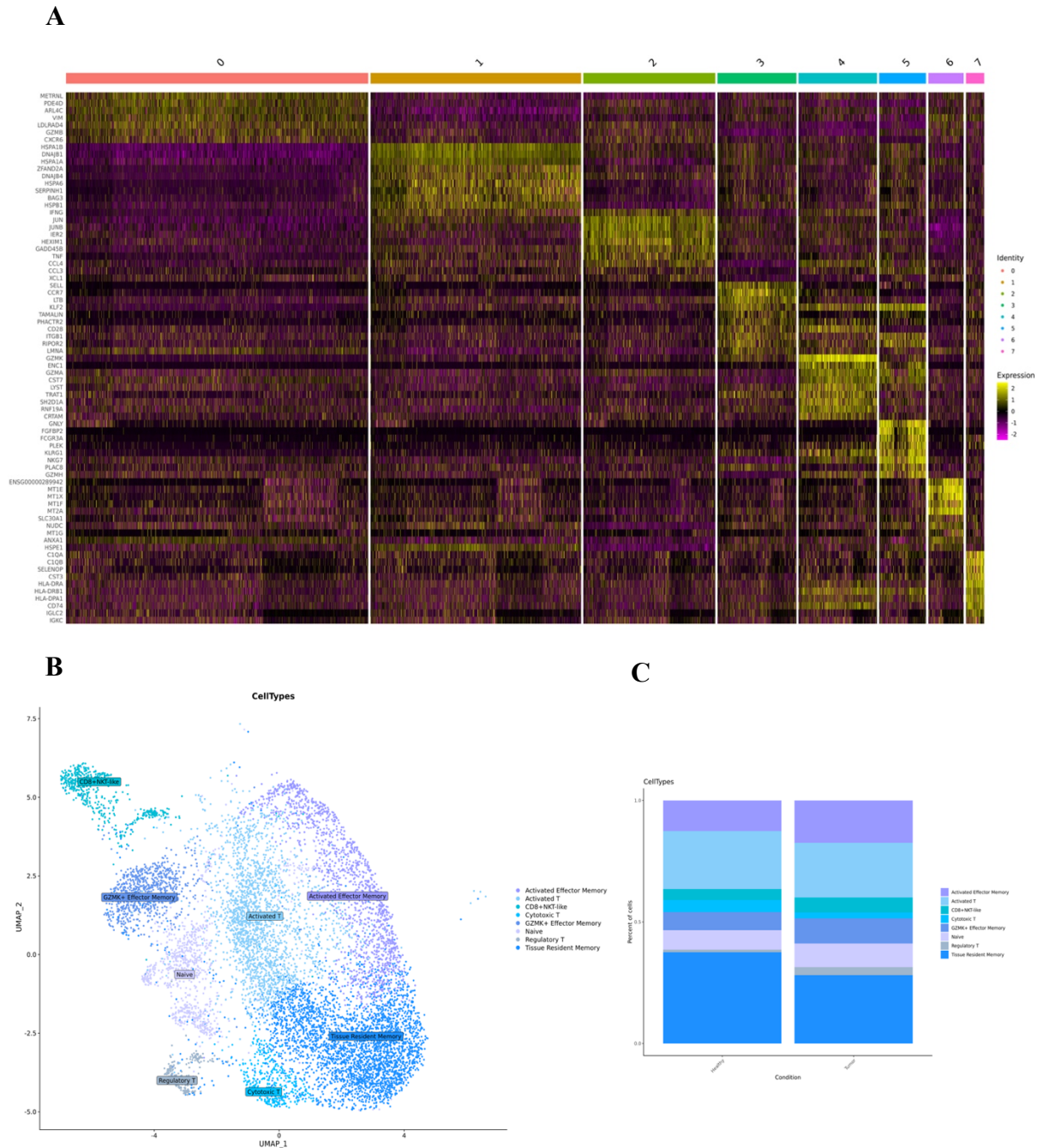


Figure 25. Single-cell analysis of CD8⁺ populations in prostate samples. (A) Heatmap depicting the expression profiles of top genes across 8 distinct single-cell clusters identified through RNA sequencing analysis. Each row represents a gene, while each column represents a single-cell cluster. The color intensity indicates the level of gene expression, with warmer colors representing higher expression levels and cooler colors indicating lower expression levels. The heatmap highlights the unique gene expression signatures characterizing each cell cluster. **(B)** Uniform Manifold Approximation and Projection (UMAP) plot illustrating the clustering of cells based on single-cell RNA sequencing data. Each point represents an individual cell, with colors indicating distinct clusters identified through unsupervised clustering algorithms. Cell clusters were annotated based on marker gene expression profiles and known cell type characteristics. **(C)** Bar plot illustrating the relative abundance of CD8⁺ T cell populations identified; Left) Health Tissue and right) PCa Tissue.

5.3.3 Characterization of transcriptional profiles in CD8+CD103+ T cells

The cells annotated as Tissue Resident Memory cells showed the ITGAE gene (encoding for the integrin alpha E protein, also known as CD103) among the main top marker genes that characterize the cluster. Even if the feature plot revealed the presence of ITGAE in various CD8 subpopulations, the combined expression of CXCR6 and ITGAE was observed within a specific region of the plot. Additionally, a Violin plot graphically displaying the expression of the ITGAE gene across the different CD8 subpopulations. The expression patterns reveal varying levels of ITGAE across the clusters, but confirmed its enrichment within the population previously defined as Tissue Resident Memory (Figure 26 A). This finding allowed us to attribute the CD8+ CD103+ population to this specific cellular subclass (Figure 26 B).

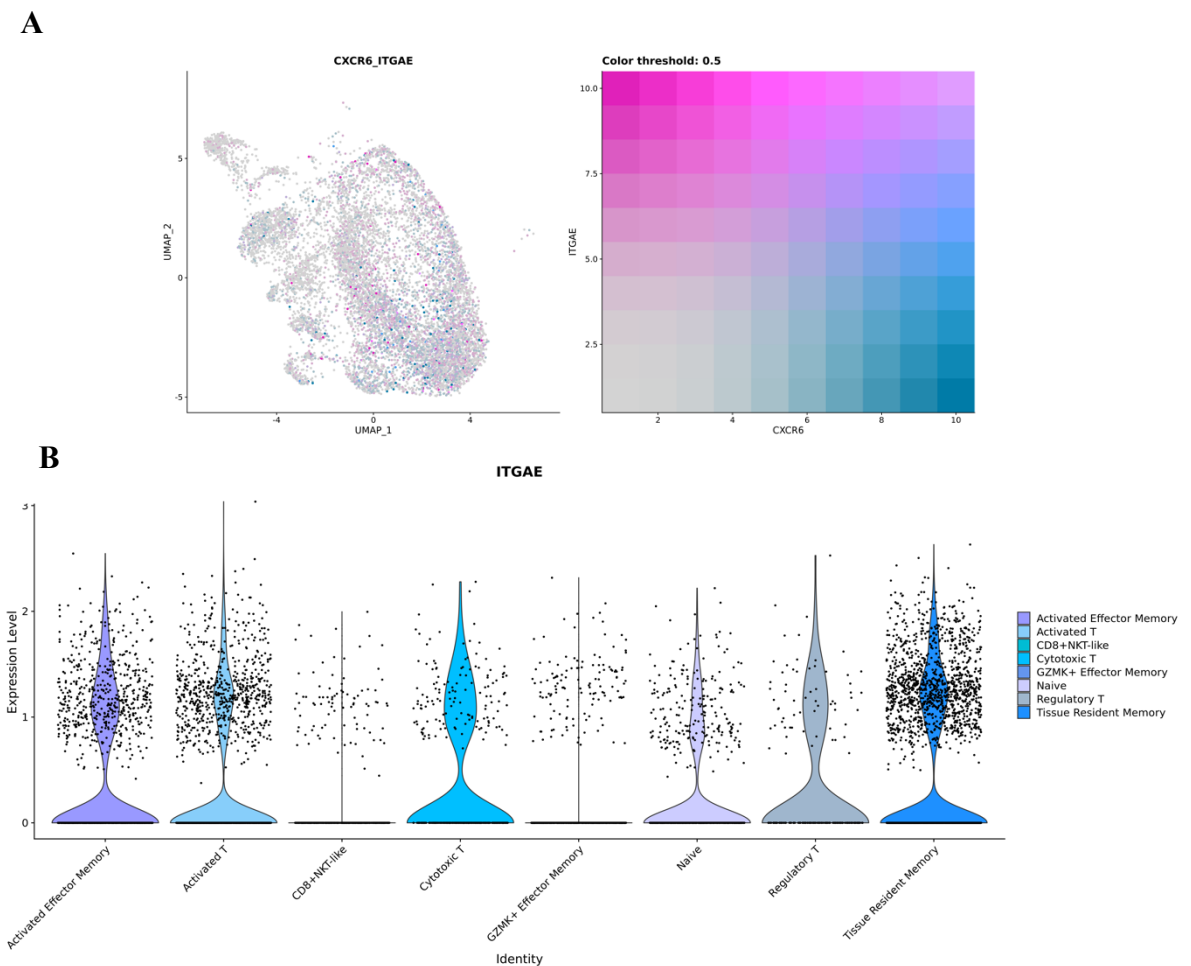


Figure 26. ITGAE gene expression in CD8+ T cells of prostate samples. (A) UMAP visualization of single-cell RNA sequencing data showing the spatial distribution of cells expressing CXCR6 (in blue) and ITGAE (in red). Each point represents an individual cell, with colors indicating the expression levels of CXCR6 and ITGAE, thresholded at 0.5. Blue points represent cells with higher expression of CXCR6, while red points indicate cells with elevated expression of ITGAE. **(B)** Violin plot displaying the expression levels of the gene ITGAE in eight distinct clusters of CD8+ T cells. Each violin plot represents the distribution of ITGAE expression within a specific cluster, with the width of the plot corresponding to the density of cells at different expression levels.

After categorizing CD103+ CD8+ cells as resembling a TRM phenotype, we sought to investigate the genes that significantly differentiate samples from tumor tissues compared to those from healthy tissues. Again, we confirmed the presence of the ITGAE gene (CD103) within our study population.

The exploration of gene expression patterns between tumor and healthy groups revealed distinct profiles, as depicted in the violin plots. Among the myriad of genes analyzed, we identified 8 of them as differentially expressed, showcasing significant alterations in their expression levels between the two cohorts. These genes, namely RGS1, IRF2BP2, IRF1, IL2RB, NFKB1, NFKB2, FAS and ICOS, exhibited notable variations in expression, with the tumor group displaying either upregulation or downregulation compared to the healthy cohort. The violin plots vividly illustrate the distribution and density of expression values for each gene, providing a comprehensive visual representation of the differential expression landscape (Figure 27). Among these genes, we identified RGS1 to be upregulated in tumor samples compared to healthy tissues, while IRF2BP2, IRF1, IL2RB, NFKB1, NFKB2, as well as FAS and ICOS to be downregulated (fold change ranging from +1.10 to -0.56).

Notably, these genes play pivotal roles in the regulation of cytokine production (RGS1, IRF2BP2, IRF1, IL2RB, NFKB1, NFKB2) or cellular vitality, particularly following antigenic stimulation (FAS and ICOS)(Peng et al., 2022). It's remarkable that all genes encoded for the measured cytokines at a protein levels (IL-2, TNF α , and IFN γ) exhibit a reduction in CD103+ CD8+ cells isolated from tumor tissues (Figure 27). At the same time, the RGS gene was found to be upregulated in tumoral TRM cells, indicating a dysfunctional profile, since its high expression has been shown to inhibit immune cell functions (von Werdt et al., 2023).

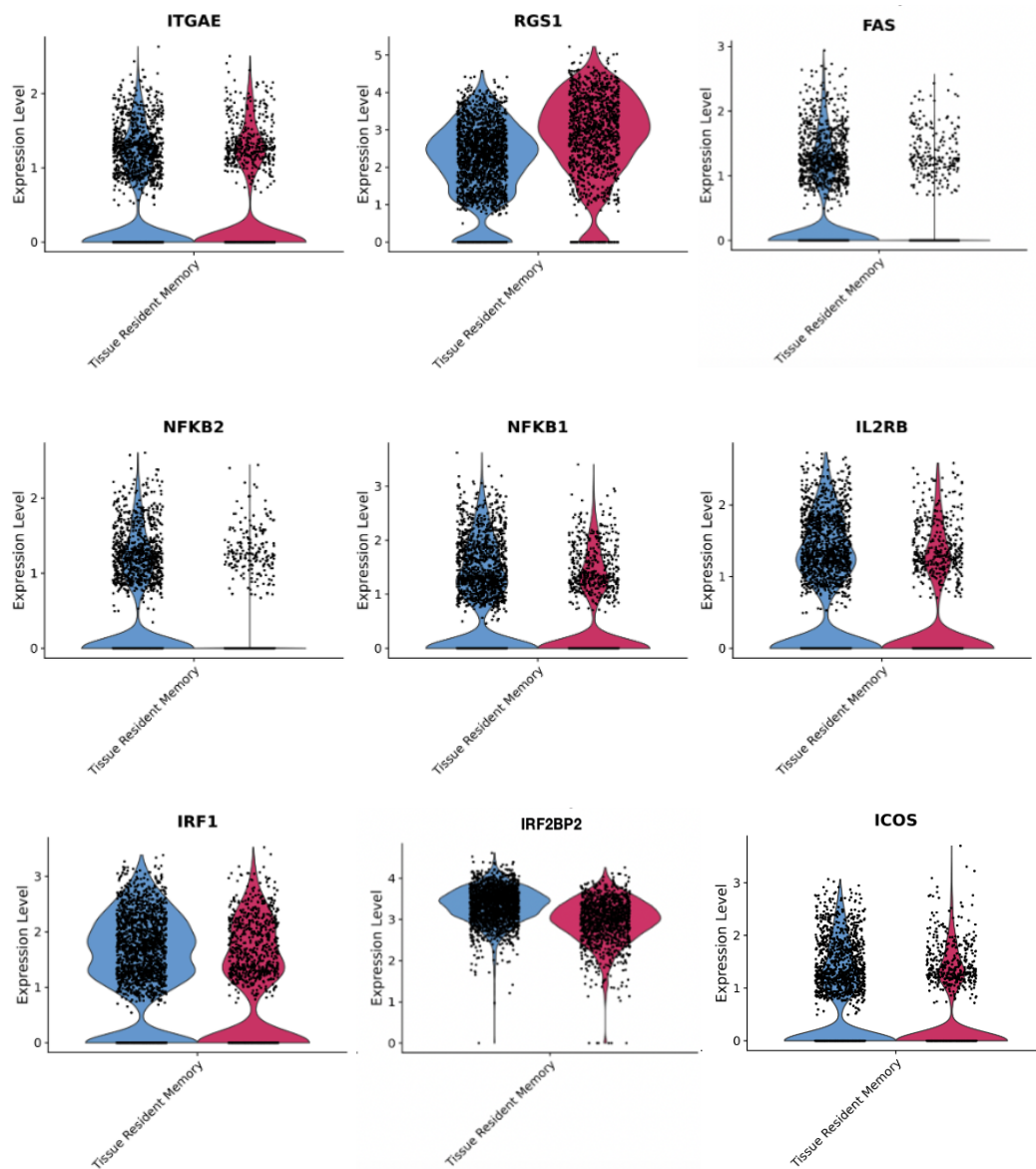


Figure 27. Differential Expression of Cytokine-Associated Genes in CD103+ CD8+ T Cells from Tumors and Healthy prostate tissue. Violin plot displaying the expression levels of 9 genes obtained from single-cell RNA sequencing analysis comparing tumor samples ($n=3$) to control samples ($n=3$). Each violin plot represents the distribution of gene expression within the two groups, with the width indicating the density of expression values. The median expression level is denoted by a horizontal line within each violin, while the interquartile range is represented by the width of the violin. Notably, gene *RGS1* exhibit significantly higher expression in tumor samples compared to controls, whereas all the other genes (*FAS*, *NFKB2*, *NFKB1*, *IL2RB*, *IRF1*, *IRF2BP2*, *ICOS*) show reduced expression in tumor samples. Gene *ITAGAE* demonstrates comparable expression levels between the two groups.

5.3.4 Flow Cytometry Analysis of Cytokine Production in CD8+ and CD8+CD103+ T Cells

To explore the functional significance of exhaustion phenotypes in CD8+ T cells, we evaluated the secretion of cytotoxic cytokines, such as granzyme B (GrzB), IL-2, TNF α , and IFN γ , in several human samples obtained from patients undergoing RP. Samples were procured through immediate evaluation of surgical margins by expert uropathologists. The study cohort comprised 39 samples, encompassing 14 disease-negative (control), 11 clinically insignificant disease (Gleason Score 6), and 14 samples of clinically significant disease (Gleason score 7-10). Patients exhibited variability in disease stage at prostate biopsy but were consistent in terms of PSA levels and other preoperative parameters (Table 7).

	Control	Insignificant PCa	Clinically Significant PCa
N patients (N 39)	14	11	14
PSA	9,3	7,9	8,4
Gleason Score	NA	6	7-10
Surgical Margines	0	0	0
Positive nodes	0	0	2

Table 7. Patient Composition and Characteristics for Flow Cytometry Analysis of Cytokine Production

After polyclonal stimulation with PMI and Ionomycin for 5 hours, we noted a gradual reduction in intracellular secretion of IL-2, TNF α , and IFN γ in CD8+ cell samples derived from individuals with CS PCa, (Gleason Score 7-10). Specifically, TNF α and IFN γ exhibited significant differences only between the control and CS PCa groups ($p < 0.01$). No reduction in GrzB production was observed across different disease grades. Regarding IL-2 production, we noted a statistically significant reduction across all three groups analyzed: Control vs. CS PCa ($p < 0.001$), Control vs. CS PCa ($p < 0.01$), and Ins Ca vs. CS PCa ($p < 0.05$) (Figure 28 B).

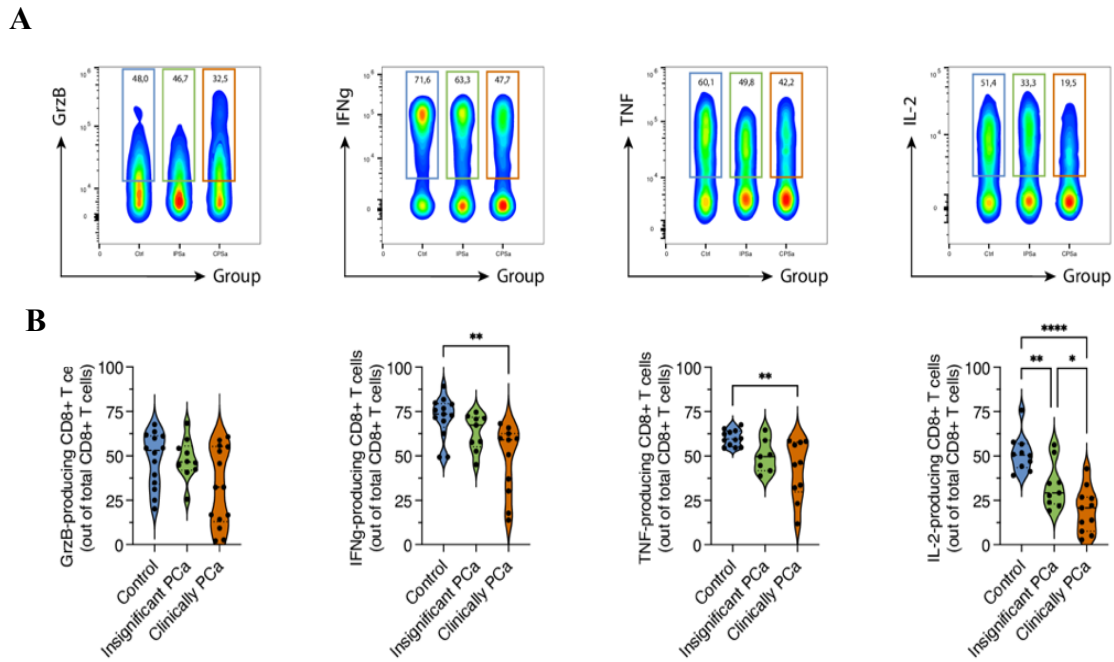


Figure 28 Cytokine production capacity of CD8⁺T cells in prostate cancer tissue samples. (A) Representative FACS plot that represent CD8⁺T cells Grzm-B, TNF- α , IFN-g and IL-2 production (Y axis) in indicated groups of patients (X axis). CD8⁺ T cells were pre-gated on Live, CD45⁺, CD4⁺, CD19⁻, CD8⁺ cells. (B) Violin plots showing frequency of Grzm-B, TNF- α , IFN-g and IL-2 producing CD8⁺T cells of indicated groups of patients stratified basing on relative level of risk disease: healthy control (blue), insignificant PCa (green) and clinically significant PCa (orange). Dots represent individual samples. Data are expressed as mean \pm SEM. Statistics: ns p-value > 0.05, * p-value \leq 0.05, ** p-value \leq 0.01, *** p-value \leq 0.001, **** p-value \leq 0.0001, Kruskal-Wallis Test.

In the gating strategy depicted (Figure 29 A), CD8⁺ T cells demonstrated the capacity to produce multiple cytokines concurrently. To investigate the capacity to produce multiple cytokines simultaneously, five subsets of cytokine-producing cells were defined in relation to the gating strategy proposed above (Figure 29 C). These scenarios range from complete production of all four cytokines (cluster 4, yellow) up to the incomplete capacity to produce any measured cytokines (cluster 0, blue). Once again, CD8⁺ cells derived from a high-grade tumor environment appear to be predominantly dysfunctional, lacking the ability to produce cytokines (Control vs. CS PCa or IPCa vs. CSPCa; p value < 0.01). Similarly, CD8⁺ cells from healthy individuals or those with low-grade disease

seem to retain their cytokine-producing activity (Figure 29 B). Consequently, we observe a transition of these cells from a multifunctional state to a dysfunctional one.

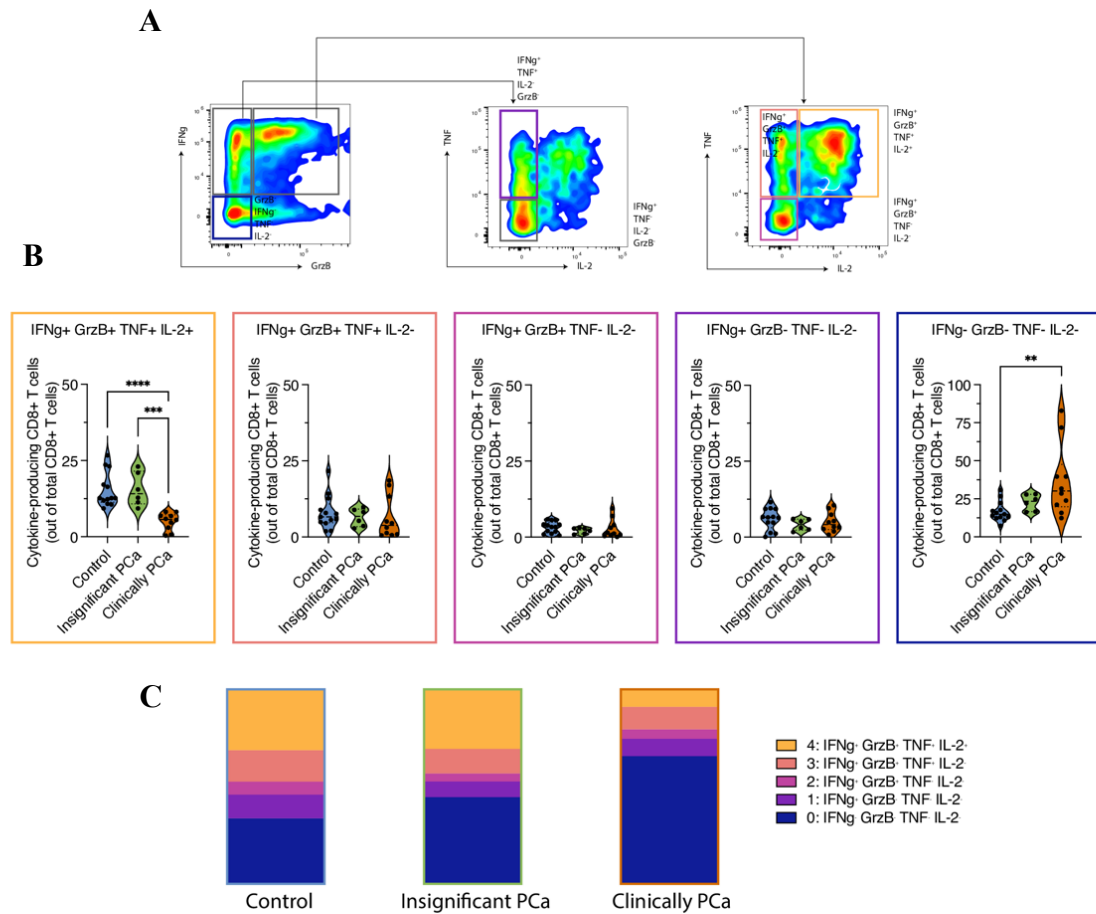


Figure 29. Reduced cytokine production capacity of CD8⁺T cells from high grade prostate cancer tissues. (A) Gating strategy utilized in order to identify indicated groups of interest of cytokine-producing CD8⁺T cells. CD8⁺T cells were pre-gated on Live, CD45⁺, CD4⁺, CD19⁻, CD8⁺ cells. (B) Violin plots showing frequency of indicated combination of cytokine-producing and non-producing CD8⁺T cells of indicated groups of patients stratified basing on relative level of risk disease: healthy control (blue), insignificant PCa (green) and clinically significant PCa (orange). Dots represent individual samples. (C) Proportion plot depicting frequency of indicated cytokine-producing CD8⁺T cell subsets in control (left), insignificant PCa (middle) and clinically significant PCa (right) patients. Data are expressed as mean ± SEM. Statistics: ** p-value ≤ 0.01, *** p-value ≤ 0.001, **** p-value ≤ 0.0001, Kruskal-Wallis Test.

After comprehending a dysfunctional state within the CD8 compartment, we aimed to focus our attention on the TRM population. This population exhibited a diminished transcriptional activity in genes encoding for IL2, TNF α , and IFN γ (Figure 27). However, we sought to confirm through intracellular flow cytometry whether they also displayed reduced cytokine production. The gating strategy for tissue-resident

memory cells comprised a CD8⁺ population doubly positive for CD103 and CD69 (Figure 30 A). This population was compared with CD8⁺ CD103⁻CD69⁻ cells.

TRM cells originating from clinically relevant tumors (Gleason Score 7-10) further confirmed their inability to produce essential cytokines crucial for homeostasis, killing, and antitumor control through flow cytometry analysis. Specifically, TRM cells from the CS PCa cohort exhibited a significant reduction when compared to healthy controls or individuals with insignificant pathologies in all studied molecules: IFN γ ($p < 0.01$), TNF α ($p < 0.05$), and IL2 ($p < 0.01$). The same trend was identified in the remaining CD8⁺ cells, which evidently displayed a general dysfunctional phenotype (Figure 30 B).

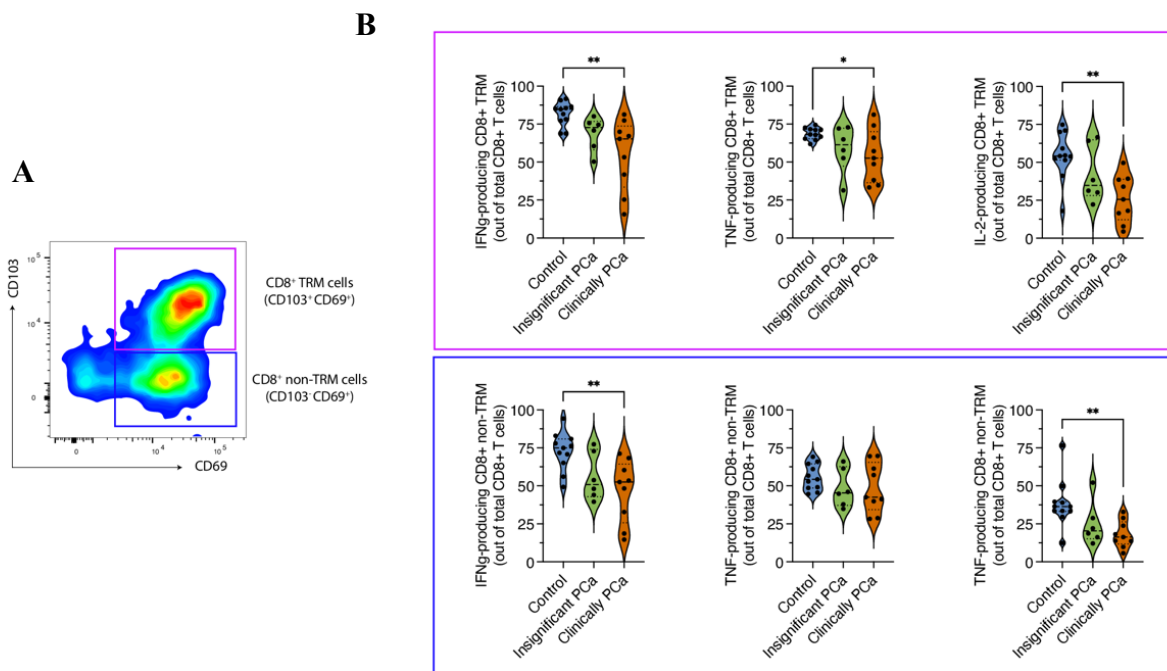


Figure 30. Reduced cytokine production capacity of tissue-resident memory CD8⁺T cells from clinically relevant tumors. (A) Gating strategy utilized in order to identify indicated groups of interest of TRM (resident memory) or non-TRM (non-resident memory) CD8⁺ T cells. CD8⁺ T cells were pre-gated on Live, CD45⁺, CD4⁻, CD19⁻, CD8⁺ cells. (B) (up) Violin plots showing frequency of IFN-g, TNF-a and IL-2 producing TRM CD8⁺T cells of indicated groups of patients stratified basing on relative level of risk disease: healthy control (blue), insignificant PCa (green) and clinically significant PCa (orange). Dots represent individual samples. (bottom) Violin plots showing frequency of IFN-g, TNF-a and IL-2 producing non-TRM CD8⁺T cells of indicated groups of patients stratified basing on relative level of risk disease: healthy control (blue), insignificant PCa (green) and clinically significant PCa (orange). Dots represent individual samples. Data are expressed as mean \pm SEM. Statistics: * p -value ≤ 0.05 , ** p -value ≤ 0.01 , Kruskal-Wallis Test.

5.3.5 Cytokine Production in CD4⁺ T Cells Using Flow Cytometry

Additionally, we deemed it appropriate to study the cytokine production in CD4 cells after investigating CD8 cells, considering the interdependence that exists between both T cell populations and the help that a CD4 T cell can provide to a CD8 T cell in an antitumoral response. Understanding the cytokine production patterns in both CD4 and CD8 cells provides a comprehensive picture of the immune response in the analyzed patients. It's interesting to note that the CD4 T cells in the TME of relevant tumors also exhibits reduced production of IL-2, IFN γ and TNF α (Figure 31), three key cytokines for the cytotoxic effector function of anti-tumoral CD8 T cells.

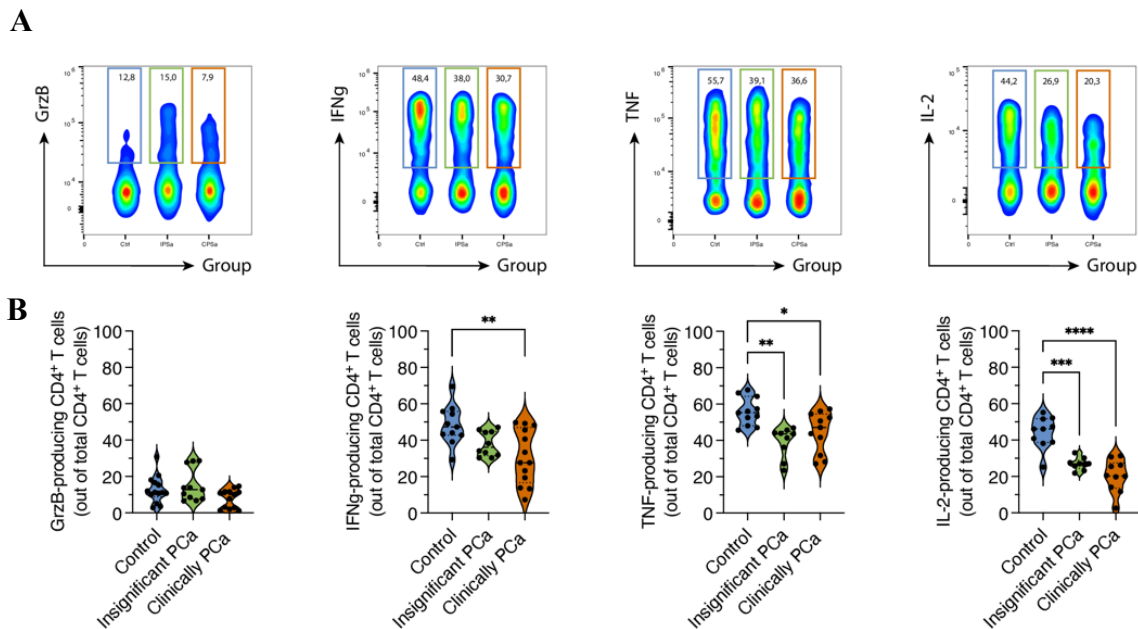


Figure 31. Reduced cytokine production capacity of CD4⁺T cells from clinically significant . (A) Representative FACS plot that represent frequency of CD4⁺T cells producing Grzm-B, TNF-a, IFN-g and IL-2 (Y axis) in indicated groups of patients (X axis). CD4⁺ T cells were pre-gated on Live, CD45⁺, CD8⁻, CD19⁻, CD4⁺ cells. (B) Violin plots showing frequency of Grzm-B, TNF-a, IFN-g and IL-2 producing CD8⁺T cells of indicated groups of patients stratified basing on relative level of risk disease: healthy control (blue), insignificant PCa (green) and clinically significant PCa (orange). Dots represent individual samples. Data are expressed as mean \pm SEM. Statistics: * p-value \leq 0.05, ** p-value \leq 0.01, **** p-value \leq 0.0001, Kruskal-Wallis Test.

6 DISCUSSION

Prostate cancer (PCa) exhibits significant heterogeneity, manifesting in diverse clinical behaviors and outcomes (N. Mottet, 2023). The delineation of prognostic classifications, such as low, intermediate, and high-risk groups, has become pivotal in guiding therapeutic decisions. Current clinical paradigms rely on various prognostic biomarkers, including genetic signatures, to refine risk stratification and personalize treatment strategies. However, while genetic markers are readily accessible in the biomedical and molecular diagnostics realm (Cucchiara et al., 2018), a thorough comprehension of the disease still requires the identification and characterization of cellular markers (Haffner et al., 2021).

Notably, the involvement of lymphocytes in the TME is emerging as a crucial determinant of cancer progression and response to therapy (Ge et al., 2022). The integration of genetic and cellular markers holds promise in enhancing the accuracy of prognostication and facilitates the selection of better therapeutic interventions for individual patients. Consequently, a holistic approach that combines genetic and cellular markers may yield more accurate assessments of PCa prognosis and guide clinicians towards the most effective treatment modalities.

Despite the significant progress that has already been achieved in characterizing the TME in terms of gene expression of infiltrating cells (Chen et al., 2021; Xin et al., 2023), the protein composition of these cells and, furthermore, their functionality, which could potentially be damped, remains certainly unclear (Hirz et al., 2023).

Numerous efforts have been undertaken to identify immunological markers in peripheral blood samples from PCa patients (Baxevanis et al., 2023; Gallazzi et al., 2021). Given the diverse cellular populations responsive to stimuli unrelated to prostate neoplasia, our study suggests the current lack of a specific cellular population capable of accurately stratifying patients across different risk classes or predicting oncological outcomes, such as disease recurrence, at least using the markers present in the study.

Consequently, our research underscores prostate tissue as the most reliable biological material for such purpose. Tumor-infiltrating lymphocytes encompass a diverse number of immune cells, exhibiting variability in specificity, differentiation, and function (Ozbek et al., 2022)(Eiva et al., 2022; Rosenberg et al., 2008). In PCa, the

characterization of specific subsets of T cells presents a formidable challenge, as conventional immune checkpoint molecules such as PD-1 (Programmed cell Death protein 1) or CTLA-4 (Cytotoxic T-Lymphocyte Associated Protein 4) inadequately discriminate between distinct T cell populations within the TME (Seidel et al., 2018). Although the blockade of PD-1 and CTLA-4 has proven effective in some malignancies by augmenting general T cell activation and effector functions, its applicability in PCa remains restricted. This limitation may stem from the heterogeneous nature of the T cell landscape (Sena et al., 2021) or the low expression observed in intratumoral T cells (M. Sharma et al., 2019). In our study, we verified that PD1 or CTLA4 expression does not change significantly between the CD4⁺ and CD8⁺ populations derived from high-grade tumor environments compared to their healthy counterparts within the same patient. A previous report has indicated that only a minority of PCa patients may derive benefits from anti-PD-L1 therapy (Vitkin et al., 2019). Additionally, intratumoral PD-L1 expression proves inadequate in identifying the subset of the population that would benefit from this therapy (Antonarakis et al., 2020b).

In this study, we validated the reliability of multiplex immunofluorescence for quantifying T cell subsets in primary prostate carcinomas. We also emphasized the importance of accurately discerning the spatial distribution of the inflammatory infiltrate. It becomes fundamentally crucial to perform a separate analysis between the intraepithelial and the stromal population. Quantifying individual cell populations, such as CD8⁺ cells, may yield contrasting results (Leclerc et al., 2016; Petitprez et al., 2019a). Moreover, we established that the infiltration of T cells into the stromal compartment could function as a potential prognostic marker for nodal metastasis. A decline in CD8⁺ T cells and an elevation in CD4⁺ cells within the stromal compartment were observed to be significantly correlated with nodal involvement in PCa patients.

In addition to spatial localization, the identification of a specific cellular subset is also of paramount importance. Our observation of elevated levels of CD4⁺ cells in the stroma may be inconsistent with recent findings indicating a significantly lower presence of CD4⁺ effector T cells in the stromal compartment of patients with nodal metastasis (Ntala et al., 2021). It is important to highlight that our data, unlike the aforementioned study, encompass the entire CD4⁺ population rather than focusing solely on specific subsets such as CD4⁺ effector cells.

Recent investigations have shed light on the presence of functionally diverse CD8⁺ subsets characterized by varying phenotypic and functional attributes, such as exhausted, effector, and memory subsets (Koh et al., 2023). These subsets play distinct roles in modulating tumor immune responses and influencing patient outcomes.

Tissue-resident memory T cells (TRMs), identified by surface markers such as CD69 and CD103, play pivotal roles in immunosurveillance and host defense within peripheral tissues (Schenkel & Masopust, 2014). Upon antigen exposure, these cells become activated and migrate to non-lymphoid tissues, where they establish a long-term residence (Masopust & Soerens, 2019). The integrin alpha subunit CD103 aids in anchoring TRMs within the tissue microenvironment by binding to E-cadherin, a molecule expressed on epithelial cells. Once stationed, TRMs display a memory phenotype, facilitating prompt and potent responses upon subsequent exposure to specific antigens. Through the release of cytokines and direct cytotoxic activity, CD8⁺CD103⁺ TRMs actively participate in immune surveillance, pathogen elimination, and regulation of tumor growth within the tissue milieu (Masopust & Soerens, 2019).

In our study, we identified the presence of CD8⁺ CD103⁺ cells in prostatic tissue. Remarkably, we observed a significant reduction in this particular cellular subset among individuals with high-PCa. Integrating this parameter into clinical predictive models has proven to be a dependable prognostic factor for aggressive disease. Several prior studies have indicated the potential involvement of CD103⁺ CD8 tumor-infiltrating lymphocytes in diverse cancer types, including lung and ovarian cancer (Masopust & Soerens, 2019; Webb et al., 2015a).

Moreover, in alignment with our results, a recent study conducted by Ganesan et al. disclosed that CD103⁺ CD8⁺ tumor-infiltrating lymphocytes in PCa displayed a gene signature characteristic of tissue-resident memory T cells (TRM) (Ganesan et al., 2017). Specifically, our single-cell data revealed an elevated expression of the CXCR6 transcript (encoding the chemokine receptor CXCR6), a crucial factor for the localization and functioning of tissue-resident T cells (L. N. Lee et al., 2011; Tse et al., 2014). Transcripts of S1PR1 (encoding the G protein-coupled receptor S1P1) and KLF2 (encoding the transcription factor KLF2) were also observed to be downregulated in TRM cells (Mackay et al., 2013). These results lend support to the idea of a common gene signature among CD103⁺ CD8 TRM cells across various tissues. Our findings are consistent with

other studies that have reported a positive prognostic role of CD8⁺ CD103⁺ in other tumor pathologies such as ovarian, (Webb et al., 2015b), bladder cancer (B. Wang et al., 2015) and breast cancer (Z.-Q. Wang et al., 2016).

Conversely, Zhou et al. have identified the presence of CD103⁺ cells as an independent prognostic factor for BCR-free survival in prostate disease (Zhou et al., 2023). The authors have associated higher CD103⁺ cell infiltration with decreased survival. However, it is crucial to note that Zhou and colleagues primarily correlated the presence of CD103⁺ T cells, not exclusively CD8⁺ CD103⁺, with oncological outcomes. Although CD8⁺ T cells were identified as the primary cellular source of CD103 (Zhou et al., 2023), other cell populations such as CD4⁺ or DCs may also co-express this marker, thereby reducing the relevance of these results.

Furthermore, our study revealed that compared to their expression in healthy tissue, CD8⁺CD103⁺ TRMs from tumors exhibited reduced expression of genes encoding products involved in cytokine release, among all the differentially expressed genes. Specifically, tumor-infiltrating TRMs display a diminished transcriptional profile of genes such as IRF2BP2, IRF1, IL2RB, NFKB1, and NFKB2.

The reduced production of INF γ (Ariotti et al., 2014; Schenkel et al., 2014), TNF α (Di Mitri et al., 2019b; Srinivasan et al., 2010), and IL2 (Boyman et al., 2015) defines an exhausted and dysfunctional profile incapable of restraining tumor progression. In fact, for TRMs, the recognition of tumor antigens leads to cytokine production and results in direct anti-tumor activity, but it also serves to alert the surrounding environment (sometimes referred to as a sensing-and-alarm function).

Functional TRM cells, on the other hand, are capable of expressing IFN- γ , TNF- α , and IL-2, triggering interferon-stimulated genes in neighboring cells, thereby allowing them to recruit leukocytes and activate DCs, NK cells to limit tumor progression (F. Castro et al., 2018; Medrano et al., 2017). The transcriptional analysis of our TRMs can also explain why, unlike other studies, high-grade tumor tissues present fewer CD8⁺ CD103⁺ cells. ICOS (Inducible T cell COStimulator) and FAS (also known as CD95) are molecules involved in T cell activation, survival, and regulation. They play critical roles in the development, maintenance, and function of various T cell subsets, including memory T cells. Specifically, ICOS signaling is important for the generation and maintenance of TRMs (Takahashi et al., 2009). FAS, on the other hand, is involved in

regulating T cell apoptosis (cell death) and can influence the survival and turnover of memory T cell populations (Arakaki et al., 2014). In our study, we demonstrated a notable decrease in ICOS or FAS signaling or expression, which could potentially affect the development, survival, or upkeep of CD103⁺ CD8⁺ T cells. Nevertheless, additional experimental evidence would be required to validate the precise role of ICOS and FAS in regulating TRMs in PCa.

Furthermore, our research highlights the importance of gating on CD39⁺ cells within the CD103⁺ CD8 population to enrich for an intratumoral T cell subset. We found that within the CD8⁺ cell population, elevated frequencies of CD103⁺CD39⁺ cells are associated with a significantly increased risk of more severe disease pathology or worse oncological outcomes. These cells also exhibit an exhausted phenotype, as evidenced by the presence of markers such as CD39. This phenomenon could be explained by chronic TCR stimulation within the tumor microenvironment, leading to increased expression of exhaustion markers (Canale et al., 2018).

Indeed, CD39 represents another potential immune inhibitory pathway, exhibiting high expression on TRMs. CD39 functions as an ectonucleotidase, catalyzing the hydrolysis of extracellular ATP and ADP into AMP. Subsequently, AMP is converted into adenosine by CD73, an ecto-5'-nucleotidase expressed by numerous tumor cell types (Antonioli et al., 2013). Adenosine serves as a potent immunoregulator; its binding to A2A receptors on T lymphocytes augments the intracellular accumulation of cAMP, resulting in the attenuation of T-cell activation. Disrupting the adenosine pathway by targeting the CD39 axis or adenosine receptors on T cells within the TME represents a potentially promising therapeutic strategy (Duhén et al., 2018). This approach aims to enhance the function and potency of TRMs, offering a novel avenue for therapeutic intervention.

In contrast to previous studies which focused only on CD8⁺ tumor infiltrating cells (Gros et al., 2014), we expanded our analysis to include CD4⁺ T cells as well. The identification of endogenous intratumor-antigen-specific T cells biomarkers in patients has predominantly centered on CD8⁺ T-cell responses (Djenidi et al., 2015; Duhén et al., 2018). However, there is increasing recognition of the importance of CD4⁺ T cells in bolstering antitumor immunity and enhancing the efficacy of immunotherapy (Borst et al., 2018; Tran et al., 2014). Our findings revealed that intratumoral CD4⁺ also exhibit deficiencies in IFN- γ , TNF- α , and IL-2 production. This supports the idea that both

intratumoral CD8⁺ and CD4⁺ play crucial roles in orchestrating antitumor immune responses, each potentially eliciting distinct antitumoral reactions. Further experiments will indeed be necessary to understand the relationship between these two cellular populations.

This study is not devoid of limitations. The low number of cases included in our molecular analysis and in the prediction of pathological outcomes is certainly the most significant. Given the substantial heterogeneity of PCa, we acknowledge that our data are derived from a specific patient population. Consequently, our findings require validation in a larger cohort with extended follow-up to confirm the prognostic significance of TRMs (CD8⁺CD103⁺CD39⁺) as a potential biomarker. Moreover, the cases analyzed in this study were meticulously selected in collaboration with expert pathologists to ensure a well-represented inflammatory infiltrate and might not represent the real scenario in all the patients. Additionally, we recognize that the inflammatory infiltrate of prostate tumors predominantly localizes around and within benign glands and stroma (De Marzo et al., 2007; Ebel et al., 2009; Sfanos et al., 2018).

For this reason, it is conceivable that immune cell populations in PCa may react to antigens associated with benign tissues or other stimuli. This observation adds complexity to the interpretation of anti-tumor immune responses within the prostate. Despite these challenges, our collaboration with specialized pathologists has facilitated the examination of intratumoral or adjacent inflammatory infiltrate using single-cell dissociation techniques (such as flow cytometry and single-cell RNA sequencing). Additionally, in single-cell analysis, we assert that isolating CD45⁺ cells from our sample has notably minimized potential confounders in transcriptomic analysis. However, a subset of stromal/epithelial cells originating from nearby tissue or tumor cells, estimated to be below 10% after internal quality control, may have had a marginal impact on the data's reliability.

This study collectively illustrates that tumor-specific resident memory cells (CD8⁺CD103⁺CD39⁺) could serve as a biomarker for identifying men at elevated risk of aggressive disease. Furthermore, this research has the potential to enhance our comprehension of prostate CD8⁺ TIL biology. Leveraging CD39 and CD103 to identify tumor-reactive CD8⁺T cells in PCa could provide crucial mechanistic insights for evaluating the efficacy of immunotherapeutic interventions.

7 MATERIALS AND METHODS

7.1 Study population

The study population consisted of patients diagnosed with PCa who underwent RP at IRCCS San Raffaele Hospital between 2017 and 2023. Formalin Fixed Paraffin Embedded (FFPE) samples for immunohistochemical and immunofluorescence analysis were selected from 67 patients. Only patients with a diagnosis of localized or locally advanced hormone-sensitive PCa, without the use of adjuvant therapy, were included. Patients with bone or visceral metastasis were excluded, while only those with lymph node metastasis were permitted. All patients were treated between 2017 and 2018 to ensure a minimum follow-up of five years for correlation with oncological outcomes such as biochemical recurrence (BCR).

Fresh samples were obtained from 80 patients undergoing surgery between March 2021 and December 2023. Peripheral blood samples were collected from these patients on the day of surgery. Similar to the tissue samples, only patients with a diagnosis of localized or locally advanced hormone-sensitive PCa without the use of adjuvant therapy, were included. Peripheral blood samples from healthy patients undergoing surgery for Benign Prostatic Hyperplasia (BPH) served as controls.

All patients involved in the study provided informed consent (URBBAN, Version 08.06.2017, and URBBAN Emendament n7-n8), indicating their full understanding and voluntary agreement to participate. This process ensures that each individual comprehends the study's purpose, procedures, potential risks, and benefits before deciding to participate. By signing the informed consent form, patients affirm their autonomy and willingness to contribute to the research.

It is worth noting that all collected samples, including tissues and blood, have been carefully stored within the Urological Research Institute (URI) Biobank. This biobanking serves as a secure repository, preserving the integrity and confidentiality of these valuable specimens for future analyses and investigations. Adherence to ethical guidelines regarding informed consent and proper sample management underscores the commitment to conducting responsible and transparent research, prioritizing patient welfare and scientific integrity.

7.2 Sample Harvesting and Pathological Examination

Surgically resected prostates were obtained from patients who underwent RP surgery at IRCCS San Raffaele Hospital (Milan, Italy). All biological material collected from patients is protected by strict privacy policies and is only harvested for research purposes after express and informed consent was provided to and signed by each patient. Prostates were harvested during the surgical procedure in an aseptic manner. Post-surgery, unfixed prostate tissue was spatially oriented and inked. Following the extemporaneous examination of surgical margins, pieces of tissue were surgically dissected from two different areas (Tumoral vs Healthy) of the peripheral zone tissue. After slicing the sample, the first and last slices were retained for standard histopathology. The residual tissue was utilized for research objectives.

7.3. Tissue digestion and cell staining

Residual tissue not used for tissue slice analysis was used for tissue digestion and cell isolation. This is our protocol for human prostate single cell suspension:

- Take the tissue (usually is preserved in PBS) and discard the medium. Smash it with a scalpel in a petri dish with 5 ml plain DMEM + collagenase IV (1mg/ml) and put it in a 15 ml Falcon tube
- Incubate the cells for 1h 30 min at 37°C rotating
- Centrifuge 1500 x 5min
- Resuspend the pellet with 5ml Trypsin (1:5 diluted) in PBS 1x
- Incubate for 5 min at 37°C
- Smash the single cell suspension in the falcon tube with a 10 ml syringe pink gauge (18G) for 10 times
- Inactivate the trypsin with 10ml DMEM complete
- Filter the cells with 40um strainer in 50ml falcon tube
- Centrifuge 1500 x 5min
- Count the cells

7.4 Isolation of peripheral blood mononuclear cells

Peripheral blood samples were first mixed with PBS and gently applied on top of Ficoll-Paque PLUS (GE Healthcare) in a stratified manner. Subsequent centrifugation was conducted without disrupting the layers. The cells residing in the intermediate layer were then retrieved, subjected to two washes with PBS, and subsequently reconstituted in 1 mL of $1 \times$ PBS + 0.04% BSA solution. Following this, cell count and viability assessments were performed.

7.5 Flow cytometry analysis

Multiparameter flow cytometry was employed to assess the surface expression of cellular subsets residing in the prostate and infiltrating it. Single-cell preparations were appropriately stained, and data acquisition was performed using the Cytex Aurora flow cytometer. Analysis was conducted utilizing FlowJo software version 10.10 (Tree Star Inc., Ashland, OR, USA). The gating strategy involved excluding dead cells, debris, aggregates, and utilizing internal negative controls. Details regarding reagents used are outlined in the accompanying Table 8.

AB	Clone	Fluorochrome	Channel	Company
CD45	HI30	BUV395	UltraViolet 355	BD
CD4	SK3	BUV563	UltraViolet 355	BD
CD14	M5E2	BUV805	UltraViolet 355	BD
CD45RA	HI100	BUV563	UltraViolet 355	BD
CD69	FN50	BUV737	UltraViolet 355	BD
CD15	W6D3	BUV496	UltraViolet 355	BD
CD28	CD28.2	BUV661	UltraViolet 355	BD
PD-1 (CD279)	EH12.1	BV421	Violet 405	BD
CD11b	ICRF44	BV605	Violet 405	BD
CD8	RPA-T8	BV650	Violet 405	BD
HLA-DR	G46-6	BV711	Violet 405	BD
CD103	Ber-ACT8	BV785	Violet 405	BioLegend
KI-67	B56	BV480	Violet 405	BD
CD244 (2B4)	C1.7	Pacific Blue	Violet 405	Campoverde
TIGIT	741182	BV421	Violet 405	BD
CD3	UCHT1	BV480	Violet 405	BD

Zombie aqua	NIR	BV510	Violet 405	BIOLEGEND
CD16	3G8	Alexa Fluor 488	Blue 488	BioLegend
CD56	NCAM16.2	BB700	Blue 488	BD
TNFa	MAb11	Alexa Fluor 488	Blue 488	BIOLEGEND
INF-Y	4S.B3	RB780	Blue 488	BD
CD134 (OX40)	ACT35	BB700	Blue 488	BD
CD163	GHI/61	PE	Yellow Green 561	BioLegend
CD152 (CTLA-4)	BNI3	PE/Dazzle 594	Yellow Green 561	BioLegend
CD11c	3.9	PE/Cyanine7	Yellow Green 561	BioLegend
Foxp3	236A/E7	PE	Yellow Green 561	BD
CD127	HIL-7R-M21	RY586	Yellow Green 561	BD
CD279 (PD-1)	EH12.2H7	PE/Dazzle 594	Yellow Green 561	Campoverde
CCR7 (CD197)	G043H7	PE/Fire 640	Yellow Green 561	Campoverde
CD39	A1	PE/Fire- 810	Yellow Green 561	Campoverde
CD27	M-T271	Pe-Cy7	Yellow Green 561	BD
CD38	S17015A	PE-Fire 700	Yellow Green 561	BIOLEGEND
IL2	MQ1-17H12	R718	Red 640	BD
CD137	4B4-1	APC	Red 640	BIOLEGEND
CD86	FUN-1	APC	Red 640	BD
CD3	UCHT1	Alexa Fluor 700	Red 640	BioLegend
CD19	SJ25C1	APC/Cyanine7	Red 640	BioLegend
CD4	SK3	APC/Fire 810	Red 640	Campoverde
Reagents				
Cytofix/Cytoperm™ Fixation/Permeabilization Kit				BD
Brilliant Stain Buffer				BD

Table 8: List of reagents and antibodies for Multiparameter flow cytometry

7.6 Separation of prostate CD45⁺ T cells

Prostate-specific CD45⁺ cells were isolated from healthy or tumoral samples by initially labeling the cells with anti-PE microbeads (Miltenyi Biotec), targeting the PE-conjugated antibodies bound to CD45. Subsequently, the labeled cells were subjected to magnetic separation using the LS autoMACS® Columns. The autoMACS® system

applies a magnetic field to separate labeled cells from the unlabeled ones, allowing for the isolation of the desired CD45+ cell population.

The antibody used in this experiment was: PE anti-human CD45 (clone HI30), cat: 304008, Biolegend.

7.7 Multiplex Ventana phenotyping

Ventana Ultra (Ventana Medical Systems), which is a fully automated immunohistochemistry staining platform, was used for our analysis.

Sample preparation typically involves the following steps:

1. **Sectioning:** The paraffin-embedded tissue blocks were sectioned into thin slices (usually around 4-5 micrometers thick) using a microtome. These sections are then mounted onto glass slides.
2. **Deparaffinization:** The tissue sections on slides are deparaffinized to remove the paraffin wax.
3. **Antigen Retrieval:** Antigen retrieval is performed to unmask epitopes and enhance antigen detection. This is typically achieved by heating the tissue sections in a buffer solution.
4. **Blocking:** Non-specific binding sites on the tissue sections are blocked using a blocking solution containing proteins such as bovine serum albumin (BSA).
5. **Primary Antibody Incubation:** The tissue sections are incubated with a primary antibody.
6. **Detection:** After washing to remove unbound primary antibody, a secondary antibody conjugated to a detection molecule, such as horseradish peroxidase (HRP) or alkaline phosphatase (AP), is applied to the tissue sections.
7. **Chromogen/Substrate Addition:** A chromogenic substrate solution, such as diaminobenzidine (DAB) for HRP or Fast Red for AP, is added to the tissue sections.
8. **Mounting:** Finally, the stained tissue sections are dehydrated, cleared, and mounted with a coverslip using a mounting medium to preserve the staining and provide optical clarity for microscopy.
9. **Counting:** A manual tally was conducted on the captured images (ImageJ software). Before manual counting, the images underwent preprocessing steps including cropping, scaling to micrometers, and separation by color channels, with removal of artifacts. A region selection tool was employed to delineate the tumor region and ascertain its area. Cell counts were then quantified and expressed as counts per square millimeter (mm²).

This is the list of antibodies used in our analysis (Table 9).

Ab	Clone	Dilution	Company
CD68 (M)	KP1 - MoAb	Ready to use	Ventana
CD163 (M2)	MRQ26 - MoAb	Ready to Use	Ventana
CD86 (M1)	E5W6H RaAb	1:75	Cell Signaling
CD4	SP35 RaAb	Ready to use	Ventana
CD8	SP57 RaAb	Ready to use	Ventana
FOXP3	263A/E7 - Leica	Ready to use	Laica
CD39	EPR20627 RaAb	1:500.	Abcam
CD8	SP239 RaAb	Ready to use	Ventana
CD103	EP206RaAb	Ready to use	Leica
DAPI			

Table 9. Reagents and Antibodies used for Multiplex Ventana phenotyping

7.8 Single cell RNA seq Experiments

Single-cell sequencing was performed using a 10 × Genomics platform. Cell suspensions of CD45+ cells from 3 patients (3 healthy and 3 tumor tissues) were prepared and vitality was assessed for each individual scRNA-seq experiment. A viability > 90% was verified for each sample.

Briefly, cell suspensions were diluted in PBS with 0.04% BSA to a final concentration of 1×10^6 cells/mL (1,000 cells per μ L). 12000 cells were loaded onto a single-cell chip for GEM generation using the 10x Genomics Chromium Controller (10× Genomics, Pleasanton, CA). 3'mRNA-seq gene expression libraries were constructed using the Chromium Single Cell 3' Library & Gel Bead Kit v2 (10x Genomics) according to the manufacturer's guidelines.

All reactions were performed in a C1000 Touch Thermal Cycler (Bio-Rad Laboratories, Hercules, CA). Twelve cycles were used for cDNA amplification, while the number of total cycles for the sample index PCR was calculated based on the cDNA concentration. Amplified cDNA and final libraries were evaluated using a Tape Station 4200 (Agilent

Technologies, Santa Clara, CA) with a high sensitivity chip. scRNA-seq libraries were sequenced on an Illumina NovaSeq6000 with the standard sequencing protocol of R1 28; I1 10; I2 10; R2 90 nt read length

Single cell encapsulation, cDNA amplification, library prep and sequencing were performed by COSR (Center for Omic Sciences).

7.9 Bioinformatic analysis

UMItool v.1.0.0 was used to map the raw reads to the assembly GRCh38 of the human genome and to obtain the gene expression level for each cell. Genecode release 44 and Ensembl release 110 were used for the annotation. The counts were then imported in the R environment v.4.0.3 and analyzed with the Seurat package v.4.3.0 (<https://satijalab.org/seurat/>).

All the six samples were first analyzed individually, following the standard Seurat pipeline. In the first filtering step, only cells with at least 200 genes and genes expressed in at least 5 cells were considered. Then, a second filtering step was applied taking into account the number of features per cell and the mitochondrial counts. Different thresholds were set based on the evaluation of these parameters in each sample. Counts were then normalized with the standard Seurat “LogNormalize” function, using a 10,000 scale factor. The FindVariableFeatures function was used to identify a subset of features that exhibit high cell-to-cell variation that were then used as input for the RunPCA function to perform the principal component analysis (PCA). The ScaleData function was used to scale the datasets related to all the six samples and both the number of features and the percentage of mitochondrial genes were regressed out. The distribution of the variable genes resulted to be unaffected by the cell cycle phases.

The integrated analysis was performed on the six samples through SelectIntegrationFeatures and FindIntegrationAnchors functions. The final integration step was then performed with the IntegrateData function. Data were scaled as described above and the clustering was carried out through the FindCluster function, using the original Louvain algorithm and considering 1-30 principal components and a 0.2 resolution.

Marker genes for each cluster were identified with the FindAllMarkers (logfc.threshold = 0.25, min.pct = 0.25). Cells were then classified using the SingleR

package, referring to the Monaco Immune Database database (MonacoG et al. (2019). RNA-Seq Signature Normalized by mRNA Abundance Allow Absolute Deconvolution of Human Immune Cell Types CellRep.26,1627-1640). Then, the top marker genes for each cluster were considered for a more detailed manually annotation.

CD8B Subset

The integrated dataset was subset to keep only cells belonging to the T cell cluster and expressing CD8B. The Seurat SplitObject function was used to obtain the single datasets belonging to each of the six sample. The NormalizeData and FindVariableFeatures were performed again on each dataset, that were then used to perform the integration again, as described above. The clustering considered 30nPCS and a 0.3 resolution.

A manually curated annotation was carried out, considering the top marker genes for each cluster obtained with the FindAllMarkers function.

Then, to better inspect the differences between tumor and healthy cells, the same function was used to perform the intracluster analysis and to detect differentially expressed genes in tumor cells versus healthy cells, considering each cluster individually.

8 REFERENCES

- Ahmed, H. U., El-Shater Bosaily, A., Brown, L. C., Gabe, R., Kaplan, R., Parmar, M. K., Collaco-Moraes, Y., Ward, K., Hindley, R. G., Freeman, A., Kirkham, A. P., Oldroyd, R., Parker, C., Emberton, M., & PROMIS study group. (2017). Diagnostic accuracy of multi-parametric MRI and TRUS biopsy in prostate cancer (PROMIS): a paired validating confirmatory study. *Lancet (London, England)*, *389*(10071), 815–822. [https://doi.org/10.1016/S0140-6736\(16\)32401-1](https://doi.org/10.1016/S0140-6736(16)32401-1)
- Alexandrov, L. B., Nik-Zainal, S., Wedge, D. C., Aparicio, S. A. J. R., Behjati, S., Biankin, A. V., Bignell, G. R., Bolli, N., Borg, A., Børresen-Dale, A.-L., Boyault, S., Burkhardt, B., Butler, A. P., Caldas, C., Davies, H. R., Desmedt, C., Eils, R., Eyfjörd, J. E., Foekens, J. A., ... Stratton, M. R. (2013). Signatures of mutational processes in human cancer. *Nature*, *500*(7463), 415–421. <https://doi.org/10.1038/nature12477>
- Amin Al Olama, A., Dadaev, T., Hazelett, D. J., Li, Q., Leongamornlert, D., Saunders, E. J., Stephens, S., Cieza-Borrella, C., Whitmore, I., Benlloch Garcia, S., Giles, G. G., Southey, M. C., Fitzgerald, L., Gronberg, H., Wiklund, F., Aly, M., Henderson, B. E., Schumacher, F., Haiman, C. A., ... Kote-Jarai, Z. (2015). Multiple novel prostate cancer susceptibility signals identified by fine-mapping of known risk loci among Europeans. *Human Molecular Genetics*, *24*(19), 5589–5602. <https://doi.org/10.1093/hmg/ddv203>
- Anderson, B. B., Oberlin, D. T., Razmaria, A. A., Choy, B., Zagaja, G. P., Shalhav, A. L., Meeks, J. J., Yang, X. J., Paner, G. P., & Eggener, S. E. (2017). Extraprostatic Extension Is Extremely Rare for Contemporary Gleason Score 6 Prostate Cancer. *European Urology*, *72*(3), 455–460. <https://doi.org/10.1016/j.eururo.2016.11.028>
- Antonarakis, E. S., Piulats, J. M., Gross-Goupil, M., Goh, J., Ojamaa, K., Hoimes, C. J., Vaishampayan, U., Berger, R., Sezer, A., Alanko, T., de Wit, R., Li, C., Omlin, A., Procopio, G., Fukasawa, S., Tabata, K., Park, S. H., Feyerabend, S., Drake, C. G., ... de Bono, J. S. (2020a). Pembrolizumab for Treatment-Refractory Metastatic Castration-Resistant Prostate Cancer: Multicohort, Open-Label Phase II KEYNOTE-199 Study. *Journal of Clinical Oncology*, *38*(5), 395–405. <https://doi.org/10.1200/JCO.19.01638>
- Antonarakis, E. S., Piulats, J. M., Gross-Goupil, M., Goh, J., Ojamaa, K., Hoimes, C. J., Vaishampayan, U., Berger, R., Sezer, A., Alanko, T., de Wit, R., Li, C., Omlin, A., Procopio, G., Fukasawa, S., Tabata, K., Park, S. H., Feyerabend, S., Drake, C. G., ... de Bono, J. S. (2020b). Pembrolizumab for Treatment-Refractory Metastatic Castration-Resistant Prostate Cancer: Multicohort, Open-Label Phase II KEYNOTE-199 Study. *Journal of Clinical Oncology*, *38*(5), 395–405. <https://doi.org/10.1200/JCO.19.01638>
- Antonioli, L., Pacher, P., Vizi, E. S., & Haskó, G. (2013). CD39 and CD73 in immunity and inflammation. *Trends in Molecular Medicine*, *19*(6), 355–367. <https://doi.org/10.1016/j.molmed.2013.03.005>
- Ao, M., Williams, K., Bhowmick, N. A., & Hayward, S. W. (2006). Transforming growth factor-beta promotes invasion in tumorigenic but not in nontumorigenic human prostatic epithelial cells. *Cancer Research*, *66*(16), 8007–8016. <https://doi.org/10.1158/0008-5472.CAN-05-4451>

- Arakaki, R., Yamada, A., Kudo, Y., Hayashi, Y., & Ishimaru, N. (2014). Mechanism of activation-induced cell death of T cells and regulation of FasL expression. *Critical Reviews in Immunology*, 34(4), 301–314. <https://doi.org/10.1615/critrevimmunol.2014009988>
- Araki, S., Omori, Y., Lyn, D., Singh, R. K., Meinbach, D. M., Sandman, Y., Lokeshwar, V. B., & Lokeshwar, B. L. (2007). Interleukin-8 is a molecular determinant of androgen independence and progression in prostate cancer. *Cancer Research*, 67(14), 6854–6862. <https://doi.org/10.1158/0008-5472.CAN-07-1162>
- Ariotti, S., Hogenbirk, M. A., Dijkgraaf, F. E., Visser, L. L., Hoekstra, M. E., Song, J.-Y., Jacobs, H., Haanen, J. B., & Schumacher, T. N. (2014). T cell memory. Skin-resident memory CD8⁺ T cells trigger a state of tissue-wide pathogen alert. *Science (New York, N.Y.)*, 346(6205), 101–105. <https://doi.org/10.1126/science.1254803>
- Arista-Nasr, J., Martinez-Benitez, B., Bornstein-Quevedo, L., Aguilar-Ayala, E., Aleman-Sanchez, C. N., & Ortiz-Bautista, R. (2016). Low grade urothelial carcinoma mimicking basal cell hyperplasia and transitional metaplasia in needle prostate biopsy. *International Brazilian Journal of Urology : Official Journal of the Brazilian Society of Urology*, 42(2), 247. <https://doi.org/10.1590/S1677-5538.IBJU.2014.0512>
- Attard, G., Belldegrun, A. S., & de Bono, J. S. (2005). Selective blockade of androgenic steroid synthesis by novel lyase inhibitors as a therapeutic strategy for treating metastatic prostate cancer. *BJU International*, 96(9), 1241–1246. <https://doi.org/10.1111/j.1464-410X.2005.05821.x>
- Ayala, G., Tuxhorn, J. A., Wheeler, T. M., Frolov, A., Scardino, P. T., Ohori, M., Wheeler, M., Spittler, J., & Rowley, D. R. (2003). Reactive stroma as a predictor of biochemical-free recurrence in prostate cancer. *Clinical Cancer Research : An Official Journal of the American Association for Cancer Research*, 9(13), 4792–4801.
- Baca, S. C., Prandi, D., Lawrence, M. S., Mosquera, J. M., Romanel, A., Drier, Y., Park, K., Kitabayashi, N., MacDonald, T. Y., Ghandi, M., Van Allen, E., Kryukov, G. V., Sboner, A., Theurillat, J.-P., Soong, T. D., Nickerson, E., Auclair, D., Tewari, A., Beltran, H., ... Garraway, L. A. (2013). Punctuated Evolution of Prostate Cancer Genomes. *Cell*, 153(3), 666–677. <https://doi.org/10.1016/j.cell.2013.03.021>
- Barbieri, C. E., & Rubin, M. A. (2015). Genomic rearrangements in prostate cancer. *Current Opinion in Urology*, 25(1), 71–76. <https://doi.org/10.1097/MOU.0000000000000129>
- Baxevanis, C. N., Stokidis, S., Goulielmaki, M., Gritzapis, A. D., & Fortis, S. P. (2023). Peripheral Blood CD8⁺ T-Lymphocyte Subsets Are Associated with Prognosis in Prostate Cancer Patients. *Onco*, 3(3), 165–174. <https://doi.org/10.3390/onco3030012>
- Beebe-Dimmer, J. L., Kapron, A. L., Fraser, A. M., Smith, K. R., & Cooney, K. A. (2020). Risk of Prostate Cancer Associated With Familial and Hereditary Cancer Syndromes. *Journal of Clinical Oncology : Official Journal of the American Society of Clinical Oncology*, 38(16), 1807–1813. <https://doi.org/10.1200/JCO.19.02808>
- Bell, K. J. L., Del Mar, C., Wright, G., Dickinson, J., & Glasziou, P. (2015). Prevalence of incidental prostate cancer: A systematic review of autopsy studies. *International Journal of Cancer*, 137(7), 1749–1757. <https://doi.org/10.1002/ijc.29538>

- Bilusic, M., Madan, R. A., & Gulley, J. L. (2017). Immunotherapy of Prostate Cancer: Facts and Hopes. *Clinical Cancer Research : An Official Journal of the American Association for Cancer Research*, 23(22), 6764–6770. <https://doi.org/10.1158/1078-0432.CCR-17-0019>
- Borst, J., Ahrends, T., Bąbała, N., Melief, C. J. M., & Kastenmüller, W. (2018). CD4+ T cell help in cancer immunology and immunotherapy. *Nature Reviews. Immunology*, 18(10), 635–647. <https://doi.org/10.1038/s41577-018-0044-0>
- Boyman, O., Kolios, A. G. A., & Raeber, M. E. (2015). Modulation of T cell responses by IL-2 and IL-2 complexes. *Clinical and Experimental Rheumatology*, 33(4 Suppl 92), S54-7.
- Bratt, O., Drevin, L., Akre, O., Garmo, H., & Stattin, P. (2016). Family History and Probability of Prostate Cancer, Differentiated by Risk Category: A Nationwide Population-Based Study. *Journal of the National Cancer Institute*, 108(10). <https://doi.org/10.1093/jnci/djw110>
- Buchbinder, E. I., & Desai, A. (2016). CTLA-4 and PD-1 Pathways: Similarities, Differences, and Implications of Their Inhibition. *American Journal of Clinical Oncology*, 39(1), 98–106. <https://doi.org/10.1097/COC.0000000000000239>
- Byar, D. P., & Mostofi, F. K. (1972a). Carcinoma of the prostate: Prognostic evaluation of certain pathologic features in 208 radical prostatectomies. *Cancer*, 30(1), 5–13. [https://doi.org/10.1002/1097-0142\(197207\)30:1<5::AID-CNCR2820300103>3.0.CO;2-S](https://doi.org/10.1002/1097-0142(197207)30:1<5::AID-CNCR2820300103>3.0.CO;2-S)
- Byar, D. P., & Mostofi, F. K. (1972b). Carcinoma of the prostate: prognostic evaluation of certain pathologic features in 208 radical prostatectomies. Examined by the step-section technique. *Cancer*, 30(1), 5–13. [https://doi.org/10.1002/1097-0142\(197207\)30:1<5::aid-cncr2820300103>3.0.co;2-s](https://doi.org/10.1002/1097-0142(197207)30:1<5::aid-cncr2820300103>3.0.co;2-s)
- Calcinotto, A., Spataro, C., Zagato, E., Di Mitri, D., Gil, V., Crespo, M., De Bernardis, G., Losa, M., Mirenda, M., Pasquini, E., Rinaldi, A., Sumanasuriya, S., Lambros, M. B., Neeb, A., Lucianò, R., Bravi, C. A., Nava-Rodrigues, D., Dolling, D., Prayer-Galetti, T., ... Alimonti, A. (2018). IL-23 secreted by myeloid cells drives castration-resistant prostate cancer. *Nature*, 559(7714), 363–369. <https://doi.org/10.1038/s41586-018-0266-0>
- Canale, F. P., Ramello, M. C., Núñez, N., Araujo Furlan, C. L., Bossio, S. N., Gorosito Serrán, M., Tosello Boari, J., Del Castillo, A., Ledesma, M., Sedlik, C., Piaggio, E., Gruppi, A., Acosta Rodríguez, E. A., & Montes, C. L. (2018). CD39 Expression Defines Cell Exhaustion in Tumor-Infiltrating CD8+ T Cells. *Cancer Research*, 78(1), 115–128. <https://doi.org/10.1158/0008-5472.CAN-16-2684>
- Carlsson, S. V., & Vickers, A. J. (2020). Screening for Prostate Cancer. *The Medical Clinics of North America*, 104(6), 1051–1062. <https://doi.org/10.1016/j.mcna.2020.08.007>
- Carvalho, G. F., Smith, D. S., Mager, D. E., Ramos, C., & Catalona, W. J. (1999). Digital rectal examination for detecting prostate cancer at prostate specific antigen levels of 4 ng./ml. or less. *The Journal of Urology*, 161(3), 835–839.
- Castro, E., Goh, C., Olmos, D., Saunders, E., Leongamornlert, D., Tymrakiewicz, M., Mahmud, N., Dadaev, T., Govindasami, K., Guy, M., Sawyer, E., Wilkinson, R., Ardern-Jones, A., Ellis, S., Frost, D., Peock, S., Evans, D. G., Tischkowitz, M., Cole, T., ... Eeles, R. (2013). Germline BRCA mutations are associated with higher risk of nodal involvement, distant metastasis, and poor survival outcomes in prostate cancer. *Journal of Clinical Oncology : Official Journal of the American*

- Society of Clinical Oncology*, 31(14), 1748–1757.
<https://doi.org/10.1200/JCO.2012.43.1882>
- Castro, F., Cardoso, A. P., Gonçalves, R. M., Serre, K., & Oliveira, M. J. (2018). Interferon-Gamma at the Crossroads of Tumor Immune Surveillance or Evasion. *Frontiers in Immunology*, 9. <https://doi.org/10.3389/fimmu.2018.00847>
- Catalona, W. J., Richie, J. P., Ahmann, F. R., Hudson, M. A., Scardino, P. T., Flanigan, R. C., DeKernion, J. B., Ratliff, T. L., Kavoussi, L. R., Dalkin, B. L., Waters, W. B., MacFarlane, M. T., & Southwick, P. C. (1994). Comparison of digital rectal examination and serum prostate specific antigen in the early detection of prostate cancer: results of a multicenter clinical trial of 6,630 men. *The Journal of Urology*, 151(5), 1283–1290. [https://doi.org/10.1016/s0022-5347\(17\)35233-3](https://doi.org/10.1016/s0022-5347(17)35233-3)
- Cecile Vicier, L. W. Y. H. A. H. C. E. M. L. and C. S. (2019). Immune infiltrate with CD8 low or PDL1 high associated with metastatic prostate cancer after radical prostatectomy (RP). https://ascopubs.org/doi/10.1200/JCO.2019.37.7_suppl.86
- Cerqueira, M. A., Ferrari, K. L., de Mattos, A. C., Monti, C. R., & Reis, L. O. (2020). T cells CD4+/CD8+ local immune modulation by prostate cancer hemi-cryoablation. *World Journal of Urology*, 38(3), 673–680. <https://doi.org/10.1007/s00345-019-02861-0>
- Chen, S., Zhu, G., Yang, Y., Wang, F., Xiao, Y.-T., Zhang, N., Bian, X., Zhu, Y., Yu, Y., Liu, F., Dong, K., Mariscal, J., Liu, Y., Soares, F., Loo Yau, H., Zhang, B., Chen, W., Wang, C., Chen, D., ... Ren, S. (2021). Single-cell analysis reveals transcriptomic remodellings in distinct cell types that contribute to human prostate cancer progression. *Nature Cell Biology*, 23(1), 87–98. <https://doi.org/10.1038/s41556-020-00613-6>
- Chi, N., Tan, Z., Ma, K., Bao, L., & Yun, Z. (2014). Increased circulating myeloid-derived suppressor cells correlate with cancer stages, interleukin-8 and -6 in prostate cancer. *International Journal of Clinical and Experimental Medicine*, 7(10), 3181–3192.
- Chu, K. C., Tarone, R. E., & Freeman, H. P. (2003). Trends in prostate cancer mortality among black men and white men in the United States. *Cancer*, 97(6), 1507–1516. <https://doi.org/10.1002/cncr.11212>
- Cortesi, F., Delfanti, G., Grilli, A., Calcinotto, A., Gorini, F., Pucci, F., Lucianò, R., Grioni, M., Recchia, A., Benigni, F., Briganti, A., Salonia, A., De Palma, M., Bicciano, S., Doglioni, C., Bellone, M., Casorati, G., & Dellabona, P. (2018). Bimodal CD40/Fas-Dependent Crosstalk between iNKT Cells and Tumor-Associated Macrophages Impairs Prostate Cancer Progression. *Cell Reports*, 22(11), 3006–3020. <https://doi.org/10.1016/j.celrep.2018.02.058>
- Criscuolo, D., Morra, F., Giannella, R., Cerrato, A., & Celetti, A. (2019). Identification of Novel Biomarkers of Homologous Recombination Defect in DNA Repair to Predict Sensitivity of Prostate Cancer Cells to PARP-Inhibitors. *International Journal of Molecular Sciences*, 20(12), 3100. <https://doi.org/10.3390/ijms20123100>
- Cucchiara, V., Cooperberg, M. R., Dall’Era, M., Lin, D. W., Montorsi, F., Schalken, J. A., & Evans, C. P. (2018). Genomic Markers in Prostate Cancer Decision Making. *European Urology*, 73(4), 572–582. <https://doi.org/10.1016/j.eururo.2017.10.036>
- Culp, M. B., Soerjomataram, I., Efsthathiou, J. A., Bray, F., & Jemal, A. (2020). Recent Global Patterns in Prostate Cancer Incidence and Mortality Rates. *European Urology*, 77(1), 38–52. <https://doi.org/10.1016/j.eururo.2019.08.005>

- Cunha, G. R., Hayward, S. W., Dahiya, R., & Foster, B. A. (1996). Smooth Muscle-Epithelial Interactions in Normal and Neoplastic Prostatic Development. *Cells Tissues Organs*, 155(1), 63–72. <https://doi.org/10.1159/000147791>
- D’Amico, A. V., Whittington, R., Malkowicz, S. B., Schultz, D., Blank, K., Broderick, G. A., Tomaszewski, J. E., Renshaw, A. A., Kaplan, I., Beard, C. J., & Wein, A. (1998). Biochemical outcome after radical prostatectomy, external beam radiation therapy, or interstitial radiation therapy for clinically localized prostate cancer. *JAMA*, 280(11), 969–974. <https://doi.org/10.1001/jama.280.11.969>
- De Marzo, A. M., Platz, E. A., Sutcliffe, S., Xu, J., Grönberg, H., Drake, C. G., Nakai, Y., Isaacs, W. B., & Nelson, W. G. (2007). Inflammation in prostate carcinogenesis. *Nature Reviews. Cancer*, 7(4), 256–269. <https://doi.org/10.1038/nrc2090>
- Derhovanessian, E., Adams, V., Hähnel, K., Groeger, A., Pandha, H., Ward, S., & Pawelec, G. (2009). Pretreatment frequency of circulating IL-17⁺ CD4⁺ T-cells, but not Tregs, correlates with clinical response to whole-cell vaccination in prostate cancer patients. *International Journal of Cancer*, 125(6), 1372–1379. <https://doi.org/10.1002/ijc.24497>
- Di Mitri, D., Mirenda, M., Vasilevska, J., Calcinotto, A., Delaleu, N., Revandkar, A., Gil, V., Boysen, G., Losa, M., Mosole, S., Pasquini, E., D’Antuono, R., Masetti, M., Zagato, E., Chiorino, G., Ostano, P., Rinaldi, A., Gnetti, L., Graupera, M., ... Alimonti, A. (2019a). Re-education of Tumor-Associated Macrophages by CXCR2 Blockade Drives Senescence and Tumor Inhibition in Advanced Prostate Cancer. *Cell Reports*, 28(8), 2156-2168.e5. <https://doi.org/10.1016/j.celrep.2019.07.068>
- Di Mitri, D., Mirenda, M., Vasilevska, J., Calcinotto, A., Delaleu, N., Revandkar, A., Gil, V., Boysen, G., Losa, M., Mosole, S., Pasquini, E., D’Antuono, R., Masetti, M., Zagato, E., Chiorino, G., Ostano, P., Rinaldi, A., Gnetti, L., Graupera, M., ... Alimonti, A. (2019b). Re-education of Tumor-Associated Macrophages by CXCR2 Blockade Drives Senescence and Tumor Inhibition in Advanced Prostate Cancer. *Cell Reports*, 28(8), 2156-2168.e5. <https://doi.org/10.1016/j.celrep.2019.07.068>
- Djenidi, F., Adam, J., Goubar, A., Durgeau, A., Meurice, G., de Montpréville, V., Validire, P., Besse, B., & Mami-Chouaib, F. (2015). CD8⁺CD103⁺ tumor-infiltrating lymphocytes are tumor-specific tissue-resident memory T cells and a prognostic factor for survival in lung cancer patients. *Journal of Immunology (Baltimore, Md. : 1950)*, 194(7), 3475–3486. <https://doi.org/10.4049/jimmunol.1402711>
- Dowty, J. G., Win, A. K., Buchanan, D. D., Lindor, N. M., Macrae, F. A., Clendenning, M., Antill, Y. C., Thibodeau, S. N., Casey, G., Gallinger, S., Marchand, L. Le, Newcomb, P. A., Haile, R. W., Young, G. P., James, P. A., Giles, G. G., Gunawardena, S. R., Leggett, B. A., Gattas, M., ... Jenkins, M. A. (2013). Cancer Risks for *MLH1* and *MSH2* Mutation Carriers. *Human Mutation*, 34(3), 490–497. <https://doi.org/10.1002/humu.22262>
- Drost, F. J., Osses, D. F., Nieboer, D., Bangma, C. H., Steyerberg, E. W., Roobol, M. J., & Schoots, I. G. (2019). Prostate MRI, with or without targeted biopsy and standard biopsy for detecting prostate cancer: A Cochrane systematic review and meta-analysis. *European Urology Supplements*, 18(1), e728–e729. [https://doi.org/10.1016/s1569-9056\(19\)30534-2](https://doi.org/10.1016/s1569-9056(19)30534-2)

- Duhen, T., Duhen, R., Montler, R., Moses, J., Moudgil, T., de Miranda, N. F., Goodall, C. P., Blair, T. C., Fox, B. A., McDermott, J. E., Chang, S.-C., Grunkemeier, G., Leidner, R., Bell, R. B., & Weinberg, A. D. (2018). Co-expression of CD39 and CD103 identifies tumor-reactive CD8 T cells in human solid tumors. *Nature Communications*, 9(1), 2724. <https://doi.org/10.1038/s41467-018-05072-0>
- Ebelt, K., Babaryka, G., Frankenberger, B., Stief, C. G., Eisenmenger, W., Kirchner, T., Schendel, D. J., & Noessner, E. (2009). Prostate cancer lesions are surrounded by FOXP3+, PD-1+ and B7-H1+ lymphocyte clusters. *European Journal of Cancer (Oxford, England : 1990)*, 45(9), 1664–1672. <https://doi.org/10.1016/j.ejca.2009.02.015>
- Eeles, R. A., Olama, A. A. Al, Benlloch, S., Saunders, E. J., Leongamornlert, D. A., Tymrakiewicz, M., Ghoussaini, M., Luccarini, C., Dennis, J., Jugurnauth-Little, S., Dadaev, T., Neal, D. E., Hamdy, F. C., Donovan, J. L., Muir, K., Giles, G. G., Severi, G., Wiklund, F., Gronberg, H., ... Easton, D. F. (2013). Identification of 23 new prostate cancer susceptibility loci using the iCOGS custom genotyping array. *Nature Genetics*, 45(4), 385–391, 391e1-2. <https://doi.org/10.1038/ng.2560>
- Eiva, M. A., Omran, D. K., Chacon, J. A., & Powell, D. J. (2022). Systematic analysis of CD39, CD103, CD137, and PD-1 as biomarkers for naturally occurring tumor antigen-specific TILs. *European Journal of Immunology*, 52(1), 96–108. <https://doi.org/10.1002/eji.202149329>
- Ellis, W. J., Chetner, M. P., Preston, S. D., & Brawer, M. K. (1994). Diagnosis of prostatic carcinoma: the yield of serum prostate specific antigen, digital rectal examination and transrectal ultrasonography. *The Journal of Urology*, 152(5 Pt 1), 1520–1525. [https://doi.org/10.1016/s0022-5347\(17\)32460-6](https://doi.org/10.1016/s0022-5347(17)32460-6)
- Epstein, J. I., Egevad, L., Amin, M. B., Delahunt, B., Srigley, J. R., Humphrey, P. A., & Grading Committee. (2015). The 2014 International Society of Urological Pathology (ISUP) Consensus Conference on Gleason Grading of Prostatic Carcinoma. *The American Journal of Surgical Pathology*, 40(2), 1. <https://doi.org/10.1097/PAS.0000000000000530>
- Epstein, J. I., Feng, Z., Trock, B. J., & Pierorazio, P. M. (2012). Upgrading and Downgrading of Prostate Cancer from Biopsy to Radical Prostatectomy: Incidence and Predictive Factors Using the Modified Gleason Grading System and Factoring in Tertiary Grades. *European Urology*, 61(5), 1019–1024. <https://doi.org/10.1016/j.eururo.2012.01.050>
- Epstein, J. I., Pizov, G., & Walsh, P. C. (1993). Correlation of pathologic findings with progression after radical retropubic prostatectomy. *Cancer*, 71(11), 3582–3593. [https://doi.org/10.1002/1097-0142\(19930601\)71:11<3582::aid-cncr2820711120>3.0.co;2-y](https://doi.org/10.1002/1097-0142(19930601)71:11<3582::aid-cncr2820711120>3.0.co;2-y)
- Epstein, J. I., Walsh, P. C., Carmichael, M., & Brendler, C. B. (1994). Pathologic and clinical findings to predict tumor extent of nonpalpable (stage T1c) prostate cancer. *JAMA*, 271(5), 368–374.
- Epstein, J. I., Zelefsky, M. J., Sjoberg, D. D., Nelson, J. B., Egevad, L., Magi-Galluzzi, C., Vickers, A. J., Parwani, A. V., Reuter, V. E., Fine, S. W., Eastham, J. A., Wiklund, P., Han, M., Reddy, C. A., Ciezki, J. P., Nyberg, T., & Klein, E. A. (2016). A Contemporary Prostate Cancer Grading System: A Validated Alternative to the Gleason Score. *European Urology*, 69(3), 428–435. <https://doi.org/10.1016/j.eururo.2015.06.046>

- Erlandsson, A., Carlsson, J., Lundholm, M., Fält, A., Andersson, S.-O., Andrén, O., & Davidsson, S. (2019). M2 macrophages and regulatory T cells in lethal prostate cancer. *The Prostate*, *79*(4), 363–369. <https://doi.org/10.1002/pros.23742>
- Escamilla, J., Schokrpur, S., Liu, C., Priceman, S. J., Moughon, D., Jiang, Z., Pouliot, F., Magyar, C., Sung, J. L., Xu, J., Deng, G., West, B. L., Bollag, G., Fradet, Y., Lacombe, L., Jung, M. E., Huang, J., & Wu, L. (2015). CSF1 receptor targeting in prostate cancer reverses macrophage-mediated resistance to androgen blockade therapy. *Cancer Research*, *75*(6), 950–962. <https://doi.org/10.1158/0008-5472.CAN-14-0992>
- Espiritu, S. M. G., Liu, L. Y., Rubanova, Y., Bhandari, V., Holgersen, E. M., Szyca, L. M., Fox, N. S., Chua, M. L. K., Yamaguchi, T. N., Heisler, L. E., Livingstone, J., Wintersinger, J., Yousif, F., Lalonde, E., Rouette, A., Salcedo, A., Houlahan, K. E., Li, C. H., Huang, V., ... Boutros, P. C. (2018). The Evolutionary Landscape of Localized Prostate Cancers Drives Clinical Aggression. *Cell*, *173*(4), 1003–1013.e15. <https://doi.org/10.1016/j.cell.2018.03.029>
- Feng, S., Cheng, X., Zhang, L., Lu, X., Chaudhary, S., Teng, R., Frederickson, C., Champion, M. M., Zhao, R., Cheng, L., Gong, Y., Deng, H., & Lu, X. (2018). Myeloid-derived suppressor cells inhibit T cell activation through nitrating LCK in mouse cancers. *Proceedings of the National Academy of Sciences of the United States of America*, *115*(40), 10094–10099. <https://doi.org/10.1073/pnas.1800695115>
- Fine, S. W., & Reuter, V. E. (2012). Anatomy of the prostate revisited: implications for prostate biopsy and zonal origins of prostate cancer. *Histopathology*, *60*(1), 142–152. <https://doi.org/10.1111/j.1365-2559.2011.04004.x>
- Fizazi, K., Drake, C. G., Beer, T. M., Kwon, E. D., Scher, H. I., Gerritsen, W. R., Bossi, A., den Eertwegh, A. J. M. van, Krainer, M., Houede, N., Santos, R., Mahammedi, H., Ng, S., Danielli, R., Franke, F. A., Sundar, S., Agarwal, N., Bergman, A. M., Ciuleanu, T. E., ... Logothetis, C. (2020). Final Analysis of the Ipilimumab Versus Placebo Following Radiotherapy Phase III Trial in Postdocetaxel Metastatic Castration-resistant Prostate Cancer Identifies an Excess of Long-term Survivors. *European Urology*, *78*(6), 822–830. <https://doi.org/10.1016/j.eururo.2020.07.032>
- Flanigan, R. C., Catalona, W. J., Richie, J. P., Ahmann, F. R., Hudson, M. A., Scardino, P. T., DeKernion, J. B., Ratliff, T. L., Kavoussi, L. R., Dalkin, B. L., Waters, W. B., MacFarlane, M. T., & Southwick, P. C. (1994). Accuracy of digital rectal examination and transrectal ultrasonography in localizing prostate cancer. *The Journal of Urology*, *152*(5 Pt 1), 1506–1509. [https://doi.org/10.1016/s0022-5347\(17\)32457-6](https://doi.org/10.1016/s0022-5347(17)32457-6)
- Fong, L., Carroll, P., Weinberg, V., Chan, S., Lewis, J., Corman, J., Amling, C. L., Stephenson, R. A., Simko, J., Sheikh, N. A., Sims, R. B., Frohlich, M. W., & Small, E. J. (2014). Activated Lymphocyte Recruitment Into the Tumor Microenvironment Following Preoperative Sipuleucel-T for Localized Prostate Cancer. *JNCI: Journal of the National Cancer Institute*, *106*(11). <https://doi.org/10.1093/jnci/dju268>
- Gallazzi, M., Baci, D., Mortara, L., Bosi, A., Buono, G., Naselli, A., Guarneri, A., Dehò, F., Capogrosso, P., Albini, A., Noonan, D. M., & Bruno, A. (2021). Prostate Cancer Peripheral Blood NK Cells Show Enhanced CD9, CD49a, CXCR4, CXCL8, MMP-9 Production and Secrete Monocyte-Recruiting and Polarizing Factors. *Frontiers in Immunology*, *11*. <https://doi.org/10.3389/fimmu.2020.586126>

- Ganesan, A.-P., Clarke, J., Wood, O., Garrido-Martin, E. M., Chee, S. J., Mellows, T., Samaniego-Castruita, D., Singh, D., Seumois, G., Alzetani, A., Woo, E., Friedmann, P. S., King, E. V., Thomas, G. J., Sanchez-Elsner, T., Vijayanand, P., & Ottensmeier, C. H. (2017). Tissue-resident memory features are linked to the magnitude of cytotoxic T cell responses in human lung cancer. *Nature Immunology*, *18*(8), 940–950. <https://doi.org/10.1038/ni.3775>
- Ge, R., Wang, Z., & Cheng, L. (2022). Tumor microenvironment heterogeneity an important mediator of prostate cancer progression and therapeutic resistance. *Npj Precision Oncology*, *6*(1), 31. <https://doi.org/10.1038/s41698-022-00272-w>
- Gevensleben, H., Dietrich, D., Golletz, C., Steiner, S., Jung, M., Thiesler, T., Majores, M., Stein, J., Uhl, B., Müller, S., Ellinger, J., Stephan, C., Jung, K., Brossart, P., & Kristiansen, G. (2016). The Immune Checkpoint Regulator PD-L1 Is Highly Expressed in Aggressive Primary Prostate Cancer. *Clinical Cancer Research: An Official Journal of the American Association for Cancer Research*, *22*(8), 1969–1977. <https://doi.org/10.1158/1078-0432.CCR-15-2042>
- Gillessen, S., Armstrong, A., Attard, G., Beer, T. M., Beltran, H., Bjartell, A., Bossi, A., Briganti, A., Bristow, R. G., Bulbul, M., Caffo, O., Chi, K. N., Clarke, C. S., Clarke, N., Davis, I. D., de Bono, J. S., Duran, I., Eeles, R., Efstathiou, E., ... Omlin, A. (2022). Management of Patients with Advanced Prostate Cancer: Report from the Advanced Prostate Cancer Consensus Conference 2021. *European Urology*, *82*(1), 115–141. <https://doi.org/10.1016/j.eururo.2022.04.002>
- Giraudet, A.-L., Kryza, D., Hofman, M., Moreau, A., Fizazi, K., Flechon, A., Hicks, R. J., & Tran, B. (2021). PSMA targeting in metastatic castration-resistant prostate cancer: where are we and where are we going? *Therapeutic Advances in Medical Oncology*, *13*, 17588359211053898. <https://doi.org/10.1177/17588359211053898>
- Giri, V. N., Hegarty, S. E., Hyatt, C., O’Leary, E., Garcia, J., Knudsen, K. E., Kelly, W. K., & Gomella, L. G. (2019). Germline genetic testing for inherited prostate cancer in practice: Implications for genetic testing, precision therapy, and cascade testing. *The Prostate*, *79*(4), 333–339. <https://doi.org/10.1002/pros.23739>
- Gleason, D. F., & Mellinger, G. T. (1974). Prediction of prognosis for prostatic adenocarcinoma by combined histological grading and clinical staging. *The Journal of Urology*, *111*(1), 58–64. [https://doi.org/10.1016/s0022-5347\(17\)59889-4](https://doi.org/10.1016/s0022-5347(17)59889-4)
- Goel, S., Shoag, J. E., Gross, M. D., Al Hussein Al Awamlh, B., Robinson, B., Khani, F., Baltich Nelson, B., Margolis, D. J., & Hu, J. C. (2020). Concordance Between Biopsy and Radical Prostatectomy Pathology in the Era of Targeted Biopsy: A Systematic Review and Meta-analysis. *European Urology Oncology*, *3*(1), 10–20. <https://doi.org/10.1016/j.euo.2019.08.001>
- Gros, A., Robbins, P. F., Yao, X., Li, Y. F., Turcotte, S., Tran, E., Wunderlich, J. R., Mixon, A., Farid, S., Dudley, M. E., Hanada, K.-I., Almeida, J. R., Darko, S., Douek, D. C., Yang, J. C., & Rosenberg, S. A. (2014). PD-1 identifies the patient-specific CD8⁺ tumor-reactive repertoire infiltrating human tumors. *The Journal of Clinical Investigation*, *124*(5), 2246–2259. <https://doi.org/10.1172/JCI73639>
- H. Matzkin, M. S. Soloway, S. H. (1992). Transitional Cell Carcinoma of the Prostate, *J. Urol.*, *146*: 1207–1212, 1991. *Journal of Urology*, *147*(6), 1630–1630. [https://doi.org/10.1016/S0022-5347\(17\)37664-4](https://doi.org/10.1016/S0022-5347(17)37664-4)

- Haas, G. P., Delongchamps, N., Brawley, O. W., Wang, C. Y., & de la Roza, G. (2008). The worldwide epidemiology of prostate cancer: perspectives from autopsy studies. *The Canadian Journal of Urology*, *15*(1), 3866–3871.
- Haffner, M. C., Guner, G., Taheri, D., Netto, G. J., Palsgrove, D. N., Zheng, Q., Guedes, L. B., Kim, K., Tsai, H., Esopi, D. M., Lotan, T. L., Sharma, R., Meeker, A. K., Chinnaiyan, A. M., Nelson, W. G., Yegnasubramanian, S., Luo, J., Mehra, R., Antonarakis, E. S., ... De Marzo, A. M. (2018). Comprehensive Evaluation of Programmed Death-Ligand 1 Expression in Primary and Metastatic Prostate Cancer. *The American Journal of Pathology*, *188*(6), 1478–1485. <https://doi.org/10.1016/j.ajpath.2018.02.014>
- Haffner, M. C., Zwart, W., Roudier, M. P., True, L. D., Nelson, W. G., Epstein, J. I., De Marzo, A. M., Nelson, P. S., & Yegnasubramanian, S. (2021). Genomic and phenotypic heterogeneity in prostate cancer. *Nature Reviews Urology*, *18*(2), 79–92. <https://doi.org/10.1038/s41585-020-00400-w>
- Hara, R., Jo, Y., Fujii, T., Kondo, N., Yokoyama, T., Miyaji, Y., & Nagai, A. (2008). Optimal Approach for Prostate Cancer Detection as Initial Biopsy: Prospective Randomized Study Comparing Transperineal Versus Transrectal Systematic 12-Core Biopsy. *Urology*, *71*(2), 191–195. <https://doi.org/10.1016/j.urology.2007.09.029>
- Hemminki, K. (2012). Familial risk and familial survival in prostate cancer. *World Journal of Urology*, *30*(2), 143–148. <https://doi.org/10.1007/s00345-011-0801-1>
- Hirz, T., Mei, S., Sarkar, H., Kfoury, Y., Wu, S., Verhoeven, B. M., Subtelny, A. O., Zlatev, D. V., Wszolek, M. W., Salari, K., Murray, E., Chen, F., Macosko, E. Z., Wu, C.-L., Scadden, D. T., Dahl, D. M., Baryawno, N., Saylor, P. J., Kharchenko, P. V., & Sykes, D. B. (2023). Dissecting the immune suppressive human prostate tumor microenvironment via integrated single-cell and spatial transcriptomic analyses. *Nature Communications*, *14*(1), 663. <https://doi.org/10.1038/s41467-023-36325-2>
- Jhunjhunwala, S., Hammer, C., & Delamarre, L. (2021). Antigen presentation in cancer: insights into tumour immunogenicity and immune evasion. *Nature Reviews Cancer*, *21*(5), 298–312. <https://doi.org/10.1038/s41568-021-00339-z>
- Kane, C. J., Eggen, S. E., Shindel, A. W., & Andriole, G. L. (2017). Variability in Outcomes for Patients with Intermediate-risk Prostate Cancer (Gleason Score 7, International Society of Urological Pathology Gleason Group 2-3) and Implications for Risk Stratification: A Systematic Review. *European Urology Focus*, *3*(4–5), 487–497. <https://doi.org/10.1016/j.euf.2016.10.010>
- Kantoff, P. W., Higano, C. S., Shore, N. D., Berger, E. R., Small, E. J., Penson, D. F., Redfern, C. H., Ferrari, A. C., Dreicer, R., Sims, R. B., Xu, Y., Frohlich, M. W., Schellhammer, P. F., & IMPACT Study Investigators. (2010). Sipuleucel-T immunotherapy for castration-resistant prostate cancer. *The New England Journal of Medicine*, *363*(5), 411–422. <https://doi.org/10.1056/NEJMoa1001294>
- Karlou, M., Tzelepi, V., & Efstathiou, E. (2010). Therapeutic targeting of the prostate cancer microenvironment. *Nature Reviews Urology*, *7*(9), 494–509. <https://doi.org/10.1038/nrur.2010.134>
- Kass, E. M., Moynahan, M. E., & Jasin, M. (2016). When Genome Maintenance Goes Badly Awry. *Molecular Cell*, *62*(5), 777–787. <https://doi.org/10.1016/j.molcel.2016.05.021>

- Koh, C.-H., Lee, S., Kwak, M., Kim, B.-S., & Chung, Y. (2023). CD8 T-cell subsets: heterogeneity, functions, and therapeutic potential. *Experimental & Molecular Medicine*, 55(11), 2287–2299. <https://doi.org/10.1038/s12276-023-01105-x>
- Kovtun, I. V., Murphy, S. J., Johnson, S. H., Cheville, J. C., & Vasmatazis, G. (2015). Chromosomal catastrophe is a frequent event in clinically insignificant prostate cancer. *Oncotarget*, 6(30), 29087–29096. <https://doi.org/10.18632/oncotarget.4900>
- Ku, S. Y., Rosario, S., Wang, Y., Mu, P., Seshadri, M., Goodrich, Z. W., Goodrich, M. M., Labbé, D. P., Gomez, E. C., Wang, J., Long, H. W., Xu, B., Brown, M., Loda, M., Sawyers, C. L., Ellis, L., & Goodrich, D. W. (2017). *Rb1* and *Trp53* cooperate to suppress prostate cancer lineage plasticity, metastasis, and antiandrogen resistance. *Science*, 355(6320), 78–83. <https://doi.org/10.1126/science.aah4199>
- Larionova, I., Tuguzbaeva, G., Ponomaryova, A., Stakheyeva, M., Cherdyntseva, N., Pavlov, V., Choinzonov, E., & Kzhyshkowska, J. (2020). Tumor-Associated Macrophages in Human Breast, Colorectal, Lung, Ovarian and Prostate Cancers. *Frontiers in Oncology*, 10, 566511. <https://doi.org/10.3389/fonc.2020.566511>
- Leclerc, B. G., Charlebois, R., Chouinard, G., Allard, B., Pommey, S., Saad, F., & Stagg, J. (2016). CD73 Expression Is an Independent Prognostic Factor in Prostate Cancer. *Clinical Cancer Research*, 22(1), 158–166. <https://doi.org/10.1158/1078-0432.CCR-15-1181>
- Lee, F., Torp-Pedersen, S. T., Siders, D. B., Littrup, P. J., & McLeary, R. D. (1989). Transrectal ultrasound in the diagnosis and staging of prostatic carcinoma. *Radiology*, 170(3), 609–615. <https://doi.org/10.1148/radiology.170.3.2644656>
- Lee, L. N., Ronan, E. O., de Lara, C., Franken, K. L. M. C., Ottenhoff, T. H. M., Tchilian, E. Z., & Beverley, P. C. L. (2011). CXCR6 is a marker for protective antigen-specific cells in the lungs after intranasal immunization against *Mycobacterium tuberculosis*. *Infection and Immunity*, 79(8), 3328–3337. <https://doi.org/10.1128/IAI.01133-10>
- Li, H., Wang, Z., Zhang, Y., Sun, G., Ding, B., Yan, L., Liu, H., Guan, W., Hu, Z., Wang, S., Cheng, F., Xu, H., Zhang, X., & Ye, Z. (2019). The Immune Checkpoint Regulator PDL1 is an Independent Prognostic Biomarker for Biochemical Recurrence in Prostate Cancer Patients Following Adjuvant Hormonal Therapy. *Journal of Cancer*, 10(14), 3102–3111. <https://doi.org/10.7150/jca.30384>
- Li, Z., Bishop, A. C., Alyamani, M., Garcia, J. A., Dreicer, R., Bunch, D., Liu, J., Upadhyay, S. K., Auchus, R. J., & Sharifi, N. (2015). Conversion of abiraterone to D4A drives anti-tumour activity in prostate cancer. *Nature*, 523(7560), 347–351. <https://doi.org/10.1038/nature14406>
- Mackay, L. K., Rahimpour, A., Ma, J. Z., Collins, N., Stock, A. T., Hafon, M.-L., Vega-Ramos, J., Lauzurica, P., Mueller, S. N., Stefanovic, T., Tschärke, D. C., Heath, W. R., Inouye, M., Carbone, F. R., & Gebhardt, T. (2013). The developmental pathway for CD103(+)CD8+ tissue-resident memory T cells of skin. *Nature Immunology*, 14(12), 1294–1301. <https://doi.org/10.1038/ni.2744>
- Mahadevia, P. S., Koss, L. G., & Tar, I. J. (1986). Prostatic involvement in bladder cancer. Prostate mapping in 20 cystoprostatectomy specimens. *Cancer*, 58(9), 2096–2102. [https://doi.org/10.1002/1097-0142\(19861101\)58:9<2096::aid-cncr2820580922>3.0.co;2-0](https://doi.org/10.1002/1097-0142(19861101)58:9<2096::aid-cncr2820580922>3.0.co;2-0)
- Maolake, A., Izumi, K., Shigehara, K., Natsagdorj, A., Iwamoto, H., Kadomoto, S., Takezawa, Y., Machioka, K., Narimoto, K., Namiki, M., Lin, W.-J., Wufuer, G., & Mizokami, A. (2017). Tumor-associated macrophages promote prostate cancer

- migration through activation of the CCL22-CCR4 axis. *Oncotarget*, 8(6), 9739–9751. <https://doi.org/10.18632/oncotarget.14185>
- Martinez, F. O., & Gordon, S. (2014). The M1 and M2 paradigm of macrophage activation: time for reassessment. *F1000prime Reports*, 6, 13. <https://doi.org/10.12703/P6-13>
- Masopust, D., & Soerens, A. G. (2019). Tissue-Resident T Cells and Other Resident Leukocytes. *Annual Review of Immunology*, 37(1), 521–546. <https://doi.org/10.1146/annurev-immunol-042617-053214>
- Massagué, J., Blain, S. W., & Lo, R. S. (2000). TGFbeta signaling in growth control, cancer, and heritable disorders. *Cell*, 103(2), 295–309. [https://doi.org/10.1016/s0092-8674\(00\)00121-5](https://doi.org/10.1016/s0092-8674(00)00121-5)
- Mateo, J., Boysen, G., Barbieri, C. E., Bryant, H. E., Castro, E., Nelson, P. S., Olmos, D., Pritchard, C. C., Rubin, M. A., & de Bono, J. S. (2017). DNA Repair in Prostate Cancer: Biology and Clinical Implications. *European Urology*, 71(3), 417–425. <https://doi.org/10.1016/j.eururo.2016.08.037>
- Mateo, J., Seed, G., Bertan, C., Rescigno, P., Dolling, D., Figueiredo, I., Miranda, S., Nava Rodrigues, D., Gurel, B., Clarke, M., Atkin, M., Chandler, R., Messina, C., Sumanasuriya, S., Bianchini, D., Barrero, M., Petermolo, A., Zafeiriou, Z., Fontes, M., ... de Bono, J. S. (2020). Genomics of lethal prostate cancer at diagnosis and castration resistance. *The Journal of Clinical Investigation*, 130(4), 1743–1751. <https://doi.org/10.1172/JCI132031>
- McNeal, J. E., Villers, A. A., Redwine, E. A., Freiha, F. S., & Stamey, T. A. (1990). Histologic differentiation, cancer volume, and pelvic lymph node metastasis in adenocarcinoma of the prostate. *Cancer*, 66(6), 1225–1233. [https://doi.org/10.1002/1097-0142\(19900915\)66:6<1225::aid-cncr2820660624>3.0.co;2-x](https://doi.org/10.1002/1097-0142(19900915)66:6<1225::aid-cncr2820660624>3.0.co;2-x)
- Medrano, R. F. V., Hunger, A., Mendonça, S. A., Barbuto, J. A. M., & Strauss, B. E. (2017). Immunomodulatory and antitumor effects of type I interferons and their application in cancer therapy. *Oncotarget*, 8(41), 71249–71284. <https://doi.org/10.18632/oncotarget.19531>
- Milowsky, M. I., Nanus, D. M., Kostakoglu, L., Sheehan, C. E., Vallabhajosula, S., Goldsmith, S. J., Ross, J. S., & Bander, N. H. (2007). Vascular Targeted Therapy With Anti-Prostate-Specific Membrane Antigen Monoclonal Antibody J591 in Advanced Solid Tumors. *Journal of Clinical Oncology*, 25(5), 540–547. <https://doi.org/10.1200/JCO.2006.07.8097>
- Montironi, R., Cheng, L., Lopez-Beltran, A., Scarpelli, M., Mazzucchelli, R., Mikuz, G., Kirkali, Z., & Montorsi, F. (2010). Original Gleason System Versus 2005 ISUP Modified Gleason System: The Importance of Indicating Which System Is Used in the Patient's Pathology and Clinical Reports. *European Urology*, 58(3), 369–373. <https://doi.org/10.1016/j.eururo.2010.04.028>
- Moyer, V. A., & U.S. Preventive Services Task Force. (2012). Screening for prostate cancer: U.S. Preventive Services Task Force recommendation statement. *Annals of Internal Medicine*, 157(2), 120–134. <https://doi.org/10.7326/0003-4819-157-2-201207170-00459>
- Mu, P., Zhang, Z., Benelli, M., Karthaus, W. R., Hoover, E., Chen, C.-C., Wongvipat, J., Ku, S.-Y., Gao, D., Cao, Z., Shah, N., Adams, E. J., Abida, W., Watson, P. A., Prandi, D., Huang, C.-H., de Stanchina, E., Lowe, S. W., Ellis, L., ... Sawyers, C. L. (2017). *SOX2* promotes lineage plasticity and antiandrogen resistance in *TP53* -

- and *RBI* -deficient prostate cancer. *Science*, 355(6320), 84–88.
<https://doi.org/10.1126/science.aah4307>
- N. Mottet. (2023). *EAU Guidelines. Edn. presented at the EAU Annual Congress Milan 2023. ISBN 978-94-92671-19-6.*
- Na, R., Zheng, S. L., Han, M., Yu, H., Jiang, D., Shah, S., Ewing, C. M., Zhang, L., Novakovic, K., Petkewicz, J., Gulukota, K., Helseth, D. L., Quinn, M., Humphries, E., Wiley, K. E., Isaacs, S. D., Wu, Y., Liu, X., Zhang, N., ... Isaacs, W. B. (2017). Germline Mutations in ATM and BRCA1/2 Distinguish Risk for Lethal and Indolent Prostate Cancer and are Associated with Early Age at Death. *European Urology*, 71(5), 740–747. <https://doi.org/10.1016/j.eururo.2016.11.033>
- Narayan, V., Barber-Rotenberg, J. S., Jung, I.-Y., Lacey, S. F., Rech, A. J., Davis, M. M., Hwang, W.-T., Lal, P., Carpenter, E. L., Maude, S. L., Plesa, G., Vapiwala, N., Chew, A., Moniak, M., Sebro, R. A., Farwell, M. D., Marshall, A., Gilmore, J., Lledo, L., ... Haas, N. B. (2022). PSMA-targeting TGFβ-insensitive armored CAR T cells in metastatic castration-resistant prostate cancer: a phase 1 trial. *Nature Medicine*, 28(4), 724–734. <https://doi.org/10.1038/s41591-022-01726-1>
- Nguyen, D. P., Li, J., & Tewari, A. K. (2014). Inflammation and prostate cancer: the role of interleukin 6 (IL-6). *BJU International*, 113(6), 986–992.
<https://doi.org/10.1111/bju.12452>
- Nicolosi, P., Ledet, E., Yang, S., Michalski, S., Freschi, B., O’Leary, E., Esplin, E. D., Nussbaum, R. L., & Sartor, O. (2019). Prevalence of Germline Variants in Prostate Cancer and Implications for Current Genetic Testing Guidelines. *JAMA Oncology*, 5(4), 523–528. <https://doi.org/10.1001/jamaoncol.2018.6760>
- Ntala, C., Salji, M., Salmond, J., Officer, L., Teodosio, A. V., Blomme, A., McGhee, E. J., Powley, I., Ahmad, I., Kruithof-de Julio, M., Thalmann, G., Roberts, E., Goodyear, C. S., Jamaspishvili, T., Berman, D. M., Carlin, L. M., Le Quesne, J., & Leung, H. Y. (2021). Analysis of Prostate Cancer Tumor Microenvironment Identifies Reduced Stromal CD4 Effector T-cell Infiltration in Tumors with Pelvic Nodal Metastasis. *European Urology Open Science*, 29, 19–29.
<https://doi.org/10.1016/j.euros.2021.05.001>
- Nyame, Y. A., Cooperberg, M. R., Cumberbatch, M. G., Eggener, S. E., Etzioni, R., Gomez, S. L., Haiman, C., Huang, F., Lee, C. T., Litwin, M. S., Lyratzopoulos, G., Mohler, J. L., Murphy, A. B., Pettaway, C., Powell, I. J., Sasieni, P., Schaeffer, E. M., Shariat, S. F., & Gore, J. L. (2022). Deconstructing, Addressing, and Eliminating Racial and Ethnic Inequities in Prostate Cancer Care. *European Urology*, 82(4), 341–351. <https://doi.org/10.1016/j.eururo.2022.03.007>
- Nyberg, T., Frost, D., Barrowdale, D., Evans, D. G., Bancroft, E., Adlard, J., Ahmed, M., Barwell, J., Brady, A. F., Brewer, C., Cook, J., Davidson, R., Donaldson, A., Eason, J., Gregory, H., Henderson, A., Izatt, L., Kennedy, M. J., Miller, C., ... Antoniou, A. C. (2020). Prostate Cancer Risks for Male BRCA1 and BRCA2 Mutation Carriers: A Prospective Cohort Study. *European Urology*, 77(1), 24–35.
<https://doi.org/10.1016/j.eururo.2019.08.025>
- Overland, M. R., Washington, S. L., Carroll, P. R., Cooperberg, M. R., & Herlemann, A. (2019). Active surveillance for intermediate-risk prostate cancer: yes, but for whom? *Current Opinion in Urology*, 29(6), 605–611.
<https://doi.org/10.1097/MOU.0000000000000671>
- Ozbek, B., Ertunc, O., Erickson, A., Vidal, I. D., Gomes-Alexandre, C., Guner, G., Hicks, J. L., Jones, T., Taube, J. M., Sfanos, K. S., Yegnasubramanian, S., & De

- Marzo, A. M. (2022). Multiplex immunohistochemical phenotyping of T cells in primary prostate cancer. *The Prostate*, 82(6), 706–722. <https://doi.org/10.1002/pros.24315>
- Pachynski, R. K., Morishima, C., Szmulewitz, R., Harshman, L., Appleman, L., Monk, P., Bitting, R. L., Kucuk, O., Millard, F., Seigne, J. D., Fling, S. P., Maecker, H. T., Duault, C., Ramchurren, N., Hess, B., D’Amico, L., Lacroix, A., Kaiser, J. C., Morre, M., ... Fong, L. (2021). IL-7 expands lymphocyte populations and enhances immune responses to sipuleucel-T in patients with metastatic castration-resistant prostate cancer (mCRPC). *Journal for ImmunoTherapy of Cancer*, 9(8), e002903. <https://doi.org/10.1136/jitc-2021-002903>
- Pan, Y., Yu, Y., Wang, X., & Zhang, T. (2020). Tumor-Associated Macrophages in Tumor Immunity. *Frontiers in Immunology*, 11, 583084. <https://doi.org/10.3389/fimmu.2020.583084>
- Parwani, A. V, Kronz, J. D., Genega, E. M., Gaudin, P., Chang, S., & Epstein, J. I. (2004). Prostate carcinoma with squamous differentiation: an analysis of 33 cases. *The American Journal of Surgical Pathology*, 28(5), 651–657.
- Pasero, C., Gravis, G., Guerin, M., Granjeaud, S., Thomassin-Piana, J., Rocchi, P., Paciencia-Gros, M., Poizat, F., Bentobji, M., Azario-Cheillan, F., Walz, J., Salem, N., Brunelle, S., Moretta, A., & Olive, D. (2016). Inherent and Tumor-Driven Immune Tolerance in the Prostate Microenvironment Impairs Natural Killer Cell Antitumor Activity. *Cancer Research*, 76(8), 2153–2165. <https://doi.org/10.1158/0008-5472.CAN-15-1965>
- Peng, C., Huggins, M. A., Wanhainen, K. M., Knutson, T. P., Lu, H., Georgiev, H., Mittelsteadt, K. L., Jarjour, N. N., Wang, H., Hogquist, K. A., Campbell, D. J., Borges da Silva, H., & Jameson, S. C. (2022). Engagement of the costimulatory molecule ICOS in tissues promotes establishment of CD8+ tissue-resident memory T cells. *Immunity*, 55(1), 98-114.e5. <https://doi.org/10.1016/j.immuni.2021.11.017>
- Petitprez, F., Fossati, N., Vano, Y., Freschi, M., Becht, E., Lucianò, R., Calderaro, J., Guédet, T., Lacroix, L., Rancoita, P. M. V., Montorsi, F., Fridman, W. H., Sautès-Fridman, C., Briganti, A., Doglioni, C., & Bellone, M. (2019a). PD-L1 Expression and CD8+ T-cell Infiltrate are Associated with Clinical Progression in Patients with Node-positive Prostate Cancer. *European Urology Focus*, 5(2), 192–196. <https://doi.org/10.1016/j.euf.2017.05.013>
- Petitprez, F., Fossati, N., Vano, Y., Freschi, M., Becht, E., Lucianò, R., Calderaro, J., Guédet, T., Lacroix, L., Rancoita, P. M. V., Montorsi, F., Fridman, W. H., Sautès-Fridman, C., Briganti, A., Doglioni, C., & Bellone, M. (2019b). PD-L1 Expression and CD8+ T-cell Infiltrate are Associated with Clinical Progression in Patients with Node-positive Prostate Cancer. *European Urology Focus*, 5(2), 192–196. <https://doi.org/10.1016/j.euf.2017.05.013>
- Pound, C. R., Walsh, P. C., Epstein, J. I., Chan, D. W., & Partin, A. W. (1997). Radical prostatectomy as treatment for prostate-specific antigen-detected stage T1c prostate cancer. *World Journal of Urology*, 15(6), 373–377.
- Preisser, F., Cooperberg, M. R., Crook, J., Feng, F., Graefen, M., Karakiewicz, P. I., Klotz, L., Montironi, R., Nguyen, P. L., & D’Amico, A. V. (2020). Intermediate-risk Prostate Cancer: Stratification and Management. *European Urology Oncology*, 3(3), 270–280. <https://doi.org/10.1016/j.euo.2020.03.002>
- Qu, X., Randhawa, G., Friedman, C., Kurland, B. F., Glaskova, L., Coleman, I., Mostaghel, E., Higano, C. S., Porter, C., Vessella, R., Nelson, P. S., & Fang, M.

- (2013). A Three-Marker FISH Panel Detects More Genetic Aberrations of AR, PTEN and TMPRSS2/ERG in Castration-Resistant or Metastatic Prostate Cancers than in Primary Prostate Tumors. *PLoS ONE*, 8(9), e74671. <https://doi.org/10.1371/journal.pone.0074671>
- Rakebrandt, N., Littringer, K., & Joller, N. (2016). Regulatory T cells: balancing protection versus pathology. *Swiss Medical Weekly*. <https://doi.org/10.4414/smw.2016.14343>
- Randazzo, M., Müller, A., Carlsson, S., Eberli, D., Huber, A., Grobholz, R., Manka, L., Mortezaei, A., Sulser, T., Recker, F., & Kwiatkowski, M. (2016). A positive family history as a risk factor for prostate cancer in a population-based study with organised prostate-specific antigen screening: results of the Swiss European Randomised Study of Screening for Prostate Cancer (ERSPC, Aarau). *BJU International*, 117(4), 576–583. <https://doi.org/10.1111/bju.13310>
- Rathi, N., McFarland, T. R., Nussenzweig, R., Agarwal, N., & Swami, U. (2021). Evolving Role of Immunotherapy in Metastatic Castration Refractory Prostate Cancer. *Drugs*, 81(2), 191–206. <https://doi.org/10.1007/s40265-020-01456-z>
- Raulet, D. H. (2003). Roles of the NKG2D immunoreceptor and its ligands. *Nature Reviews. Immunology*, 3(10), 781–790. <https://doi.org/10.1038/nri1199>
- Rebuzzi, S. E., Rescigno, P., Catalano, F., Mollica, V., Vogl, U. M., Marandino, L., Massari, F., Pereira Mestre, R., Zanardi, E., Signori, A., Buti, S., Bauckneht, M., Gillessen, S., Banna, G. L., & Fornarini, G. (2022). Immune Checkpoint Inhibitors in Advanced Prostate Cancer: Current Data and Future Perspectives. *Cancers*, 14(5). <https://doi.org/10.3390/cancers14051245>
- Richie, J. P., Catalona, W. J., Ahmann, F. R., Hudson, M. A., Scardino, P. T., Flanigan, R. C., deKernion, J. B., Ratliff, T. L., Kavoussi, L. R., Dalkin, B. L., Waters, W. B., MacFarlane, M. T., & Southwick, P. C. (1993). Effect of patient age on early detection of prostate cancer with serum prostate-specific antigen and digital rectal examination. *Urology*, 42(4), 365–374.
- Rifkin, M. D., Zerhouni, E. A., Gatsonis, C. A., Quint, L. E., Paushter, D. M., Epstein, J. I., Hamper, U., Walsh, P. C., & McNeil, B. J. (1990). Comparison of Magnetic Resonance Imaging and Ultrasonography in Staging Early Prostate Cancer. *New England Journal of Medicine*, 323(10), 621–626. <https://doi.org/10.1056/NEJM199009063231001>
- Rosenberg, S. A., Restifo, N. P., Yang, J. C., Morgan, R. A., & Dudley, M. E. (2008). Adoptive cell transfer: a clinical path to effective cancer immunotherapy. *Nature Reviews. Cancer*, 8(4), 299–308. <https://doi.org/10.1038/nrc2355>
- Ross, H. M., Kryvenko, O. N., Cowan, J. E., Simko, J. P., Wheeler, T. M., & Epstein, J. I. (2012a). Do adenocarcinomas of the prostate with Gleason score (GS) ≤ 6 have the potential to metastasize to lymph nodes? *The American Journal of Surgical Pathology*, 36(9), 1346–1352. <https://doi.org/10.1097/PAS.0b013e3182556dcd>
- Ross, H. M., Kryvenko, O. N., Cowan, J. E., Simko, J. P., Wheeler, T. M., & Epstein, J. I. (2012b). Do Adenocarcinomas of the Prostate With Gleason Score (GS) ≤ 6 Have the Potential to Metastasize to Lymph Nodes? *The American Journal of Surgical Pathology*, 36(9), 1346–1352. <https://doi.org/10.1097/PAS.0b013e3182556dcd>
- Rouvière, O., Puech, P., Renard-Penna, R., Claudon, M., Roy, C., Mège-Lechevallier, F., Decaussin-Petrucci, M., Dubreuil-Chambardel, M., Magaud, L., Remontet, L., Ruffion, A., Colombel, M., Crouzet, S., Schott, A.-M., Lemaitre, L., Rabilloud, M., Grenier, N., & MRI-FIRST Investigators. (2019). Use of prostate systematic

- and targeted biopsy on the basis of multiparametric MRI in biopsy-naive patients (MRI-FIRST): a prospective, multicentre, paired diagnostic study. *The Lancet Oncology*, 20(1), 100–109. [https://doi.org/10.1016/S1470-2045\(18\)30569-2](https://doi.org/10.1016/S1470-2045(18)30569-2)
- Runcie, K., Budman, D. R., John, V., & Seetharamu, N. (2018). Bi-specific and tri-specific antibodies- the next big thing in solid tumor therapeutics. *Molecular Medicine (Cambridge, Mass.)*, 24(1), 50. <https://doi.org/10.1186/s10020-018-0051-4>
- Sanchez-Ortiz, R. F., Troncoso, P., Babaian, R. J., Lloreta, J., Johnston, D. A., & Pettaway, C. A. (2006). African-American men with nonpalpable prostate cancer exhibit greater tumor volume than matched white men. *Cancer*, 107(1), 75–82. <https://doi.org/10.1002/cncr.21954>
- Sawczuk, I., Tannenbaum, M., Olsson, C. A., & deVere White, R. (1985). Primary transitional cell carcinoma of prostatic periurethral ducts. *Urology*, 25(4), 339–343.
- Schaeffer, E. M., Srinivas, S., Adra, N., An, Y., Barocas, D., Bitting, R., Bryce, A., Chapin, B., Cheng, H. H., D'Amico, A. V., Desai, N., Dorff, T., Eastham, J. A., Farrington, T. A., Gao, X., Gupta, S., Guzzo, T., Ippolito, J. E., Kuettel, M. R., ... Freedman-Cass, D. A. (2023). Prostate Cancer, Version 4.2023, NCCN Clinical Practice Guidelines in Oncology. *Journal of the National Comprehensive Cancer Network : JNCCN*, 21(10), 1067–1096. <https://doi.org/10.6004/jnccn.2023.0050>
- Schalken, J., & Fitzpatrick, J. M. (2016). Enzalutamide: targeting the androgen signalling pathway in metastatic castration-resistant prostate cancer. *BJU International*, 117(2), 215–225. <https://doi.org/10.1111/bju.13123>
- Schally, A. V., Block, N. L., & Rick, F. G. (2017). Discovery of LHRH and development of LHRH analogs for prostate cancer treatment. *The Prostate*, 77(9), 1036–1054. <https://doi.org/10.1002/pros.23360>
- Schellhammer, P. F., Bean, M. A., & Whitmore, W. F. (1977). Prostatic involvement by transitional cell carcinoma: pathogenesis, patterns and prognosis. *The Journal of Urology*, 118(3), 399–403. [https://doi.org/10.1016/s0022-5347\(17\)58039-8](https://doi.org/10.1016/s0022-5347(17)58039-8)
- Schenkel, J. M., Fraser, K. A., Beura, L. K., Pauken, K. E., Vezys, V., & Masopust, D. (2014). T cell memory. Resident memory CD8 T cells trigger protective innate and adaptive immune responses. *Science (New York, N.Y.)*, 346(6205), 98–101. <https://doi.org/10.1126/science.1254536>
- Schenkel, J. M., & Masopust, D. (2014). Tissue-resident memory T cells. *Immunity*, 41(6), 886–897. <https://doi.org/10.1016/j.immuni.2014.12.007>
- Schildberg, F. A., Klein, S. R., Freeman, G. J., & Sharpe, A. H. (2016). Coinhibitory Pathways in the B7-CD28 Ligand-Receptor Family. *Immunity*, 44(5), 955–972. <https://doi.org/10.1016/j.immuni.2016.05.002>
- Schott, D. S., Pizon, M., Pachmann, U., & Pachmann, K. (2017). Sensitive detection of PD-L1 expression on circulating epithelial tumor cells (CETCs) could be a potential biomarker to select patients for treatment with PD-1/PD-L1 inhibitors in early and metastatic solid tumors. *Oncotarget*, 8(42), 72755–72772. <https://doi.org/10.18632/oncotarget.20346>
- Sciarra, A., Barentsz, J., Bjartell, A., Eastham, J., Hricak, H., Panebianco, V., & Witjes, J. A. (2011). Advances in magnetic resonance imaging: How they are changing the management of prostate cancer. *European Urology*, 59(6), 962–977. <https://doi.org/10.1016/j.eururo.2011.02.034>

- Seidel, J. A., Otsuka, A., & Kabashima, K. (2018). Anti-PD-1 and Anti-CTLA-4 Therapies in Cancer: Mechanisms of Action, Efficacy, and Limitations. *Frontiers in Oncology*, 8, 86. <https://doi.org/10.3389/fonc.2018.00086>
- Sena, L. A., Denmeade, S. R., & Antonarakis, E. S. (2021). Targeting the spectrum of immune checkpoints in prostate cancer. *Expert Review of Clinical Pharmacology*, 14(10), 1253–1266. <https://doi.org/10.1080/17512433.2021.1949287>
- Sexton, W. J., Lance, R. E., Reyes, A. O., Pisters, P. W., Tu, S. M., & Pisters, L. L. (2001). Adult prostate sarcoma: the M. D. Anderson Cancer Center Experience. *The Journal of Urology*, 166(2), 521–525. [https://doi.org/10.1016/s0022-5347\(05\)65974-5](https://doi.org/10.1016/s0022-5347(05)65974-5)
- Sfanos, K. S., Bruno, T. C., Maris, C. H., Xu, L., Thoburn, C. J., DeMarzo, A. M., Meeker, A. K., Isaacs, W. B., & Drake, C. G. (2008). Phenotypic Analysis of Prostate-Infiltrating Lymphocytes Reveals TH17 and Treg Skewing. *Clinical Cancer Research*, 14(11), 3254–3261. <https://doi.org/10.1158/1078-0432.CCR-07-5164>
- Sfanos, K. S., Yegnasubramanian, S., Nelson, W. G., & De Marzo, A. M. (2018). The inflammatory microenvironment and microbiome in prostate cancer development. *Nature Reviews Urology*, 15(1), 11–24. <https://doi.org/10.1038/nrur.2017.167>
- Sharma, M., Yang, Z., & Miyamoto, H. (2019). Immunohistochemistry of immune checkpoint markers PD-1 and PD-L1 in prostate cancer. *Medicine*, 98(38), e17257. <https://doi.org/10.1097/MD.00000000000017257>
- Sharma, P., Krainer, M., Saad, F., Castellano, D., Bedke, J., Kwiatkowski, M., Patnaik, A., Procopio, G., Wiechno, P., Kochuparambil, S. T., Thomas, C., Arranz Arijia, J. A., McCune, S. L., Hansen, S., Daugaard, G., Amin, N. P., Wang, Y., David, J. M., & Pachynski, R. K. (2023). Nivolumab plus ipilimumab for the treatment of post-chemotherapy metastatic castration-resistant prostate cancer (mCRPC): Additional results from the randomized phase 2 CheckMate 650 trial. *Journal of Clinical Oncology*, 41(6_suppl), 22–22. https://doi.org/10.1200/JCO.2023.41.6_suppl.22
- Singh, A., Dees, S., & Grewal, I. S. (2021). Overcoming the challenges associated with CD3+ T-cell redirection in cancer. *British Journal of Cancer*, 124(6), 1037–1048. <https://doi.org/10.1038/s41416-020-01225-5>
- Slovin, S. F., Wang, X., Hullings, M., Arauz, G., Bartido, S., Lewis, J. S., Schöder, H., Zanzonico, P., Scher, H. I., Sadelain, M., & Riviere, I. (2013). Chimeric antigen receptor (CAR⁺) modified T cells targeting prostate-specific membrane antigen (PSMA) in patients (pts) with castrate metastatic prostate cancer (CMPC). *Journal of Clinical Oncology*, 31(6_suppl), 72–72. https://doi.org/10.1200/jco.2013.31.6_suppl.72
- Srinivasan, S., Kumar, R., Koduru, S., Chandramouli, A., & Damodaran, C. (2010). Inhibiting TNF-mediated signaling: a novel therapeutic paradigm for androgen independent prostate cancer. *Apoptosis*, 15(2), 153–161. <https://doi.org/10.1007/s10495-009-0416-9>
- Stamey, T. A., Freiha, F. S., McNeal, J. E., Redwine, E. A., Whittemore, A. S., & Schmid, H. P. (1993). Localized prostate cancer. Relationship of tumor volume to clinical significance for treatment of prostate cancer. *Cancer*, 71(3 Suppl), 933–938. [https://doi.org/10.1002/1097-0142\(19930201\)71:3+<933::aid-cncr2820711408>3.0.co;2-1](https://doi.org/10.1002/1097-0142(19930201)71:3+<933::aid-cncr2820711408>3.0.co;2-1)
- Stamey, T. A., Yang, N., Hay, A. R., McNeal, J. E., Freiha, F. S., & Redwine, E. (1987). Prostate-Specific Antigen as a Serum Marker for Adenocarcinoma of the

- Prostate. *New England Journal of Medicine*, 317(15), 909–916.
<https://doi.org/10.1056/NEJM198710083171501>
- Subudhi, S. K., Vence, L., Zhao, H., Blando, J., Yadav, S. S., Xiong, Q., Reuben, A., Aparicio, A., Corn, P. G., Chapin, B. F., Pisters, L. L., Troncoso, P., Tidwell, R. S., Thall, P., Wu, C.-J., Zhang, J., Logothetis, C. L., Futreal, A., Allison, J. P., & Sharma, P. (2020). Neoantigen responses, immune correlates, and favorable outcomes after ipilimumab treatment of patients with prostate cancer. *Science Translational Medicine*, 12(537). <https://doi.org/10.1126/scitranslmed.aaz3577>
- Sung, H., Ferlay, J., Siegel, R. L., Laversanne, M., Soerjomataram, I., Jemal, A., & Bray, F. (2021). Global Cancer Statistics 2020: GLOBOCAN Estimates of Incidence and Mortality Worldwide for 36 Cancers in 185 Countries. *CA: A Cancer Journal for Clinicians*, 71(3), 209–249. <https://doi.org/10.3322/caac.21660>
- Takahashi, N., Matsumoto, K., Saito, H., Nanki, T., Miyasaka, N., Kobata, T., Azuma, M., Lee, S.-K., Mizutani, S., & Morio, T. (2009). Impaired CD4 and CD8 effector function and decreased memory T cell populations in ICOS-deficient patients. *Journal of Immunology (Baltimore, Md. : 1950)*, 182(9), 5515–5527.
<https://doi.org/10.4049/jimmunol.0803256>
- Takenaka, A., Hara, R., Ishimura, T., Fujii, T., Jo, Y., Nagai, A., & Fujisawa, M. (2008). A prospective randomized comparison of diagnostic efficacy between transperineal and transrectal 12-core prostate biopsy. *Prostate Cancer and Prostatic Diseases*, 11(2), 134–138. <https://doi.org/10.1038/sj.pcan.4500985>
- Taneja, S. S. (2018). Re: MRI-Targeted or Standard Biopsy for Prostate-Cancer Diagnosis. *The Journal of Urology*, 200(4), 697–699.
<https://doi.org/10.1016/j.juro.2018.07.026>
- Tang, B., de Castro, K., Barnes, H. E., Parks, W. T., Stewart, L., Böttinger, E. P., Danielpour, D., & Wakefield, L. M. (1999). Loss of responsiveness to transforming growth factor beta induces malignant transformation of nontumorigenic rat prostate epithelial cells. *Cancer Research*, 59(19), 4834–4842.
- Tannock, I. F., de Wit, R., Berry, W. R., Horti, J., Pluzanska, A., Chi, K. N., Oudard, S., Théodore, C., James, N. D., Turesson, I., Rosenthal, M. A., Eisenberger, M. A., & TAX 327 Investigators. (2004). Docetaxel plus prednisone or mitoxantrone plus prednisone for advanced prostate cancer. *The New England Journal of Medicine*, 351(15), 1502–1512. <https://doi.org/10.1056/NEJMoa040720>
- Têtu, B., Ro, J. Y., Ayala, A. G., Johnson, D. E., Logothetis, C. J., & Ordonez, N. G. (1987). Small cell carcinoma of the prostate. Part I. A clinicopathologic study of 20 cases. *Cancer*, 59(10), 1803–1809. [https://doi.org/10.1002/1097-0142\(19870515\)59:10<1803::aid-cnrc2820591019>3.0.co;2-x](https://doi.org/10.1002/1097-0142(19870515)59:10<1803::aid-cnrc2820591019>3.0.co;2-x)
- Thompson, I. M., Pauler, D. K., Goodman, P. J., Tangen, C. M., Lucia, M. S., Parnes, H. L., Minasian, L. M., Ford, L. G., Lippman, S. M., Crawford, E. D., Crowley, J. J., & Coltman, C. A. (2004). Prevalence of Prostate Cancer among Men with a Prostate-Specific Antigen Level ≤ 4.0 ng per Milliliter. *New England Journal of Medicine*, 350(22), 2239–2246. <https://doi.org/10.1056/NEJMoa031918>
- Tran, E., Turcotte, S., Gros, A., Robbins, P. F., Lu, Y.-C., Dudley, M. E., Wunderlich, J. R., Somerville, R. P., Hogan, K., Hinrichs, C. S., Parkhurst, M. R., Yang, J. C., & Rosenberg, S. A. (2014). Cancer immunotherapy based on mutation-specific CD4+ T cells in a patient with epithelial cancer. *Science (New York, N.Y.)*, 344(6184), 641–645. <https://doi.org/10.1126/science.1251102>

- Tsaur, I., Brandt, M. P., Juengel, E., Manceau, C., & Ploussard, G. (2021). Immunotherapy in prostate cancer: new horizon of hurdles and hopes. *World Journal of Urology*, *39*(5), 1387–1403. <https://doi.org/10.1007/s00345-020-03497-1>
- Tse, S.-W., Radtke, A. J., Espinosa, D. A., Cockburn, I. A., & Zavala, F. (2014). The chemokine receptor CXCR6 is required for the maintenance of liver memory CD8⁺ T cells specific for infectious pathogens. *The Journal of Infectious Diseases*, *210*(9), 1508–1516. <https://doi.org/10.1093/infdis/jiu281>
- Van der Kwast, T. H., & Roobol, M. J. (2013). Defining the threshold for significant versus insignificant prostate cancer. *Nature Reviews. Urology*, *10*(8), 473–482. <https://doi.org/10.1038/nrurol.2013.112>
- van der Leest, M., Cornel, E., Israël, B., Hendriks, R., Padhani, A. R., Hoogenboom, M., Zamecnik, P., Bakker, D., Setiasti, A. Y., Veltman, J., van den Hout, H., van der Lelij, H., van Oort, I., Klaver, S., Debruyne, F., Sedelaar, M., Hannink, G., Rovers, M., Hulsbergen-van de Kaa, C., & Barentsz, J. O. (2019). Head-to-head Comparison of Transrectal Ultrasound-guided Prostate Biopsy Versus Multiparametric Prostate Resonance Imaging with Subsequent Magnetic Resonance-guided Biopsy in Biopsy-naïve Men with Elevated Prostate-specific Antigen: A Large Prospective Mu. *European Urology*, *75*(4), 570–578. <https://doi.org/10.1016/j.eururo.2018.11.023>
- Vandenbon, A., & Diez, D. (2020). A clustering-independent method for finding differentially expressed genes in single-cell transcriptome data. *Nature Communications*, *11*(1), 4318. <https://doi.org/10.1038/s41467-020-17900-3>
- Venkitaraman, A. R. (2002). Cancer Susceptibility and the Functions of BRCA1 and BRCA2. *Cell*, *108*(2), 171–182. [https://doi.org/10.1016/S0092-8674\(02\)00615-3](https://doi.org/10.1016/S0092-8674(02)00615-3)
- Vis, A. N., van der Sluis, T. M., Al-Itejawi, H. H. M., van Moorselaar, R. J. A., & Meuleman, E. J. H. (2015). Risk of disease flare with LHRH agonist therapy in men with prostate cancer: myth or fact? *Urologic Oncology*, *33*(1), 7–15. <https://doi.org/10.1016/j.urolonc.2014.04.016>
- Vitek, R. A., Huang, W., Geiger, P. G., Heninger, E., Lang, J. M., Jarrard, D. F., Beebe, D. J., & Johnson, B. P. (2022). Fresh tissue procurement and preparation for multicompartiment and multimodal analysis of the prostate tumor microenvironment. *The Prostate*, *82*(7), 836–849. <https://doi.org/10.1002/pros.24326>
- Vitkin, N., Nersesian, S., Siemens, D. R., & Koti, M. (2019). The Tumor Immune Contexture of Prostate Cancer. *Frontiers in Immunology*, *10*. <https://doi.org/10.3389/fimmu.2019.00603>
- von Werdt, D., Gungor, B., Barreto de Albuquerque, J., Gruber, T., Zysset, D., Kwong Chung, C. K. C., Corrêa-Ferreira, A., Berchtold, R., Page, N., Schenk, M., Kehrl, J. H., Merkler, D., Imhof, B. A., Stein, J. V., Abe, J., Turchinovich, G., Finke, D., Hayday, A. C., Corazza, N., & Mueller, C. (2023). Regulator of G-protein signaling 1 critically supports CD8⁺ TRM cell-mediated intestinal immunity. *Frontiers in Immunology*, *14*, 1085895. <https://doi.org/10.3389/fimmu.2023.1085895>
- Wang, B., Wu, S., Zeng, H., Liu, Z., Dong, W., He, W., Chen, X., Dong, X., Zheng, L., Lin, T., & Huang, J. (2015). CD103⁺ Tumor Infiltrating Lymphocytes Predict a Favorable Prognosis in Urothelial Cell Carcinoma of the Bladder. *Journal of Urology*, *194*(2), 556–562. <https://doi.org/10.1016/j.juro.2015.02.2941>

- Wang, E. (2013). Understanding genomic alterations in cancer genomes using an integrative network approach. *Cancer Letters*, 340(2), 261–269. <https://doi.org/10.1016/j.canlet.2012.11.050>
- Wang, L., Lu, B., He, M., Wang, Y., Wang, Z., & Du, L. (2022). Prostate Cancer Incidence and Mortality: Global Status and Temporal Trends in 89 Countries From 2000 to 2019. *Frontiers in Public Health*, 10, 811044. <https://doi.org/10.3389/fpubh.2022.811044>
- Wang, Z.-Q., Milne, K., Derocher, H., Webb, J. R., Nelson, B. H., & Watson, P. H. (2016). CD103 and Intratumoral Immune Response in Breast Cancer. *Clinical Cancer Research*, 22(24), 6290–6297. <https://doi.org/10.1158/1078-0432.CCR-16-0732>
- Webb, J. R., Milne, K., & Nelson, B. H. (2015a). PD-1 and CD103 Are Widely Coexpressed on Prognostically Favorable Intraepithelial CD8 T Cells in Human Ovarian Cancer. *Cancer Immunology Research*, 3(8), 926–935. <https://doi.org/10.1158/2326-6066.CIR-14-0239>
- Webb, J. R., Milne, K., & Nelson, B. H. (2015b). PD-1 and CD103 Are Widely Coexpressed on Prognostically Favorable Intraepithelial CD8 T Cells in Human Ovarian Cancer. *Cancer Immunology Research*, 3(8), 926–935. <https://doi.org/10.1158/2326-6066.CIR-14-0239>
- Webb, J. R., Milne, K., Watson, P., Deleeuw, R. J., & Nelson, B. H. (2014). Tumor-infiltrating lymphocytes expressing the tissue resident memory marker CD103 are associated with increased survival in high-grade serous ovarian cancer. *Clinical Cancer Research : An Official Journal of the American Association for Cancer Research*, 20(2), 434–444. <https://doi.org/10.1158/1078-0432.CCR-13-1877>
- Winkler, J., Abisoye-Ogunniyan, A., Metcalf, K. J., & Werb, Z. (2020). Concepts of extracellular matrix remodelling in tumour progression and metastasis. *Nature Communications*, 11(1), 5120. <https://doi.org/10.1038/s41467-020-18794-x>
- Wood, D. P., Montie, J. E., Pontes, J. E., Medendorp, S. V., & Levin, H. S. (1989). Transitional Cell Carcinoma of the Prostate in Cystoprostatectomy Specimens Removed for Bladder Cancer. *Journal of Urology*, 141(2), 346–349. [https://doi.org/10.1016/S0022-5347\(17\)40762-2](https://doi.org/10.1016/S0022-5347(17)40762-2)
- Wu, X., Jin, C., Wang, F., Yu, C., & McKeehan, W. L. (2003). Stromal cell heterogeneity in fibroblast growth factor-mediated stromal-epithelial cell cross-talk in premalignant prostate tumors. *Cancer Research*, 63(16), 4936–4944.
- Xin, S., Liu, X., Li, Z., Sun, X., Wang, R., Zhang, Z., Feng, X., Jin, L., Li, W., Tang, C., Mei, W., Cao, Q., Wang, H., Zhang, J., Feng, L., & Ye, L. (2023). ScRNA-seq revealed an immunosuppression state and tumor microenvironment heterogeneity related to lymph node metastasis in prostate cancer. *Experimental Hematology & Oncology*, 12(1), 49. <https://doi.org/10.1186/s40164-023-00407-0>
- Xu, L., Chen, X., Shen, M., Yang, D.-R., Fang, L., Weng, G., Tsai, Y., Keng, P. C., Chen, Y., & Lee, S. O. (2018). Inhibition of IL-6-JAK/Stat3 signaling in castration-resistant prostate cancer cells enhances the NK cell-mediated cytotoxicity via alteration of PD-L1/NKG2D ligand levels. *Molecular Oncology*, 12(3), 269–286. <https://doi.org/10.1002/1878-0261.12135>
- Xu, Y., Song, G., Xie, S., Jiang, W., Chen, X., Chu, M., Hu, X., & Wang, Z.-W. (2021). The roles of PD-1/PD-L1 in the prognosis and immunotherapy of prostate cancer. *Molecular Therapy : The Journal of the American Society of Gene Therapy*, 29(6), 1958–1969. <https://doi.org/10.1016/j.ymthe.2021.04.029>

- Yanagisawa, N., Li, R., Rowley, D., Liu, H., Kadmon, D., Miles, B. J., Wheeler, T. M., & Ayala, G. E. (2008). Reprint of: Stromogenic prostatic carcinoma pattern (carcinomas with reactive stromal grade 3) in needle biopsies predicts biochemical recurrence-free survival in patients after radical prostatectomy. *Human Pathology*, *39*(2), 282–291. <https://doi.org/10.1016/j.humpath.2007.04.025>
- Yokokawa, J., Cereda, V., Remondo, C., Gulley, J. L., Arlen, P. M., Schlom, J., & Tsang, K. Y. (2008). Enhanced Functionality of CD4+CD25highFoxP3+ Regulatory T Cells in the Peripheral Blood of Patients with Prostate Cancer. *Clinical Cancer Research*, *14*(4), 1032–1040. <https://doi.org/10.1158/1078-0432.CCR-07-2056>
- Yuanquan Yang, K. A. C. V. A. O. W. B. B. X. E. K. J. M. K. G. Q. L. S. G. P. B. C. M. A. P.-S. P. K. and G. S. C. (2018). Association of high CD8+ tumor infiltrating lymphocytes at prostatectomy with improved survival of prostate cancer patients. *J Clin Oncol* *36*:5068–5068.
- Zareba, P., Zhang, J., Yilmaz, A., & Trpkov, K. (2009). The impact of the 2005 International Society of Urological Pathology (ISUP) consensus on Gleason grading in contemporary practice. *Histopathology*, *55*(4), 384–391. <https://doi.org/10.1111/j.1365-2559.2009.03405.x>
- Zhang, Y., Campbell, B. K., Stylli, S. S., Corcoran, N. M., & Hovens, C. M. (2022). The Prostate Cancer Immune Microenvironment, Biomarkers and Therapeutic Intervention. *Uro*, *2*(2), 74–92. <https://doi.org/10.3390/uro2020010>
- Zhou, Q., Ou, Y., Dai, X., Chen, X., Wu, S., Chen, W., Hu, M., Yang, C., Zhang, L., & Jiang, H. (2023). Prevalence of tumour-infiltrating CD103+ cells identifies therapeutic-sensitive prostate cancer with poor clinical outcome. *British Journal of Cancer*, *128*(8), 1466–1477. <https://doi.org/10.1038/s41416-023-02183-4>
- Zhu, M.-L., Partin, J. V., Bruckheimer, E. M., Strup, S. E., & Kyprianou, N. (2008). TGF-beta signaling and androgen receptor status determine apoptotic cross-talk in human prostate cancer cells. *The Prostate*, *68*(3), 287–295. <https://doi.org/10.1002/pros.20698>
- Zumsteg, Z. S., Zelefsky, M. J., Woo, K. M., Spratt, D. E., Kollmeier, M. A., McBride, S., Pei, X., Sandler, H. M., & Zhang, Z. (2017). Unification of favourable intermediate-, unfavourable intermediate-, and very high-risk stratification criteria for prostate cancer. *BJU International*, *120*(5B), E87–E95. <https://doi.org/10.1111/bju.13903>

